Year : 2020

Impaired fetal growth and human umbilical vein dysfunction

Beaumann Manon

UNIL | Université de Lausanne
Faculté de biologie et de médecine

Département Femme-Mère-Enfant

Impaired fetal growth and human umbilical vein dysfunction

Thèse de doctorat ès sciences de la vie (PhD)

présentée à la

Faculté de biologie et de médecine
de l'Université de Lausanne

par

Manon BEAUMANN

Master de l'Université de Lausanne

Jury

Prof. Lucas Liaudet, Président
Prof. Jean-François Tolsa, Directeur de thèse
Dre Anne-Christine Peyter, Co-directrice de thèse
Prof. Jean-Christophe Rozé, Expert
Prof. Laurent Storme, Expert

Lausanne
(2020)

UNIL | Université de Lausanne
Faculté de biologie et de médecine

Département Femme-Mère-Enfant

Impaired fetal growth and human umbilical vein dysfunction

Thèse de doctorat ès sciences de la vie (PhD)

présentée à la

Faculté de biologie et de médecine
de l'Université de Lausanne

par

Manon BEAUMANN

Master de l'Université de Lausanne

Jury

Prof. Lucas Liaudet, Président
Prof. Jean-François Tolsa, Directeur de thèse
Dre Anne-Christine Peyter, Co-directrice de thèse
Prof. Jean-Christophe Rozé, Expert
Prof. Laurent Storme, Expert

Lausanne
(2020)

UNIL | Université de Lausanne
Faculté de biologie et de médecine

Ecole Doctorale
Doctorat ès sciences de la vie

Imprimatur

Vu le rapport présenté par le jury d'examen, composé de

Président·e	Monsieur	Prof.	Lucas	**Liaudet**
Directeur·trice de thèse	Monsieur	Prof.	Jean-François	**Tolsa**
Co-directeur·trice	Madame	Dre	Anne-Christine	**Peyter**
Expert·e·s	Monsieur	Prof.	Laurent	**Storme**
	Monsieur	Prof.	Jean-Christophe	**Rozé**

le Conseil de Faculté autorise l'impression de la thèse de

Madame Manon Beaumann

Master en biologie médicale, Université de Lausanne

intitulée

Impaired fetal growth and human umbilical vein dysfunction

Date de l'examen : 17 novembre 2020

Date d'émission de l'imprimatur : Lausanne, le 19 janvier 2021

pour le Doyen
de la Faculté de biologie et de médecine

Prof. Niko GELDNER
Directeur de l'Ecole Doctorale

Acknowledgements

To begin, I would like to thank all members of my thesis comity for the attention that you paid for this work. Thanks to Prof. Lucas Liaudet to accept to chair this comity and to Prof. Jean-Christophe Rozé and Prof. Laurent Storme to accept to be the experts of this thesis. I would like to thank you for your time and your interest.

A warm thanks to Prof. Jean-François Tolsa and Dre Anne-Christine Peyter to give me the opportunity to do my thesis in their lab, to their trust and their management. Thanks Jean-François to allowed me to participate at the SLECR congress in Montreal with you. It was a wonderful opportunity with great people and I will remember for a long time. Thanks Anne-Christine to your constant devotion, your help, your kindness. Thank you to have shared your wide knowledge with me, to your numerous advises and your coaching in every scientific skill.

I would like to thank all colleagues of the Neonatal Research Laboratory. Thanks to my great technician Steeve Menétrey to all things that you learned me, to your conscientious and rigorous science, to all laugh, all jokes that we shared with the team. Thanks to Dre Sandrine Gremlich-Irrausch to your advises and simply the interesting discussions that we had. Thanks to all students and trainees too, for your contribution to the lab project, to Eulalia Orozco Fernandez and Sabrina Rivera to become some true friends. A big thanks to Dre Catherine Yzydorczyk, to your friendship, your collaboration, your help in the lab as outside, your precious advises. Thanks to all shared moments. I am going to miss it.

I would also like to thank my friends and my family, specially my parents without whom I could not be there today. Thanks to your unwavering support during every obstacle that I have encountered.

Finally, a special thanks to Rogério, to your support during these thesis years and particularly at the end. Thanks to share every moment with me, either good as bad ones. Now, the real life starts.

Thank you all to have helped me to grow up.

Abstract

Introduction: Intrauterine growth restriction (IUGR) is defined as a failure of the fetus to reach its full growth potential. It is a common complication affecting about 8% of all pregnancies. IUGR is a leading cause of perinatal mortality and morbidity, and is associated with an increased risk to develop cardiovascular and metabolic diseases in adulthood. Adequate fetal growth is primarily determined by the availability of oxygen and nutrients brought by the fetoplacental circulation. In human, umbilical vascular tone is mainly regulated by the nitric oxide (NO)/cyclic guanosine monophosphate (cGMP) signaling pathway. We therefore hypothesized that IUGR could be associated with alterations in the regulation of umbilical circulation, and particularly in the NO/cGMP relaxing pathway.

Methods: Umbilical cords were collected soon after birth in term newborns. Different functional and molecular analyses were performed to investigate changes occurring in growth-restricted ("IUGR") neonates compared to appropriate for gestational age (AGA) controls, with a particular attention to the umbilical vein (UV).

Results: Functional experiments showed an impaired NO-induced smooth muscle relaxation in UV of IUGR females, significantly improved by a pre-incubation with a non-specific phosphodiesterases (PDEs) inhibitor. Molecular analyses showed several alterations in the NO/cGMP pathway in IUGR females, but not in males. At the endothelium level, a decrease in endothelial NO synthase (eNOS) protein content was found in IUGR males, but not in females. Finally, investigations relative to the oxidative stress status did not show any difference between UV of AGA and IUGR neonates.

Conclusion: This study highlighted many differences in UV reactivity and molecular components between females and males. We can therefore hypothesize that regulation of vasorelaxation differs between both sexes and that mechanisms implicated in the alteration of the NO/cGMP pathway and thus the development of IUGR are sex-specific. Moreover, the beneficial effects of PDEs inhibition suggest that PDEs could represent promising targets for therapeutic intervention.

Résumé

Introduction : Le retard de croissance intra-utérin (RCIU) est une incapacité du fœtus à atteindre son plein potentiel de croissance. Cette complication fréquente, affectant environ 8% des grossesses, est une cause majeure de mortalité et morbidité périnatales. Le RCIU est associé à un risque accru de développer des maladies cardiovasculaires et métaboliques à l'âge adulte. Une croissance fœtale adéquate est principalement déterminée par la disponibilité en oxygène et en nutriments apportés par la circulation fœto-placentaire. Chez l'homme, le tonus vasculaire ombilical est principalement régulé par la voie de signalisation de l'oxyde nitrique (NO) et de la guanosine monophosphate cylique (GMPc). Nous avons donc émis l'hypothèse que le RCIU pourrait être associé à des altérations dans la régulation de la circulation ombilicale, en particulier dans la voie de relaxation du NO/GMPc.

Méthodes : Les cordons ombilicaux ont été collectés juste après la naissance chez des nouveau-nés à terme. Des analyses fonctionnelles et moléculaires ont été réalisées pour investiguer les changements présents chez les nouveau-nés "RCIU" comparés à ceux ayant un poids approprié pour leur âge gestationnel (AGA), avec une attention particulière pour la veine ombilicale (VO).

Résultats : Les expériences fonctionnelles ont montré que la relaxation induite par le NO était altérée dans la VO des filles RCIU et significativement améliorée en présence d'un inhibiteur non-spécifique des phosphodiestérases (PDEs). Les analyses moléculaires ont montré plusieurs altérations dans la voie du NO/GMPc chez les filles RCIU, mais pas chez les garçons. Au niveau de l'endothélium, il y avait une diminution de la protéine NO synthase endothéliale (eNOS) chez les garçons RCIU, mais pas chez les filles. Enfin, les investigations relatives au stress oxydatif n'ont pas montré de différence entre les VO de nouveau-nés AGA et RCIU.

Conclusion : Cette étude a mis en évidence des différences dans la réactivité et les composants moléculaires de la VO entre les filles et les garçons. Cela suggère que la régulation de la vasorelaxation diffère entre les sexes et que les mécanismes impliqués dans l'altération de la voie du NO/GMPc et le développement du RCIU sont spécifiques au sexe. De plus, les effets bénéfiques de l'inhibition des PDEs suggèrent que les PDEs pourraient représenter des cibles prometteuses pour une intervention thérapeutique.

List of Abbreviations

5-HT	Serotonin
ACOG	American College of Obstetrics and Gynecology
ADMA	Asymmetric dimethylarginine
AEBSF	4-(2-aminoethyl)benzenesulfonyl fluoride hydrochloride
AGA	Appropriate for gestational age
ART	Assisted reproductive technologies
AUC	Area under the curve
BH_4	Tetrahydrobiopterin
BMI	Body mass index
Ca^{2+}	Calcium
CaM	Calcium-activated-calmodulin
cAMP	Cyclic adenosine monophosphate
cGMP	Cyclic guanosine monophosphate
CHAPS	3-[(3-cholamidopropyl)dimethylammonio]-1-propanesulfonate
CPM	Confined placental mosaicism
CTG	Cardiotocography
CVUE	Chronic villitis of unknown etiology
DAF-2 DA	4,5-diaminofluorescein diacetate
DAPI	4,6-Diamidine-2-phenylindole dihydrochloride
DEA/NO	2-(N,N-Diethylamino)-diazenolate-2-oxide
DHE	Dihydroethidium
DMF	N,N-dimethylformamide
DOHaD	Developmental Origins of Health and Disease
EGF	Epidermal growth factor
eNOS	Endothelial nitric oxide synthase
FABP	Fatty acid binding protein
FGF	Fibroblast growth factor

FOAD	Fetal origin of adult disease
GTP	Guanosine triphosphate
HSP90	Heat shock protein 90
IBMX	3-isobutyl-1-methylxanthine
IGF	Insulin-liked growth factor
iNOS	Inducible nitric oxide synthase
IUGR	Intrauterine growth restriction
LBW	Low birth weight
MCI	Marginal cord insertion
NADPH	Nicotinamide adenine dinucleotide phosphate
NEC	Necrotizing enterocolitis
NLA	N^G-nitro-L-arginine
nNOS	Neuronal nitric oxide synthase
NO	Nitric oxide
NOS	Nitric oxide synthase
O_2^-	Superoxide anion
PBS	Phosphate buffered saline
PDE	Phosphodiesterase
PDGF	Platelet-derived growth factor
PKG	Protein kinase G
PPHN	Persistent pulmonary hypertension of the newborn
ROP	Retinopathy of prematurity
ROS	Reactive oxygen species
RT	Room temperature
SA-β-gal	Senescence-associated β-galactosidase
SGA	Small for gestational age
sGC	Soluble guanylyl cyclase
SIRT1	Sirtuin 1
SMC	Smooth muscle cell
SOD	Superoxide dismutase

STRIDER	Sildenafil Therapy in Dismal Prognosis Early Onset Fetal Growth Restriction
US	Ultrasound
VCI	Velamentous cord insertion
WHO	World Health Organization

Table of Contents

List of Figures

List of Tables

Introduction

1. Fetal development and regulation

1.1 Fetal growth physiology

The fetal growth is an extremely complex and organized process, characterized by the tissue construction, the size increasing and the structures maturation. It is a multifactorial phenomenon depending on genetic and environmental factors. It lasts during the entire pregnancy, so 266 days or 38 gestational weeks. However, in obstetrics, the time of pregnancy is usually calculated from the first day of the last menstruations and the term is fixed at 40 weeks of amenorrhea [1].

The intrauterine development is separated in two successive stages: the embryonic stage and the fetal stage. The embryonic stage starts from the fertilization until the 8th gestational week. It comprises the embryogenesis and the apparition of 90% of the adult tissue structures. The fetal stage starts at the 9th gestational week until the end of pregnancy. It is characterized by the maturation and the growth of organs. Both processes evolve at the same time. The maturation has a qualitative aspect and consists in the cellular differentiation, whereas the growth has a quantitative aspect and includes two phenomena, the cellular hyperplasia (growth by increase of cell number) and the cellular hypertrophy (growth by increase of the cell size). During the 20 first weeks, the fetal growth takes place principally by hyperplasia, then by hypertrophy [1].

During the pregnancy, the growth can be evaluated by the measurement of the size (or stature, in centimeters) and estimation of the weight (in grams). The statural growth is linked to the skeleton, whereas the weight growth is proportional to the placental growth. On average, between the 8th and the 38th gestational week, the fetal size increases from 3 to 50 centimeters and the weight from 5 to 3500 grams (Table 1). These increases are not necessarily homogenous. In human, the weight growth is slow until the 23th gestational week, then accelerates to reach a peak near the 34th gestational week. In contrast, the statural growth

reaches a maximum at the 20th gestational week followed by a progressive slowdown until the term (Fig. 1) [1].

Table 1: Fetal growth represented by gestational age and the corresponding size and weight.

Gestation (months)	**Size** (centimeters)	**Weight** (grams)
3	11	70
4	15	200
5	30	500
6	36	1200
7	40	1700
8	45	2400
9	50	3500

Fetal size and weight increase with the gestational age, but not with the same dynamic (Adapted from [2]).

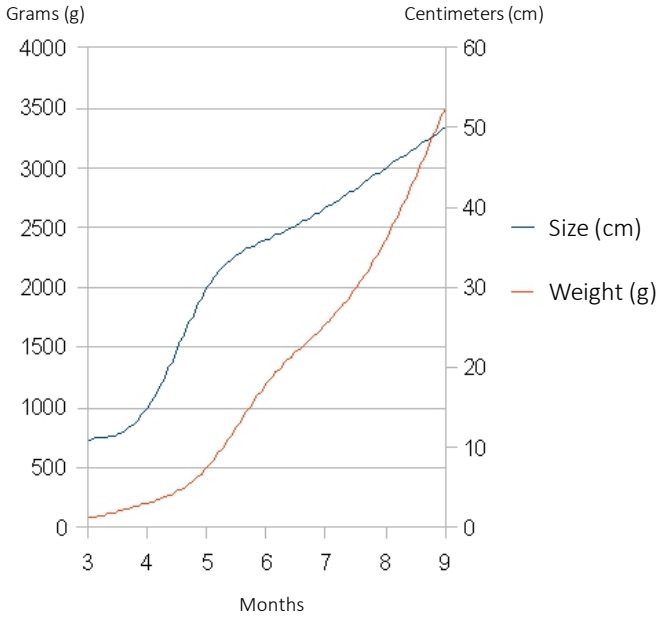

Figure 1: Curves of fetal statural and weight growth.
During the fetal development, size and weight increases are not linear and not correlated (Adapted from [2]).

The intrauterine growth requires a continuous energy intake adapted to every pregnancy period. Every quantitative or qualitative modification of this intake will cause impairments of the fetal growth, as the intrauterine growth restriction (IUGR) or the macrosomia [1]. The maternal gestational weight gain, defined as the amount of weight a pregnant woman gained between the time of conception and the onset of labor, is one of the key markers of intrauterine nutritional environment [3]. Weight gain during pregnancy comprises the products of

conception (fetus, placenta, amniotic fluid), the increases of various maternal tissues (uterus, breast, blood, extracellular extravascular fluid) and the increases in maternal fat stores [4]. The weight gain recommendation depends on the woman pregravid weight status. With a normal body mass index (BMI), this gain should be included between 11 to 16 kilograms (Table 2) [5].

Table 2: Recommended total weight gain in pregnant women according to BMI.

Weight-for-height category	Recommended total gain (kg)
Low (BMI < 19.8)	12.5–18
Normal (BMI 19.8–26.0)	11.5–16
High (BMI > 26.0–29.0)[2]	7–11.5

The recommended weight gain during pregnancy depends on the pregravid BMI. More the BMI is high, more the recommended weight gain is low [6].

1.2 Fetal growth regulation

The fetal growth is controlled by maternal, placental and fetal factors, and it is inextricably linked to the placental growth. Among the factors that will control the growth, the fetal and placental energetic metabolism and the hormonal regulation by the fetoplacental unit are essential.

1.2.1 Prenatal nutrition and metabolism

As previously discussed, the maternal weight gain plays an important role and a positive correlation between the maternal weight gain and the fetal weight is observed (Fig. 2). The optimal fetal development depends mainly on a continuous intake of nutrients (glucose, amino acids, lipids, vitamins and micronutrients) and oxygen (O_2), brought by the maternal circulation, and on the capacity of the placenta and the fetus to use them [7]. Energy cost of pregnancy includes energy deposited in maternal and fetal tissues, and the increase in energy expenditure attributed to maintenance and physical activity. Hytten and Chamberlain developed a theoretical model to estimate the energy requirements during pregnancy for well-nourished women (Table 3). The theoretical cost of a pregnancy is estimated to 85’000 kcal.

The energy costs are shared between the protein deposition (5000 kcal), the fat deposition (35'000 kcal), the increase of the basal metabolism (35'000 kcal) and the additional needs (10'000 kcal) [4].

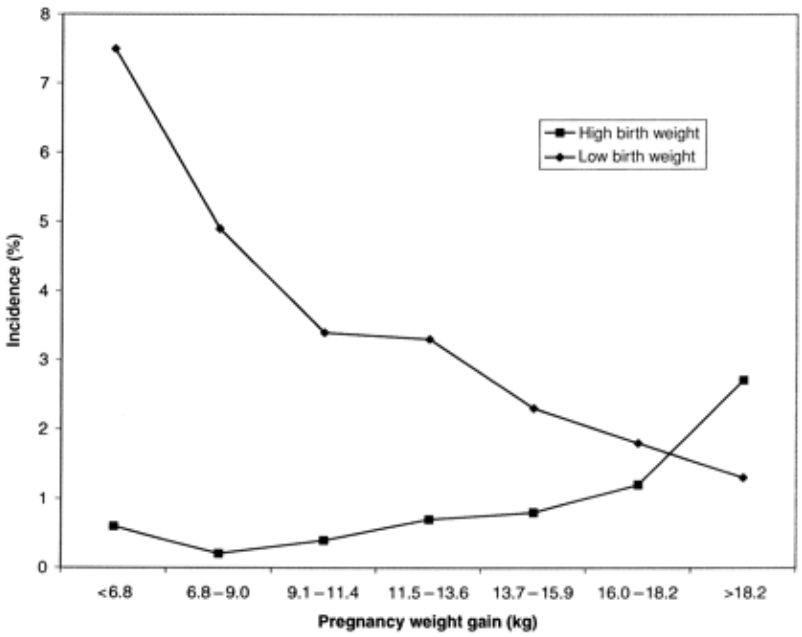

Figure 2: Incidence of low and high birth weight related to pregnancy weight gain.
More the maternal weight gain is low, more the incidence of LBW is high [6].

Table 3: Hytten and Chamberlain's theoretical model of cumulative energy cost of pregnancy.

Rates of tissue deposition	0–10 weeks*	10–20 weeks	20–30 weeks	30–40 weeks	Cumulative total (g)
Weight gain ($g day^{-1}$)**	12	48	64	57	12 500
Protein deposition ($g day^{-1}$)**	0.64	1.84	4.76	6.10	925
Fat deposition ($g day^{-1}$)**	5.85	24.80	21.85	3.30	3825
Factorial estimation of energy cost of pregnancy	**0–10 weeks***	**10–20 weeks**	**20–30 weeks**	**30–40 weeks**	**Cumulative total (kJ)**
Protein deposition ($kJ day^{-1}$)	15	43	112	143	21 698
Fat deposition ($kJ day^{-1}$)	233	986	869	131	152 001
Increment in basal metabolic rate ($kJ day^{-1}$)	187	414	620	951	149 440
Efficiency of energy utilisation ($kJ day^{-1}$)***	44	144	160	122	32 314
Total energy cost of pregnancy ($kJ day^{-1}$)	477	1586	1761	1347	355 460

*Interval (56 d) computed from last menstrual period.
**Total weight gain of 12.5 kg, protein deposition of 925 g, fat deposition 3.825 kg taken as 23.42 $kJ g^{-1}$ for protein and 39.75 $kJ g^{-1}$ for fat.
***Efficiency of energy utilisation taken as 0.90.

Energy cost of pregnancy includes energy deposited in maternal and fetal tissues, and the increase in energy expenditure attributed to maintenance and physical activity [8].

The glucose plays an important role in the fetal energetic intakes and the fetus is entirely dependent on the maternal intake. Indeed, the fetal production of glucose is almost non-

existent in human [9]. In physiological conditions, the fetal glycaemia being lower than the maternal glycaemia, the glucose transfer is done by facilitated diffusion through the placenta and follows the concentration gradient. The fetus oxidized glucose fraction represents 60% of the total captured glucose [10]. The remaining 40% are used for the fetal growth and the glycogen and triglyceride synthesis. The increase of intake causes a low increase of fetal metabolism. The excess is kept in reserves in the form of fat and glycogen [1].

The free fatty acids less contribute to the oxidant fetus metabolism. They are principally used to create lipidic and glucidic stocks. The placental transfer of the fatty acids is done by simple diffusion and by fatty acid binding protein (FABP), but the placenta is able to preferentially transfer some polyinsatured fatty acids to the fetus. Some fatty acids, such as linoleic acid or arachidonic acid, are not synthetized by mammals, therefore the placenta allows a preferential transfer of these fatty acids brought by the supply, approximately 1.5 to 3 times higher than for oleic acid [11].

The amino acids are brought to the fetus by an active transfer mechanism against a concentration gradient. They will contribute to the fetal protein synthesis and directly participate to the fetal growth. However, a part of amino acids transferred to the fetus will also be used as energetic substrate and will be oxidized [7].

The lactate constitutes also an important energetic substrate for the fetus. Indeed, the lactate production by the placenta leads to a fetoplacental lactate transfer equivalent to 50% of the glucose production [1].

1.2.2 Hormonal regulation

Maternal, fetal and placental growth factors play an important role in the gestation maintenance and the fetal growth modulation. Hormones have a sensor role of the oxygen and nutrient bioavailability. They can stimulate or inhibit the fetal growth by acting on the fetal metabolism. Hormones will control the fetal growth by regulation of the cell proliferation, apoptosis and differentiation in numerous fetal tissues [12].

Insulin is the main anabolic hormone of the fetus. It is synthetized by the pancreatic β-cells. Like all polypeptidic hormones, the insulin cannot cross the placental barrier. Thus, the fetal

insulinemia depends on the fetal insulin secretion. Insulin is an important growth hormone *in utero* across a range of species. Its deficiency causes growth retardation. In contrast, induction of fetal hyperinsulinemia has less consistent effects on intrauterine growth [12]. In contrast to tissue growth, tissue differentiation during late gestation appears to proceed normally in both hypo- and hyperinsulinemic fetuses [13]. Insulin stimulates fetal growth, in part, by its anabolic effects on glucose and amino acid metabolism [12].

Insulin will activate the insulin-like growth factor (IGF) and indirectly allows the fetal growth. In addition to IGF 1 and 2, there are numerous other growth factors that locally act of paracrine or autocrine manner, like epidermal growth factor (EGF), fibroblast growth factor (FGF) and platelet-derived growth factor (PDGF). Generally, the growth stimulatory hormones act as signals of nutrient plenty and rise in concentration in the fetus with increase in the availability of glucose, amino acids and oxygen [14].

The main growth inhibitory hormones *in utero* appear to be the glucocorticoids, although other hyperglycemic hormones, such as glucagon and catecholamines, have been shown to influence fetal metabolism and the biochemical composition of specific fetal tissues [15]. These hormones act as signals of nutrient insufficiency and rise in concentration in response to fetal hypoxemia and hypoglycemia [12]. Administration of glucocorticoids to either the mother or the fetus during late gestation leads to fetal growth retardation in several species including humans. The degree of fetal growth retardation depends on the dose and type of glucocorticoid used, the frequency and route of its administration and on the fetal sex and gestational age [15]. At the cellular level, glucocorticoids alter receptors, enzymes, ion channels and transporters and also change expression of various growth factors, cytoskeletal proteins, myelination, binding proteins, clotting factors, gap and tight junction proteins and of various components in intracellular signaling pathways involved in growth [12, 13, 16, 17]. Therefore, glucocorticoids act to switch the cell cycle from tissue accretion to tissue differentiation in preparation for delivery. However, if this switch occurs prematurely due to stress-induced glucocorticoid overexposure, the normal pattern of intrauterine growth will be altered and inappropriate tissue development can occur for the stage of gestation with long-term consequences for tissue function much later in life [18].

1.3 Impaired fetal growth and fetal programming

During the pregnancy, the fetus, following a fast growth, is very sensitive to food intake modifications. A decrease of intakes or a lower capacity of the fetoplacental unit to bring oxygen and nutrients to the fetus can induce an IUGR. An intrauterine environment modification will be perceived by the fetus, which will try to adapt to it. This adaptation goes through a key process called "fetal programming". This re-programming will allow to optimize the fetal development and maturation taking into account of adverse intrauterine conditions.

1.3.1 The Barker's hypothesis

The concept of "fetal programming" is born in the 1980's with the work of Pr. David Barker. With his colleagues, they observed that the rate of mortality due to coronary heart disease in adulthood was tightly correlated to the birth weight. Indeed, adults born with a low birth weight (LBW) (less than 2500 grams) had a significantly higher risk to dye following a coronary heart disease than those born with a normal weight. Pr. Barker therefore hypothesized than children born with a LBW were exposed to a higher risk to develop cardiovascular diseases in adulthood [19, 20]. Since, other epidemiological studies had confirmed the Barker's hypothesis and showed that the impairment of fetal growth improves the risk to develop a wide range of chronic diseases in adulthood (coronary heart disease, hypertension, type 2 diabetes, obesity, hypertension). Such observations led to the concept of the Developmental Origins of Health and Disease (DOHaD) [21-23].

1.3.2 Fetal programming

Adverse conditions during early life that alter growth and development have long-term consequences on the cardiovascular health of an individual across their lifespan. Impaired growth during fetal life also impacts the cardiovascular health of the next generation [24] implicating epigenetic processes [25] in the etiology of diseases having their origins during fetal life and early development. Epigenetic processes involve heritable changes in gene function and expression that occur in the absence of changes in the DNA sequence [26]. These processes include alterations in the methylation pattern of the DNA, modifications of the histones or

changes in small non-coding RNAs. In a general manner, the methylation promotes genes inactivation, while the demethylation causes their activation. The histones modification regulates the DNA packaging, which promotes or limits the access to the genes [23, 27, 28]. The epigenetic modifications are induced by the environment (alimentation, smoking, stress) and cause changes in gene expression in the fetus allowing to adapt to an adverse intrauterine environment. It is the hypothesis of the "thrifty phenotype" [29]. However, these modifications can be inappropriate if they do not correspond to the extrauterine conditions and then predispose the neonate to develop different diseases in adulthood. For example, an intrauterine environment with poor nutritive intakes supposes that the nutrient availability in the postnatal environment will be also limited. However, in developed countries, the extrauterine environment is rich in nutrients, so the fetus will be not adapted and thus predisposed to develop obesity and cardiometabolic diseases (Fig. 3).

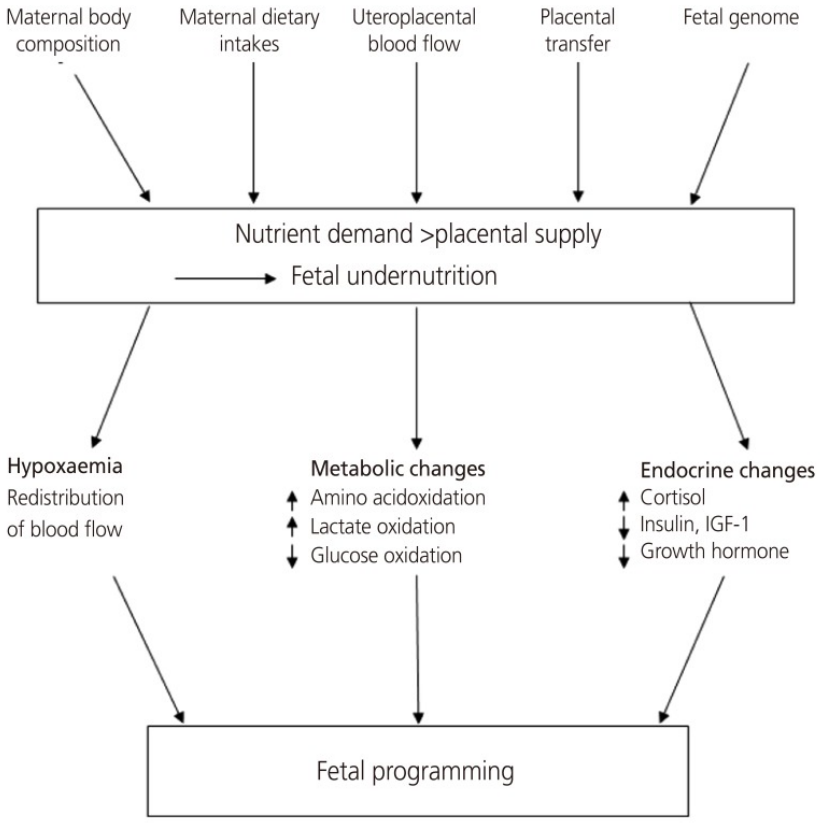

Figure 3: Fetal adaptations to undernutrition.
Numerous factors can lead to an adaptive process to maintain *in utero* immediate survival of the fetus which can have adverse consequences in adulthood [30].

Therefore, an adaptive process to maintain *in utero* immediate survival of the fetus can have adverse consequences in adulthood when there is a difference between the intra- and extrauterine environment. Epidemiological studies of people born during the Dutch Famine in Winter 1944-1945 allowed to highlight the importance of an appropriate nutrition during pregnancy, but also the impact of the exposure window to an undernutrition on the fetal programming. Birth records from the Dutch Famine Birth cohort indicate that exposure to famine during late gestation is associated with a reduction in birth weight, whereas early gestational exposure is associated with increased prevalence of coronary heart disease [31, 32].

2. Fetoplacental circulation

2.1 Fetoplacental circulation components

The fetoplacental circulation links the maternal and fetal circulations during pregnancy, ensuring adequate gas and nutrients exchange and consequently fetal growth. The hemodynamic properties of the fetoplacental circulation change throughout pregnancy as the placenta develops and in turn adapts the uterine circulation.

2.1.1 Placenta

The placenta is formed from the zygote at the start of each pregnancy and thus have the same genetic composition as the fetus. It is a roughly discoid organ, which, at term, measures approximately 22 cm in diameter, 2.5 cm thick at the center and weighs 500 g. Its surfaces are the chorionic plate that faces the fetus and to which the umbilical cord is attached and the basal plate that is adjoined to the maternal endometrium. Between these plates, there is a cavity called intervillous space, into which there are the chorionic villi, attached to the deep surface of the chorionic plate. Each villus, surrounded by the syncytiotrophoblast, represents an independent maternal–fetal exchange unit (Fig. 4) [33].

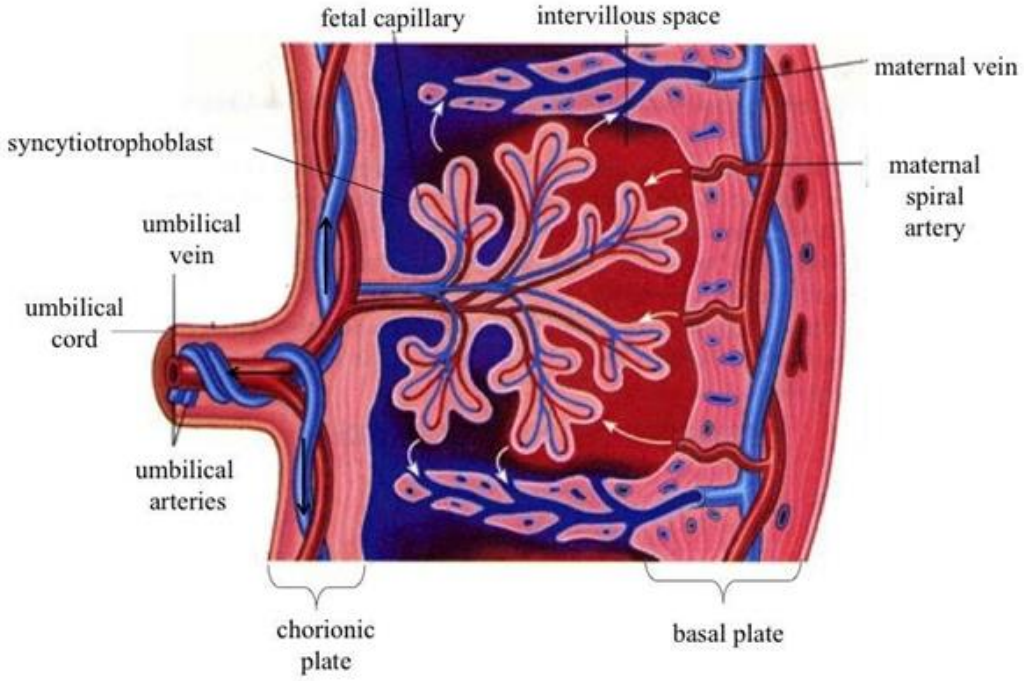

Figure 4: Placental structure and circulation.
Maternal blood enters the intervillous space via the spiral arteries. Nutrients and gases are transported across the syncytiotrophoblast surrounding the chorionic villi and enter the fetal circulation. Oxygenated blood reaches the fetus through the UV and deoxygenated blood is carried back to the placenta via the UAs [34].

Circulation of fetal and maternal blood in the placenta occurs in two separate compartments (fetoplacental and uteroplacental) and there is no mixing of maternal and fetal blood [35]. The syncytiotrophoblast is considered as the functional part of the placental barrier. Three main processes mediate the transplacental passage of nutrients, hormones, waste products and drugs across the intact placental membranes: passive diffusion, carrier-mediated transport and transcytosis [36].

2.1.2 Umbilical cord

The umbilical cord starts its formation since the 5th gestational week and has a progressive growth until the 28th gestational week. At the term of pregnancy, it measures approximately 50 to 60 cm long. It contains two umbilical arteries (UAs) that spiral around a unique umbilical vein (UV), surrounded by Wharton's jelly and, finally, by amniotic epithelial membrane (Fig. 5) [37].

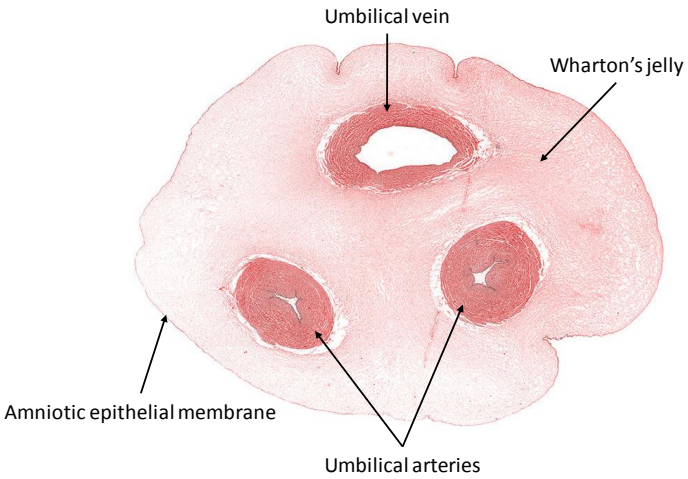

Figure 5: Umbilical cord structure.
Umbilical cord is composed of two UAs and one UV surrounded by Wharton's jelly and an amniotic epithelial membrane (Adapted from [38]).

The umbilical cord diameter and area increase as a function of gestational age. The progressive increase in the umbilical cord diameter and area up to the 32th gestational week followed by a reduction of umbilical cord thickness can be explained by the reduction of the water content of Wharton's jelly near the end of the pregnancy (Fig. 6) [39].

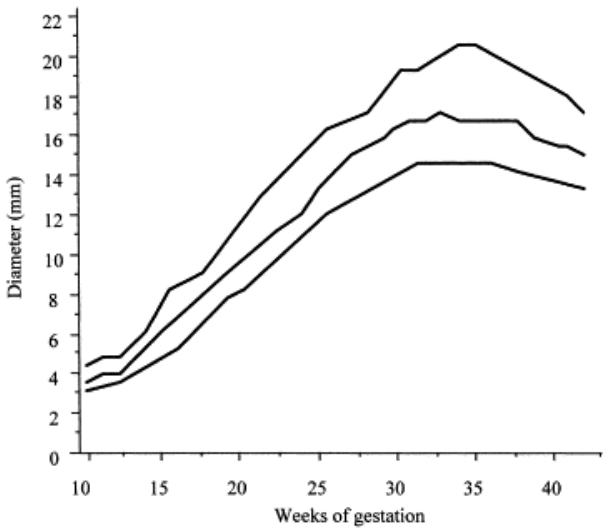

Figure 6: Umbilical cord diameter according to gestational age.
The lines represent, from bottom to top, the 10th, 50th and 90th percentiles [37].

The diameter of the UAs increases from 1.2 ± 0.4 mm at 16 gestational weeks to 4.2 ± 0.4 mm at term gestation and the UV diameter varies from 2 ± 0.6 mm at 16 weeks of gestation to 8.2 ± 0.8 mm at term [37].

From the 3rd gestational week, the arterial and venous systems within the embryo are developing. The arterial system is initially established as the paired dorsal aortae from which the aortic arches originate, while the primitive venous system is initially made up of the umbilical, vitelline and cardinal systems. During the 4th gestational week, two UAs branch from the paired dorsal aortae to become connected to the vascular network of the umbilical cord [40] and during the 5th week, this connection is obliterated [40-42]. The UVs are originally also bilateral and drain into the right and left sinus horns of the sinus venosus. The connections regress in the second month of pregnancy with complete regression of the right UV as the left UV persists and forms its connection to the ductus venosus within the developing liver [41, 42]. With the initiation of fetal heart pumping around the 4th gestational week, the UV carries oxygenated blood from the placenta to the fetus and the UAs carry deoxygenated blood with waste products from the fetus to the placenta (Fig. 7) [42].

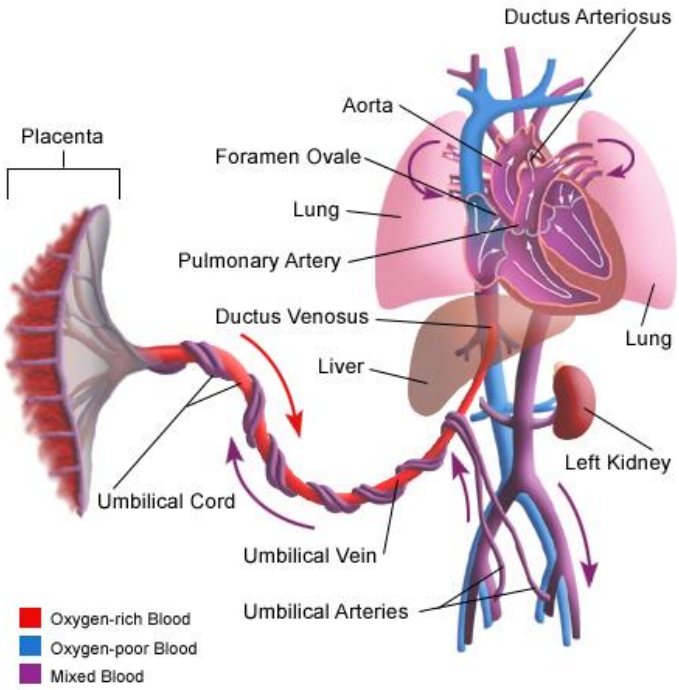

Figure 7: Fetoplacental circulation anatomy.
UV brings oxygenated blood from the placenta to the fetus and UAs carry deoxygenated blood and metabolic wastes from the fetus to the placenta [43].

The Wharton's jelly plays an important protective role for the umbilical vessels. It is constituted of a spongy network of interlacing collagen fibers in which the vessels are anchored by

numerous thick collagen bundles [44]. Furthermore, several studies have speculated that the Wharton's jelly plays a metabolic role in maintaining the normal function of the umbilical cord vessels. Takechi *et al.* demonstrated that some cells, similar to myofibroblasts and normally present in the Wharton's jelly, can function in both fibrogenesis and cell contraction, and may participate in the regulation of umbilical blood flow [45].

At birth, the umbilical cord is coiled, the coiling degree resulting of the fetal activity. Inside, umbilical vessels also undergo a coiling movement. Traditionally, the coiling has been considered a feature of the umbilical cord that protects it from compressive forces during labor [46].

The umbilical cord insertion site to the placenta can be central, eccentric, marginal or velamentous. Central and eccentric insertions account for more than 90% of term placentas. Marginal cord insertion (MCI) and velamentous cord insertion (VCI) are classed as abnormal placental cord insertions. In MCI, the cord inserts at the side of the placenta, but still comes directly from the placental mass. In VCI, the umbilical vessels insert into the membranes, thus the vessels cross between the amnion and the chorion before reaching the placenta (Fig. 8). VCI occurs in approximately 1% of singleton pregnancies and MCI in approximately 7% [47, 48].

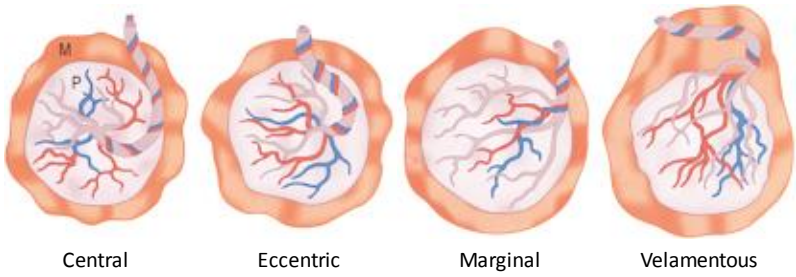

Figure 8: Different umbilical cord insertions in the placenta.
Central and eccentric insertions are considered as normal, while marginal and velamentous insertions are abnormal and can be responsible of pregnancy complications [49].

2.2 Fetoplacental circulation regulation

The fetoplacental circulation differs from systemic vascular beds. Indeed, it is not innervated [50], it is a low-resistance-high-flow circulation [51] and it contains deoxygenated arterial blood

relative to that present in the venous arm [52]. The placenta lacking neuronal innervation suggests that local physical (oxygenation, flow rate), paracrine (endothelial cell-derived nitric oxide) and circulating (angiotensin II) factors contribute to blood flow regulation in small fetoplacental vessels [53].

2.2.1 Nitric oxide and vascular relaxation

Nitric oxide (NO) is one of the critical components of the vasculature, regulating key signaling pathways. In macrovessels, NO acts to suppress cell inflammation as well as cell adhesion. In this way, it inhibits thrombosis and promotes blood flow. It also allows to limit vessel constriction and vascular wall remodeling. In microvessels, and particularly capillaries, NO, along with growth factors, is important in promoting angiogenesis [54].

Nitric oxide synthase (NOS) enzymes catalyze the nicotinamide adenine dinucleotide phosphate (NADPH) and tetrahydrobiopterin (BH_4)-dependent oxidation of L-arginine to L-citrulline to produce NO [55]. Intracellular L-arginine availability is a rate-limiting factor in cellular NO production; argininosuccinate lyase that converts L-citrulline back to L-arginine is important to synthesize not only intracellular L-arginine, but also to use extracellular L-arginine for NOS-dependent NO synthesis [56].

There are three mammalian NOS isoforms: neuronal (nNOS), endothelial (eNOS) and inducible (iNOS). In endothelial cells, eNOS catalyzes the oxidation of L-arginine to NO and L-citrulline, with the assistance of BH_4, oxygen and NADPH as cofactors [57]. Increased intracellular calcium (Ca^{2+}) in response to stressors displaces the inhibitor caveolin from calmodulin (CaM), thus activating eNOS. The eNOS dimerization [58], its phosphorylation at the serine residue 1177 [59] and the dephosphorylation of threonin 495 [60] also play a critical role in eNOS activation. NO diffuses to vascular smooth muscle cell and causes relaxation by activating soluble guanylyl cyclase (sGC), that increases intracellular cyclic guanosine monophosphate (cGMP) concentration (Fig. 9) [61].

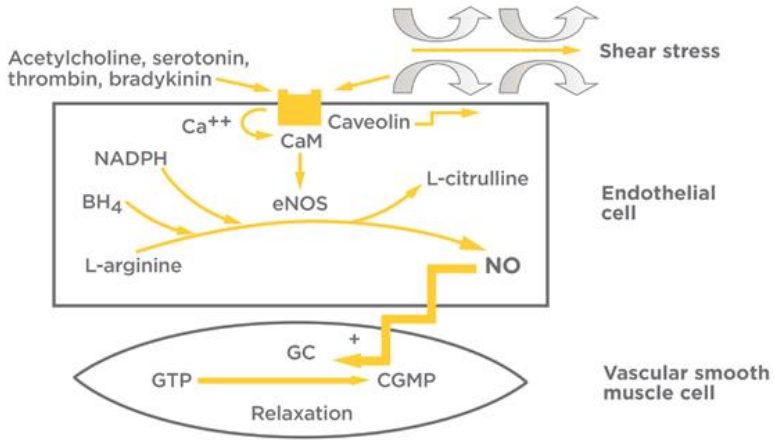

Figure 9: NO-derived relaxation pathway.
NO is a key element in the way of vascular relaxation. Produced in the endothelium, it moves in the smooth muscle to activate an enzymatic cascade [62].

The increase in cGMP mediates, among others, the activation of the cGMP-dependent protein kinase or protein kinase G (PKG), which phosphorylates a number of biologically important targets and is implicated in the regulation of smooth muscle relaxation, platelet disaggregation, gastrointestinal motility, blood flow, neuronal plasticity, erectile function, lower urinary tract functions, endothelial permeability and cardiac protection [63-68]. NO as the "first messenger" in the NO/cGMP/PKG signaling pathway initiates a cascade of phosphorylation reactions in which the magnitude of each step is enzymatically amplified, a process that is critical for the resulting physiological effects [69].

2.2.2 Impaired regulation of fetoplacental circulation

Alterations in the fetoplacental circulation can be identified using the ultrasound (US) Doppler technique. In case of an abnormal development of the fetoplacental vascular anatomy leading to a reduction in the placental surface area for maternal–fetal gas exchange, clinical manifestations occur via increased pulsatility in UA Doppler waveforms. These changes in Doppler velocimetry may precede acute fetal deterioration by up to seven days [70, 71]. Uterine artery Doppler can also identify placental insufficiency due to the most frequent pathology, namely maternal vascular malperfusion of the placenta [72]. In the umbilical cord, NO plays an important role in the regulation of the fetoplacental blood flow. Thus, an alteration in the NO/cGMP pathway can have consequences on the fetus development.

NO-derived relaxation and intrauterine growth restriction

The bioavailability of NO produced by eNOS can be affected at multiple levels, including eNOS mRNA or protein expression, availability of its substrate L-arginine, availability of its cofactors, interactions with proteins like caveolin and heat shock protein 90 (Hsp90), posttranslational modifications, and reaction of NO with superoxide (O_2^-) anion to produce peroxynitrite [73].

As an essential cofactor, BH_4 is necessary for optimal eNOS activity. Thus, when BH_4 levels are inadequate, due to enhanced oxidation, eNOS becomes unstable and uncoupled, leading to less NO production and more O_2^- generation resulting in endothelial dysfunction. Moreover, the interaction between NO and O_2^- leads to the formation of peroxynitrite, a potent oxidant, which further oxidizes BH_4 [74, 75]. In addition, endogenous asymmetric dimethylarginine (ADMA), a derivative of L-arginine, can act to competitively inhibit eNOS (Fig. 10) [76, 77]. It is also possible that a decreased intracellular L-arginine content caused by arginase may lead to eNOS uncoupling. The expression of arginase in endothelial cells can compete with eNOS for their common substrate and downregulate eNOS activity [78, 79].

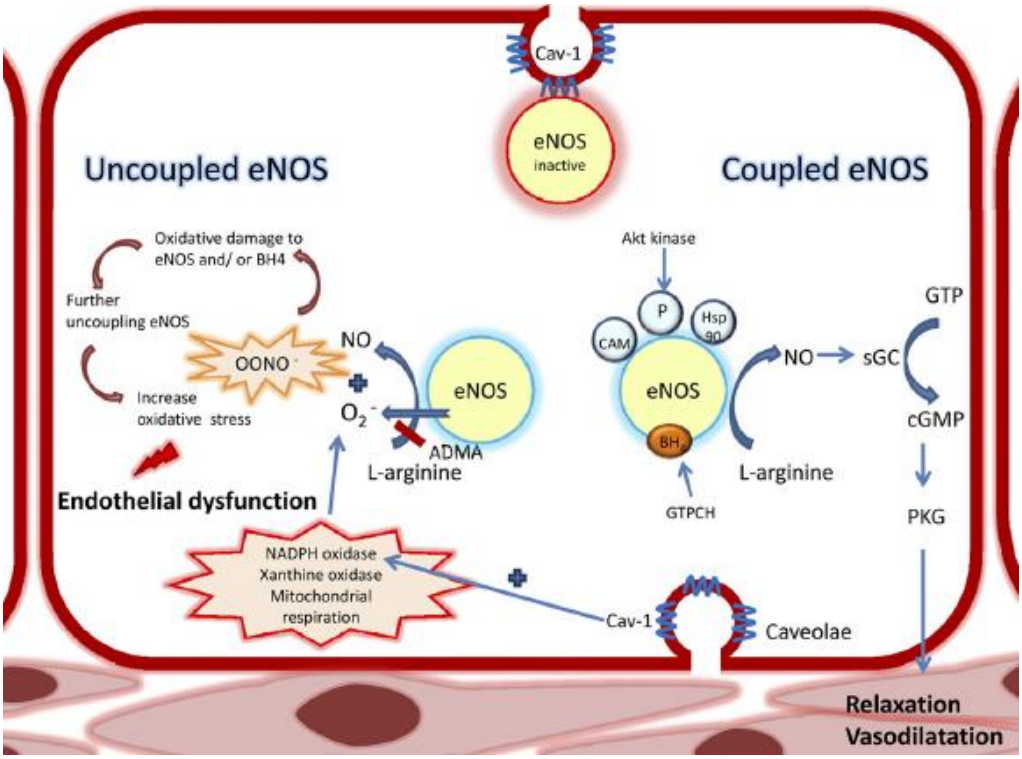

Figure 10: Central role of eNOS uncoupling in the pathogenesis of endothelial dysfunction.
When eNOS is uncoupled, it produces O_2^- in place to NO, leading to the formation of peroxynitrite, thus increasing the oxidative stress [77].

Many studies had shown that preterm infants and pregnant women could present with L-arginine deficiency [80, 81], and that impaired arginine transport into endothelial cells was observed in the umbilical endothelium from IUGR infants [82]. One meta-analysis concluded that L-arginine supplementation is superior to placebo in increasing birth weight and prolonging gestational age at labor of IUGR fetuses [83].

In the smooth muscle cell (SMC), cGMP level is primarily determined by the balance between activities of the guanylyl cyclases and cyclic nucleotide phosphodiesterases (PDEs) that break down cGMP. An imbalance in this equilibrium can decrease the concentration of cGMP, reducing the PKG activation and the vascular relaxation [69]. Peyter *et al.* have demonstrated that *ex vivo* NO-induced relaxation, directly stimulated by administration of exogenous NO, was significantly decreased in UV of growth-restricted females, supposing an alteration in the muscular part of the NO/cGMP signaling pathway, while, in contrast, growth-restricted males seemed to have an impaired vasoconstriction [84]. Though gender differences are often observed in the field of DOHaD [85], the observed sexual dimorphism remains to be elucidated. These differences in vascular reactivity were probably due to differential expression and/or regulation of molecular components of the NO/cGMP signaling pathway, as well as in vasoconstrictive mechanisms [84]. Some studies have shown a positive effect of Sildenafil citrate, a phosphodiesterase inhibitor (PDE5-selective inhibitor), versus placebo, with improvement in umbilical and middle cerebral arteries Doppler velocimetries. Indeed, PDE inhibitors act by blocking the enzymes that break down cGMP, which mediates the effects of NO in the body and leads to vascular relaxation [83]. However, other studies showed controversial effects, with no reduction in risk of perinatal death or major neonatal morbidity. In particular, the Sildenafil Therapy in Dismal Prognosis Early Onset Fetal Growth Restriction (STRIDER) consortium was designed to study a potential improvement of placental circulation by sildenafil through its effects on the uteroplacental circulation. However, the Dutch STRIDER trial suggested that sildenafil may increase the risk of neonatal pulmonary hypertension, because an increase of cases was observed in the Sildenafil study group [86].

3. Low birth weight and intrauterine growth restriction

3.1 Definition and epidemiology

The birth weight is determined by two processes, the time of the pregnancy and the rate of fetal growth. A LBW is defined by the World Health Organization (WHO) as a weight at birth below to 2500 grams. It can therefore be due to a short gestation time, an IUGR or a combination of both [87]. IUGR occurs when the fetus does not reach its full intrauterine potential for growth and development [88]. The incidence of IUGR varies among countries, populations and races [89]. Approximately, IUGR concerns 5 to 10% of pregnancies in developed countries and corresponds to 30 million newborns per year worldwide [90]. Fetuses with IUGR present a greater risk of perinatal morbidity and mortality and long-term health defects [88].

Four biometric measures are commonly used for IUGR assessment: biparietal diameter, head circumference, abdominal circumference and femur length. The biometric measurements are then combined to generate an estimated fetal weight [91]. IUGR is generally diagnosed with a statistical deviation from fetal weight reported to gestational age in the population of reference, with percentile limits of 10, 5, or 3 (Fig. 11). However, these limits also include fetuses that are small for gestational age (SGA). In contrast to IUGR, which presents an abnormal growth curve with a "growth curve break" due to an abnormal growth deceleration, SGA includes healthy but constitutionally small fetuses, with limited but harmonious fetal growth, that have a lower risk of abnormal perinatal outcomes. Even if the WHO defines IUGR as an estimated fetal weight below the 3th percentile [88], the American College of Obstetrics and Gynecology (ACOG) defines IUGR as an estimated fetal weight below the 10th percentile for gestational age. This is the most commonly used classification [92].

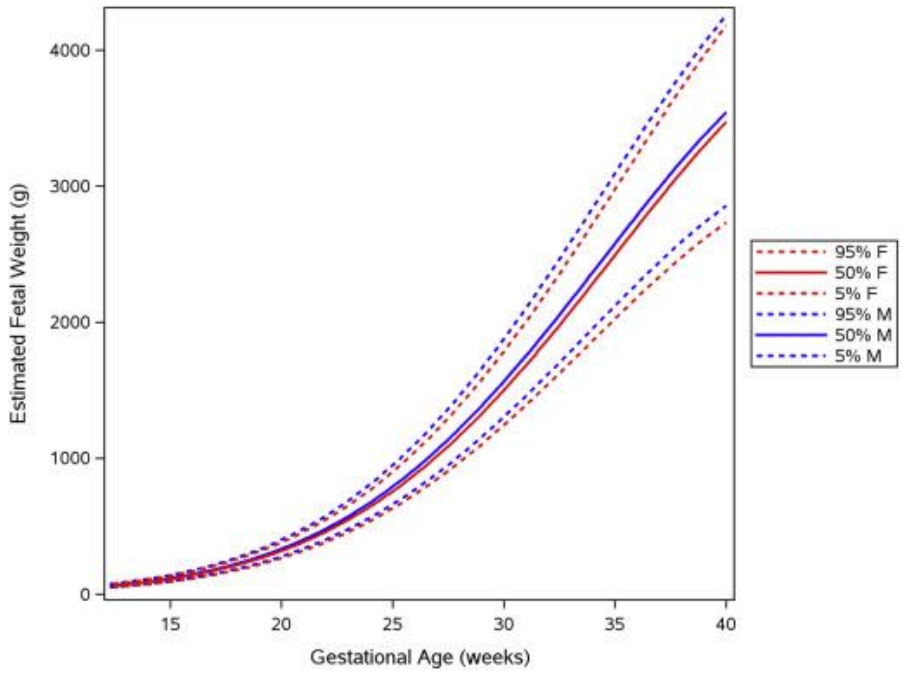

Figure 11: WHO sex-specific growth percentiles for estimated fetal weight.
This graph, representing the range of adequate estimated fetal weight in function of gestational age, is used to classify fetuses and neonates [93].

They exist mainly two types of IUGR based on the anthropometric measurements: asymmetrical (type 1) and symmetrical (type 2) IUGR. The asymmetric type of IUGR develops when oxygen or nutrient supply to the fetus is reduced during the last trimester of pregnancy due to a decreased functional capacity of the placenta. These babies normally only have a slightly reduced length, a significantly reduced weight and therefore a reduced ponderal index. This type of retardation has a clinical interest with increasing substrate demands during the last trimester [94]. It can induce severe damage and even finally stillbirth. This is the most frequent type of growth retardation. As the growth potential of the fetus is normal, the term "hypotrophic" IUGR is used. Postnatal catch-up growth is frequently observed. The symmetrical or hypoplastic IUGR is present in early pregnancy and due to intrinsic causes. In contrast to hypotrophic IUGR, the postnatal catch-up growth is rare in this group of patients [95].

3.2 Etiology of intrauterine growth restriction

The etiologies of IUGR generally can be divided into fetal, placental and maternal factors. Fetal factors include genetic conditions and congenital anomalies, whereas placental factors involve

abnormally implanted or formed placentas. Maternal factors include infection, malnutrition, impaired uterine perfusion of the placenta, drug use and various medical conditions [96].

3.2.1 Fetal causes

Fetal causes of IUGR include fetal chromosomal abnormalities, genetic syndromes, congenital anomalies or infections, metabolic disorders, and multiple gestations.

Chromosomal abnormalities

Fetal chromosomal abnormalities concern 7 to 19% of total IUGR infants born. The most common chromosomal anomalies are trisomies 13 (Patau syndrome), 18 (Edwards syndrome) and 21 (Down syndrome) [97].

Genetic syndromes

Genetic syndromes known to cause IUGR include Bloom syndrome, Russell-Silver syndrome, Cornelia-de-Lange syndrome, Mulibrey Nanism syndrome, Rubenstein-Taybi syndrome, Fanconi syndrome, Dubowitz syndrome, Seckel syndrome, Johanson-Blizzard syndrome, Roberts syndrome and De Sanctis-Cacchione syndrome [98].

Congenital anomalies

Congenital anomalies, which are known to result in 1 to 2% of IUGR fetuses, includes tracheo-esophageal fistula, congenital heart disease [99], congenital diaphragmatic hernia [100], abdominal wall defects, such as omphalocele and gastrochisis, neural tube defect like anencephaly and anorectal malformation.

Congenital infections

Congenital infection concerns around 5% of the total IUGR cases. In developed countries, the common infections include toxoplasmosis and cytomegalovirus. In the developing countries, the common causes are malaria, congenital HIV infection, syphilis and rubella [89].

Metabolic disorders

Metabolic disorders which have been reported to result in IUGR include agenesis of pancreas, congenital absence of Langerhans islets, congenital lipodystrophy, galactosemia, gangliosidosis type I, hypophosphatasia, inclusion-cell disease, Leprechaunism, fetal phenylketonuria and transient neonatal diabetes mellitus [101].

Multiple gestations

Finally, multiple gestations are also reported to be associated with about 3% of IUGR cases. Indeed, twin fetuses grow normally till 28 weeks of gestation and then physiologically decrease their growth rate [102].

3.2.2 Placental causes

Interactions between maternal and fetal circulations in the placenta are fundamental for adequate exchanges of nutrients and oxygen. Therefore, every difference between placental supply and fetal nutritional or respiratory demands results in impaired fetal growth. Heinonen *et al.* conducted a study to evaluate an association between placental weight and birth weight in appropriate for gestational age (AGA) and SGA infants and reported that placenta of SGA infants was 24% smaller than that of AGA newborns. These results were also confirmed by Peyter *et al.* with a reduction of approximately 27% in placental weight of growth-restricted compared to AGA neonates [84]. Placental actual weight was also lower in SGA infants than in AGA neonates of the same birth weight [103].

Placental causes of IUGR include a wide range of pathologies such as abnormal placental and umbilical insertions, impaired placental circulation and different placental affections.

Placental disorders and umbilical cord abnormalities

In the IUGR placenta, there is a decrease in number and surface area of terminal villi, representing a malfunction of vascularization. Doppler velocimetry investigations of umbilical vessels and uterine arteries have shown an increased vascular resistance in these vessels in IUGR fetuses and this occurs secondary to inadequate trophoblast invasion of the spiral arteries

[104]. Furthermore, an altered circulation is also observed in the presence of single umbilical artery or true knot [105].

Velamentous cord insertion (*placenta praevia*), placental abruption and placental infarct result in decreased transfer of nutrients to the fetus leading to IUGR [105].

Placental affections

Placental infection like placental malaria is a major cause of fetal growth restriction. Indeed, the complement system is a central component of innate host defense and is activated in malaria-infected individuals [106]. Complement C5a and C5a receptor levels are increased with PM. C5a having shown to influence angiogenesis [107], its increase leads to a placental vascular insufficiency because of dysregulated angiogenic factors that are required for placental vascular remodeling during fetal growth [108].

Confined placental mosaicism (CPM) refers to chromosomal mosaicism (usually involving a trisomy) found in the placenta, but not in the fetus. Wilkins-Haug *et al.* reported that CPM occurred significantly more in placentas of IUGR infants compared to AGA newborns. These abnormal placentas presented greater decidual vasculopathy, infarction and intervillous thrombus formation [109].

Chronic villitis of unknown etiology (CVUE) is characterized by focal areas of inflammation with mononuclear cells and areas of fibrinoid necrosis in chorionic villi. CVUE is detected in 7 to 33% of placentas, mainly with IUGR, unexplained prematurity, pre-eclampsia, perinatal asphyxia and intrauterine fetal death.

Szentpéteri *et al.* observed that the placental endoglin gene was significantly overexpressed in the IUGR group, associated with a significant higher placental endoglin protein level. Hence, they concluded that increased placental gene expression of endoglin results in vascular dysfunction leading to chronic fetal hypoxia [110].

3.2.3 Maternal causes

A wide range of maternal behaviors and diseases can be responsible of impaired fetal growth and LBW.

Maternal physiology

Extremes of maternal age (less than 16 years and more than 35 years) have been found to be risk factors for IUGR [111].

The maternal height is slightly correlated to birth weight. A study showed that tall women had bigger infants than shorter women [112]. Furthermore, a woman born with a LBW has a higher risk to give birth to a LBW infant [113].

Maternal diseases

Various maternal diseases have an effect on blood circulation resulting in a decrease in uteroplacental blood flow and leading to IUGR. These various diseases include hypertensive disorders (gestational and non-gestational), insulin-dependent diabetes mellitus associated with vasculopathy, congenital cyanotic heart disease, restrictive pneumopathies, chronic renal disease, autoimmune diseases (collagenoses, systemic lupus erythematosus, antiphospholipid syndrome), hereditary or acquired thrombophilia, hyperhomocysteinemia, sickle cell disease and severe anemia [88, 98]. There is also a strong association between pre-eclampsia and IUGR due to deficient trophoblast invasion [114].

Preconceptional health and pregnancy diet

Numerous nutritive elements play a crucial role in the fetus development. Already the preconceptional diet can have an effect on future fetal growth [115]. Studies demonstrated that delivering a SGA infant is more common in women who consume a diet consisting mainly of red and processed meat and high fat dairy [116], whereas a Mediterranean diet reduces the risk [115].

Furthermore, the maternal weight gain during the pregnancy is a well predictive element for fetal health. Indeed, there is an increased risk of delivering LBW infants in preconceptional underweight women [117]. Increased weight gain during pregnancy in underweight women reduces the risk of IUGR [118]. On the other hand, a preconceptional high BMI is also a risk factor for IUGR, as it is associated with diabetes, hypertension or hypercholesterolemia, which can affect fetal growth. Large population studies showed an association between maternal obesity and IUGR [119, 120].

Finally, even if the preconception BMI is normal, a poor weight gain during pregnancy is associated with a higher rate of IUGR [121].

Tobacco, alcohol and drug exposures

Environmental nicotine exposure may be associated with lower birth weight and smoking reduces birth weight by approximately 150 to 200 g [122]. Smoking brings higher levels of carbon monoxide in maternal blood, which are 15% higher in fetal blood, leading to secondary fetal tissue hypoxemia [123]. Moreover, nicotine alone causes adverse vasoconstrictive effects in blood circulation [89]. Different studies showed that passive smoking also results in IUGR [124, 125].

A heavy maternal drinking is associated with fetal alcohol syndrome, but already a moderate alcohol consumption may be associated with IUGR [126, 127].

Maternal intake of illicit drugs like marijuana, cocaine or amphetamine during pregnancy is associated with impaired fetal growth, increasing the risk of SGA and LBW [128, 129].

Various medications, such as warfarin, steroids, anticonvulsants, antineoplastic agents, anti-metabolites and folic acid antagonists result in IUGR [130].

Maternal infections

Maternal infections and parasite infestations, such as hepatitis C, HIV, TORCH (Toxoplasma, Other agents, Rubella, Cytomegalovirus and Herpes simplex infections leading to similar symptoms called TORCH syndrome), malaria, tuberculosis, urinary tract infections and bacterial vaginosis are implicated in IUGR [131-133].

Maternal stress and depression

Numerous studies reported consistent associations between maternal antenatal depression and anxiety, and birth size and postnatal growth rates [134]. Maternal anxiety is significantly associated with an increased risk of LBW [135], while a prenatal depression increased risk for preterm birth, LBW and IUGR [136].

Frequency of pregnancies

IUGR is associated with a short or very long inter-pregnancy interval. Zhu *et al.* showed that when compared to infants conceived 18 to 23 months after a birth, infants conceived less than six months after a birth had higher risks of LBW, preterm birth and SGA. Similarly, the infants conceived 120 months or more after a birth had higher risks of these three adverse outcomes [137].

Assisted reproductive technologies

The use of assisted reproductive technologies (ART) is a risk factor for IUGR both independently in singleton pregnancies and also as a result of multiple gestation pregnancies [138].

High altitude residence

Women living at high altitudes have compromised placental blood flow because of reduced blood volume and also have reduced oxygen carrying capacity leading to IUGR [139].

3.2.4 Genetic causes

In addition to previous causes, polymorphisms in maternal, placental and fetal genes encoding for proteins and hormones have also been shown to affect fetal growth [89].

3.3 Diagnosis of intrauterine growth restriction

Standard diagnostic tools include a detailed maternal and familial history for risk factors for IUGR, a maternal physical examination including maternal preconceptional weight and height, nutritional status, fundal height, fetal palpation, cardiotocography (CTG) and US with Doppler echography. The initial element for IUGR diagnosis includes exact gestational dating and fetal weight estimation. Appropriate gestational age should be calculated with both last menstrual period and crown-rump length in the first trimester. Then, the fetal weight can be estimated using biometric measures (biparietal diameter, head circumference, abdominal circumference and femur length) in the second trimester [140].

Identifying SGA and IUGR babies in the antenatal period is a major challenge in obstetrics with up to 80% not detected before birth [141]. In most studies, IUGR is conflated with SGA during this period, and yet there is a fundamental distinction between a birth weight that is SGA and an infant with growth restriction [142, 143]. SGA infants are small but healthy and may be subjected to unnecessary interventions. In addition, growth-restricted infants who have a birth weight above the 10th percentile may be falsely classified as normally grown [144].

A recent consensus definition of IUGR was proposed to help the identification of newborn infants at risk for poor outcome, facilitate future research, aid in the verification of antenatal diagnoses of IUGR and facilitate the comparison of different cohorts. This consensus was established by a Delphi survey conducted among experts in the field of neonatal growth. The resulting consensus definition states that growth restriction in the newborn is characterized by a birth weight less than the 3th percentile on population-based or customized growth charts or by at least 3 out of 5 of the following points: birth weight below the 10th percentile on population-based or customized growth charts, head circumference below the 10th percentile, length below the 10th percentile, prenatal diagnosis of fetal growth restriction, maternal pregnancy information (hypertension or pre-eclampsia) [145].

3.4 Consequences of intrauterine growth restriction

3.4.1 Short-term effects

The IUGR is an important cause of perinatal mortality and morbidity. The acute neonatal consequences of IUGR include metabolic and hematological disturbances and disrupted thermoregulation. Severely affected IUGR infants, deprived of oxygen and nutrients, may have difficult cardiopulmonary transition with perinatal asphyxia, meconium aspiration or persistent pulmonary hypertension of the newborn (PPHN). Immediate neonatal complications include hypothermia, hypoglycemia, hyperglycemia, hypocalcemia, polycythemia, jaundice, feeding difficulties, feed intolerance, necrotizing enterocolitis (NEC), late onset sepsis, pulmonary hemorrhage and retinopathy of prematurity (ROP) [146, 147].

3.4.2 Long-term effects

IUGR infants are at risk for impaired growth and neurodevelopment and are prone to develop adult onset disease in their infancy.

Long-term physical growth

There are many postnatal factors determining the postnatal growth of an IUGR baby, such as the cause of the growth retardation, the postnatal nutritional intake, the economic status of parents and the surrounding social environment. IUGR infants with a symmetrical IUGR have a poor postnatal growth and remain small throughout life. In comparison, asymmetrical IUGR has better prognosis and such infants have a good postnatal growth, depending upon optimal environment and adequate postnatal caloric intake provided to these neonates [148-150].

Long-term neurodevelopmental outcomes

IUGR infants have a high probability to develop subtle to major cognitive and neurodevelopmental abnormalities when compared with AGA infants born at the same gestational age. The neurodevelopmental outcome of IUGR infants depends on the type of IUGR and perinatal events. The common neurological problems seen in these children include [66–69] lower scores on cognitive testing, school difficulties or requirement of special education, a gross motor and minor neurologic dysfunction, behavioral problems (attention deficit hyperactivity syndrome), a growth failure, a reduced strength and work capacity, a cerebral palsy, a low social competence, a poor academic performance, a lower intelligence and a poor perceptual performance [151-154].

Fetal origins of adult diseases

Barker and then other investigators observed that babies who were born with a LBW, when grew to age of 50 to 70 years, had a high incidence of coronary heart disease, diabetes mellitus, hyperinsulinemia and hypercholesterolemia. Three different hypotheses have been proposed for this association, namely the fetal insulin hypothesis and mature onset diabetes of the young (MODY) genes, the thrifty genotype and the thrifty phenotype (Barker's hypothesis) [155]. The

latter is the most accepted for explanation of fetal origin of adult disease (FOAD). This hypothesis suggests that, when the intrauterine environment is poor, the fetus adapts to this hostile environment to survive *in utero*. These adaptations include prioritization of brain growth at the expense of other tissues such as muscles, liver and pancreas, reduced production and sensitivity to the fetal insulin and IGF-1 and also up-regulation of the hypothalamo–pituitary–adrenal axis. This metabolic programming makes the fetus to adapt to poor postnatal nutrition, but when nutrition during postnatal life is normal or excessive, fetal programming proves to be inadequate, thus leading to abnormal growth and making them susceptible to FOAD (Fig. 12) [156].

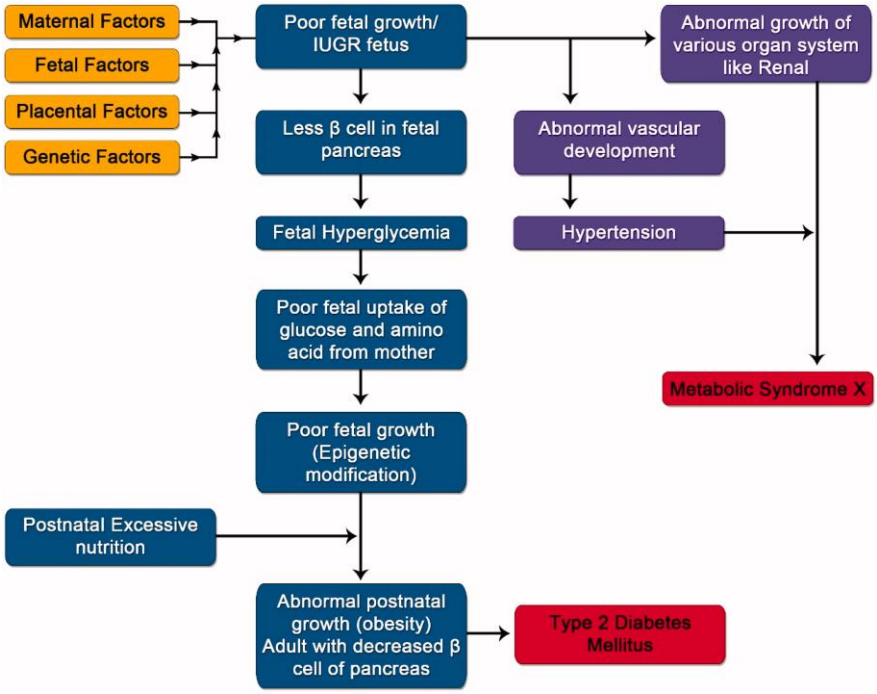

Figure 12: Barker's hypothesis (thrifty phenotype) in growth-restricted infants.
When the intrauterine environment is poor, the fetus adapts to this hostile environment to survive *in utero*, but that causes also an inadequate preparation for extrauterine environment [157].

3.5 Management of intrauterine growth restriction

Giving the wide range of different IUGR etiologies, identifying the cause is essential to choose an adapted approach to manage IUGR.

To start, women should be screened for clinical risk factors for IUGR by means of a complete history. They should stop smoking, drink alcohol or use drugs, which are known to promote the

development of IUGR. If an IUGR is suspected, detailed ultrasound examination of the placenta (looking for evidence of a small, thickened placenta, or abnormal morphology) and uterine artery Dopplers should be considered. Low-dose aspirin should be recommended to women with a previous history of placental insufficiency syndrome including IUGR and pre-eclampsia, but also for women with two or more current risk factors in pregnancy including pregestational hypertension, obesity, maternal age above 40 years, history of use of ART, pregestational diabetes mellitus (type I or II), multiple gestation, previous history of placental abruption and previous history of placental infarction. Maternal administration of corticosteroids is indicated if there is a significant possibility of delivery before the 34^{th} gestational week, as administration may positively affect umbilical Doppler measurements. If delivery was not indicated prior to 37 weeks in a patient diagnosed with IUGR, expectant management with close fetal and maternal surveillance versus delivery should be discussed after 37 weeks [142].

However, there is currently no efficient mean to prevent or limit the development of IUGR. Understanding the implicated mechanisms is therefore necessary to better manage this pathology and its adverse outcomes.

Aim of the study

IUGR is a leading cause of perinatal mortality and morbidity affecting approximately 5 to 10% of all pregnancies. Moreover, it is also linked to an increased risk to develop chronic diseases in adulthood, in particular cardiovascular and metabolic diseases. Then, IUGR is a major challenge of public health worldwide. Unfortunately, the mechanisms implicated in IUGR remain poorly understood today. Placental insufficiency is often associated to IUGR development as proven by several studies. Ultrasonographic Doppler investigations on placental and umbilical vessels showed an impaired circulation in IUGR fetuses. NO plays a key role in the regulation of umbilical circulation thanks to its vasorelaxant properties. Therefore, even if few studies evaluated the contribution of the umbilical vessels, it is likely that an altered regulation of the NO/cGMP signaling pathway could be associated with IUGR. Thus, we hypothesized that placental insufficiency and the resultant reduction in oxygen and/or nutrients delivery to the fetus could be associated with alterations in the umbilical circulation, especially in the NO/cGMP-dependent vasorelaxation, contributing to IUGR development.

Our research team previously showed that NO-induced relaxation was impaired in UV of IUGR females compared to AGA newborns, but unaffected in males.

The aim of the present study was thus to identify sex-specific cellular and molecular mechanisms implicated in the impaired regulation of UV vascular tone in case of IUGR, with a particular attention to the NO/cGMP signaling pathway.

Materials and Methods

The present study was designed to investigate sex-specific alterations in the UV of IUGR compared to AGA neonates, with a particular attention to the NO/cGMP relaxing pathway. The endothelium-independent relaxation of isolated UV was investigated in organ chambers (OCs). The modifications occurring in molecular components implicated in the NO/cGMP pathway were determined by western blotting analyses of relative protein content or by enzymatic activity measurements, completed by tissular investigations on histological sections. Females and males were analyzed separately in order to determine sex-specific alterations.

1. Patients

The present study was approved by the ethical committee of the Faculty of Biology and Medicine of the University of Lausanne (protocol number 134/08).

Umbilical cords of newborns delivered at the Maternity of the University Hospital CHUV in Lausanne (Switzerland) were collected from 2009. Demographic and medical data were retrospectively collected for each patient from the digital medical record system of our institution.

1.1 Inclusion/exclusion criteria

Inclusion criteria were term (≥ 37 accomplished weeks of gestation) singleton pregnancies of either IUGR or AGA fetuses.

Exclusion criteria were fetal abnormalities, genetic syndromes, mothers presenting with HIV, hepatitis A, B or C, pre-eclampsia, single UA, and neonates with a birth weight above the 90th percentile.

1.2 Classification

Newborns were dichotomized into two categories, based on their body weight at birth: "IUGR" and "AGA". Samples were assigned to the "AGA" group when birth weight was between the 10th and 90th percentile, and to the "IUGR" group when birth weight was below the 10th percentile. The percentile classification was determined using a growth centile calculator, which consisted on an Excel file using a formula based on data extracted from growth charts endorsed by the Swiss Society of Pediatrics [158]. When available, prenatal data (e.g. estimated fetal weight) were used to determine whether a growth curve break occurred, namely a significant change in percentiles, in order to distinguish "IUGR" from constitutive SGA. Female and male neonates were studied separately. However, since prenatal growth follow-up or other parameters like ultrasound Doppler measurements were not available for all patients, our subjects were retroactively reclassified according to the criteria of the "Consensus Based Definition of Growth Restriction in the Newborn" published in The Journal of Pediatrics (2018) [145]. This allowed a more rigorous postnatal classification of our patients. Subjects who did not reach these criteria were excluded from the initial groups.

2. Sample collection

The proximal part (close to the fetus) of the umbilical cord was collected at delivery and used within 24 h. A 10 to 15 cm segment was cut as close as possible to the fetus and kept, until dissection, at 4°C in deoxygenated modified Krebs-Ringer solution (118.3 mM NaCl, 4.7 mM KCl, 2.5 mM $CaCl_2$, 1.2 mM $MgSO_4$, 1.2 mM KH_2PO_4, 25.0 mM $NaHCO_3$, and 11.1 mM glucose), prepared by bubbling with 21% O_2 and 5% CO_2, balanced with nitrogen, during about 30 min [84]. Before dissection, the diameter of the collected cord segment was measured at three different places, using a digital caliper, to calculate the average umbilical cord diameter for each patient.

For technical reasons, it was not possible to perform all types of experiments on each umbilical cord. In particular, all experiments requiring freshly isolated vessels (organ bath experiments, cGMP production and PDEs activity) were performed on different patients. In contrast,

homogenates analyzed by western blot were prepared with frozen UV segments dissected from umbilical cords used for the experiments mentioned above. However, we checked that each subset of samples used for the various experiments was representative of the entire population included in this study. In particular, we verified that the growth parameters were significantly reduced in IUGR compared to AGA neonates used for each type of experiments.

3. Isolated vessel tension studies

UV reactivity was investigated as previously described [84]. Briefly, UV was dissected, cut into small rings (4 to 5 mm length) and placed into vertical organ chambers filled with 10 ml modified Krebs-Ringer solution, bubbled with 21% O_2 and 5% CO_2, and maintained at 37.5°C. A 2 g stretch tension was applied to each vessel ring, followed by 20 min equilibration before washing. Stretch/equilibration/wash steps were repeated still three times, in order to get the vessels to their optimal resting tension. After equilibration, N^G-nitro-L-arginine (NLA, 10^{-4} M) and indomethacin (10^{-5} M) were added in order to exclude possible interference of endogenous synthesis of NO and prostanoids. In some experiments, 3-isobutyl-1-methylxanthine (IBMX, 10^{-4} M), a non-specific inhibitor of PDEs, was also added to investigate the contribution of PDEs in NO-induced relaxation. Vascular rings were then preconstricted with serotonin (5-HT, 10^{-5} M) or an analogue of thromboxan A_2 (U46619, 10^{-6} M), before relaxant response to cumulative doses of the NO-donor 2-(N,N-Diethylamino)-diazenolate-2-oxide (DEA/NO, 10^{-8} to 10^{-4} M) was tested. Change in tension induced by DEA/NO was expressed as percent of the initial contraction induced by the vasoconstrictor. Area under the curve (AUC) was calculated for each relaxation curve using Prism 8.0.

An additional set of experiments was performed to investigate simultaneously, in vascular rings isolated from the same UV, the relaxation induced by DEA/NO (10^{-10} to 10^{-4} M) in the presence or absence of IBMX, as well as spontaneous relaxation observed in the absence of the relaxing agent.

4. Western blotting analyses

The relative amounts of specific proteins in UV homogenates were investigated by western blot. Flash-frozen UV were crushed in a cryogenic mortar, homogenized in lysis buffer (50 mM HEPES, 1 mM EDTA, 1 mM EGTA, 10% glycerol, 1 mM DTT, 5 µg/ml pepstatin, 3 µg/ml aprotinin, 10 µg/ml leupeptin, 0.1 mM 4-(2-aminoethyl)benzenesulfonyl fluoride hydrochloride (AEBSF), 1 mM sodium vanadate, 50 mM sodium fluoride, and 20 mM 3-[(3cholamidopropyl)dimethylammonio]-1-propanesulfonate (CHAPS)), and centrifuged for 10 min at 3'000 g at 4°C. Supernatant protein concentration was quantified using a BCA protein assay kit (Pierce). Samples were diluted in Laemmli buffer (Tris-HCl pH 6.8, 2% SDS, 10% glycerol, 0.1% bromophenol blue, 4% 2-mercaptoethanol), to reach a concentration of 40 or 80 µg per lane, depending on the protein, and were heated for 5 min at 95°C before loading on a 7.5% polyacrylamide gel. Proteins were fractioned by SDS-PAGE (1 h 35 min, 0.05 A) and transferred to a nitrocellulose membrane (overnight, 30 V, 4°C). After a 30 min blocking in 1% casein solution (Vector) at room temperature (RT), membranes were immunoblotted (overnight at 4°C, or 1 h at RT) using specific antibodies targeted against sGC (1:10'000, Abcam), PKG (1:1'000, Stressgen), eNOS (1:1'000, Cell Sign), catalase (1:100, Santa Cruz), SOD1 (1:5'000, Santa Cruz), SOD2 (1:1'000, Cell Sign), SOD3 (1:100, Santa Cruz), SIRT1 (1:1'000, Cell Sign) or actinin (1:250, Sigma), diluted in 1% casein solution containing 0.1% Tween. Blots were then incubated with an anti-mouse or anti-rabbit antibody (LICOR) diluted 1:10'000 in 1% casein solution (1 h, RT). Target proteins were visualized using an Odyssey Infrared Imaging System (LICOR). The amount of each specific protein was quantified using ImageJ software and normalized to the actinin content.

For each experimental group, samples from 40 patients were randomly distributed into 4 pools, in order to limit the influence of individual variability on the results. To allow comparison between the different membranes and between groups, the specific protein content measured in each pool was reported to the amount measured in a "standard" sample, constituted of proteins extracted from 6 additional patients (3 AGA males and 3 AGA females), which were not included in the pools.

Some experiments were also performed using individual samples rather than pools of patients in order to validate the usefulness of pools as described above. For that purpose, individual patients were randomly selected in each pool in order to investigate sGC and PKG protein content. To allow comparison between the different membranes and groups, the target protein content measured in each sample was reported to the amount measured in the same "standard" sample as for experiments using pools of patients.

Finally, some western blots were performed on non-denatured proteins. For each experimental group, samples from 12 patients were randomly distributed into 4 pools. To compare samples between the different membranes and between groups, the specific protein content measured in each pool was reported to the amount measured in a "standard" sample, constituted of non-denatured proteins extracted from 6 additional patients (3 AGA males and 3 AGA females), which were not included in the pools. For this experiment, the differences are that crushed samples were homogenized in 1 ml non-denaturing lysis buffer (50 mM HEPES, 1 mM EDTA, 1 mM EGTA, 10% glycerol, 5 µg/ml pepstatin, 3 µg/ml aprotinin, 10 µg/ml leupeptin, 0.1 mM AEBSF, 1 mM sodium vanadate, 50 mM NaF and 100 mM maleimide). Samples were then diluted in non-denaturing Laemmli buffer (without β-mercaptoethanol, but with 100 mM maleimide) and were loaded without heating at 95°C. The continuation of the experiment was identical as described above.

4.1 Western blotting analyses with different extraction methods

Some western blots were performed on individual samples previously extracted using two different methods. After that flash-frozen UV were crushed in a cryogenic mortar, each individual resulting sample was shared in two parts. One part was homogenized in classic denaturing lysis buffer (50 mM HEPES, 1 mM EDTA, 1 mM EGTA, 10% glycerol, 1 mM DTT, 5 µg/ml pepstatin, 3 µg/ml aprotinin, 10 µg/ml leupeptin, 0.1 mM AEBSF, 1 mM sodium vanadate, 50 mM sodium fluoride, and 20 mM CHAPS) and the other part was homogenized in non-denaturing lysis buffer (50 mM HEPES, 1 mM EDTA, 1 mM EGTA, 10% glycerol, 5 µg/ml

pepstatin, 3 µg/ml aprotinin, 10 µg/ml leupeptin, 0.1 mM AEBSF, 1 mM sodium vanadate, 50 mM NaF and 100 mM maleimide). After a 3 h incubation, samples were centrifuged for 30 min at 10'000 g at 4°C. After recovery of supernatants, pellets from the non-denaturated part were re-extracted with the denaturing lysis buffer described above. After a new 3 h incubation, samples were centrifuged for 30 min at 10'000 g at 4°C and supernatants collected. The protein concentration was quantified using a BCA protein assay kit in the three types of supernatants: the supernatant resulting from the denaturating extraction, the supernatant recovered after the non-denaturating extraction and the supernatant resulting from the second extraction of proteins contained in the pellet of the non-denaturating extraction. Samples were diluted in Laemmli buffer, to reach a protein concentration of 40 µg per lane, and were heated for 5 min at 95°C before loading on a 7.5% polyacrylamide gel. Proteins were fractioned by SDS-PAGE (1 h 35 min, 0.05 A) and transferred to a nitrocellulose membrane (overnight, 30 V, 4°C). A Ponceau coloration (Sigma) was performed on membranes to visualize all proteins, before they were rinsed. After a 30 min blocking in 1% casein solution (Vector) at RT, membranes were immunoblotted (overnight at 4°C, or 1 h at RT) using specific antibodies targeted against PKG (1:1'000, Stressgen) or actinin (1:250, Sigma), diluted in 1% casein solution containing 0.1% Tween. Blots were then incubated with an anti-mouse or anti-rabbit antibody (LICOR) diluted 1:10'000 in 1% casein solution (1 h, RT). Target proteins were visualized using an Odyssey Infrared Imaging System (LICOR). The amount of each specific protein was quantified using ImageJ software and normalized to the actinin content or to the total amount of proteins visible with the Ponceau coloration.

5. Enzymatic activity analyses

5.1 cGMP production in isolated umbilical veins

UV was dissected, cut into small rings (4 to 5 mm length) and incubated in modified Krebs-Ringer solution (37.5°C, bubbled with 21% O_2 and 5% CO_2). All measurements were performed in the presence of indomethacin (10^{-5} M) and NLA (10^{-4} M), such as in isolated vessel tension studies. Several conditions were tested at the same time on vascular rings from the same UV.

IBMX (10^{-4} M) was used to prevent the degradation of cGMP. After a 20 min equilibration period, DEA/NO (10^{-4} M) was added in the bath. After a 4 min incubation, UV rings were quickly frozen in liquid nitrogen in order to stop the reaction. Vascular rings were crushed in a cryogenic mortar and homogenized in 0.1 N HCl. The cGMP content was quantified in homogenates using the direct cGMP ELISA Kit (Enzo Life Sciences) according to the manufacturer's instructions. Samples with high cGMP content (vessel rings treated with DEA/NO +/- IBMX) were processed using the classical procedure, whereas samples with low cGMP content (vessel rings in basal conditions or treated with IBMX alone) were tested using the acetylation procedure. For each sample, cGMP content was normalized by the corresponding protein content, quantified using the BCA protein assay kit, and expressed as pmol cGMP/mg protein/min.

5.2 PDEs activity in umbilical vein homogenates

The PDEs activity was quantified in UV homogenates using a cyclic nucleotide phosphodiesterase assay kit (Enzo Life Sciences) according to the manufacturer's instructions. Briefly, flash-frozen vein segments were crushed in a cryogenic mortar, and 450 mg was mixed with 1 ml Assay Buffer containing 20 mM CHAPS using a tissue grinder. Homogenates were then sonicated and centrifuged for 10 min at 3'000 g at 4°C. A buffer exchange was performed using Pierce™ Protein Concentrators PES, 3K MWCO, 0.5 mL, in order to remove excess free phosphate, which interferes with the BIOMOL® GREEN reagent of the kit. cGMP or cyclic adenosine monophosphate (cAMP) degradation was tested in the absence or presence of IBMX 10^{-4} M. Enzymatic reaction was performed during 20 min at 30°C in Assay buffer containing 0.5 mM $MgCl_2$, 0.2 mM $CaCl_2$ and 2 µM calmodulin. Results were measured at 620 nm in a microplate reader (NanoQuant, Tecan). For each sample, total and IBMX-sensitive PDEs activities were normalized by the corresponding protein content, quantified using the BCA protein assay kit, and expressed as nmol cGMP/mg protein/min.

5.3 Beta-galactosidase activity in umbilical vein homogenates

The β-galactosidase activity was quantified in UV homogenates using a fluorometric assay kit (BioVision) according to the manufacturer's instructions. Flash-frozen vein segments were crushed in a cryogenic mortar, and 15 mg was mixed with 300 µl Assay buffer. Homogenates were centrifuged for 5 min at 10'000 g at 4°C. Supernatants were loaded on a 96-well plate before addition of β-Gal substrate. Fluorescence of fluorescein, produced by β-galactosidase, was measured immediately in a microplate reader with fluorescence detection (Victor^3, PerkinElmer) in kinetic mode for 45 min at 37°C. For each sample, fluorescence was normalized by the corresponding protein content, quantified using the BCA protein assay kit.

5.4 Superoxide detection by chemiluminescence

O_2^- production in umbilical vessels was evaluated using the oxidative fluorescent dye dihydroethidium (DHE) in comparison to a negative control (autofluorescence detection). In the presence of O_2^-, DHE is oxidized to fluorescent ethidium bromide, which is trapped in DNA by intercalation. Segments of 1 cm were cut in fresh umbilical cord, included in OCT gel (Tissue-Tek) and put in dry ice. Frozen umbilical cord segments in OCT blocks were cut into 5 µm thick sections with a cryostat at -20°C and thaw-mounted on microscope slides (Superfrost® Plus, Thermo Scientific). Tissue slices were washed with phosphate buffered saline (PBS) 1X, quickly fixed with a fixative solution (BioVision) for 15 min and washed again twice with PBS 1X. A pre-incubation solution containing N,N-dimethylformamide (DMF, Cell Sign) or apocynin (0.5 M diluted in DMF, Millipore) was added for 15 min at 37°C. Then, the pre-incubation solution was removed to put the incubation solution for 45 min at 37°C, in a light-protected humidified chamber. Three incubation solutions were prepared, with either DMF, or DMF and DHE (10^{-3} M, Sigma), or DHE (10^{-3} M) and apocynin (0.5 M diluted in DMF). Tissue slices were washed twice with PBS 1X, mounted with Fluoromount-G mounting medium containing 4,6-diamidino-2-phenylindole (DAPI, Interchim), covered with a coverslip and let overnight at RT. Images were obtained using a Nikon Eclipse Ti microscope with dedicated optical assistance imaging software

(NIS-Elements Viewer version 4.5), at a magnification of 4x, and evaluated with ImageJ software.

6. Data analyses

Statistical analyses were performed using Prism 8.0 (GraphPad Software, San Diego, CA). The test used to analyze each type of experiment is specified in the figure/table legends. The differences were considered statistically significant when $P < 0.05$.

Results

1. Demographic data

Table 4 displays maternal and neonatal characteristics of each group. Gestational and maternal age at delivery were similar in all groups. As expected, body weight, length and head circumference at birth were significantly reduced in IUGR neonates compared to AGA. Ponderal index, placental weight and umbilical cord diameter were also significantly lower in IUGR than AGA newborns, while the body to placental weight ratio was significantly increased.

Table 4: Demographic data related to patients included in the present study.

	Females		
	AGA	**IUGR**	***P*-value**
Number of patients included	163	98	
Gestational age (weeks)	39.6 ± 1.0	39.4 ± 1.1	> 0.9999
Birth weight (g)	3312 ± 302	2551 ± 262 *	**< 0.0001**
Length (cm)	49.1 ± 1.6	46.5 ± 2.0 *	**< 0.0001**
Head circumference (cm)	34.5 ± 1.1 †	32.7 ± 1.1 *	**< 0.0001**
Ponderal index (g/cm^3)	2.82 ± 0.24	2.55 ± 0.28 *	**< 0.0001**
Placental weight (g)	617 ± 119	420 ± 84 *	**< 0.0001**
Body to placental weight ratio	5.52 ± 0.92	6.29 ± 1.14 *	**< 0.0001**
Umbilical cord diameter (mm)	12.0 ± 2.1	10.6 ± 2.0 *	**< 0.0001**
Maternal age (years)	31.9 ± 5.2	31.3 ± 5.3	> 0.9999
Smoking (yes/no)	15 / 71 (77 n/a)	17 / 50 (31 n/a) †	0.2381 #
	Males		
	AGA	**IUGR**	***P*-value**
Number of patients included	153	92	
Gestational age (weeks)	39.5 ± 1.0	39.2 ± 1.2	0.4951
Birth weight (g)	3442 ± 303	2588 ± 302 *	**< 0.0001**
Length (cm)	49.8 ± 1.7	46.8 ± 1.9 *	**< 0.0001**
Head circumference (cm)	35.1 ± 1.0 †	33.1 ± 1.2 *	**< 0.0001**
Ponderal index (g/cm^3)	2.77 ± 0.22	2.53 ± 0.21 *	**< 0.0001**
Placental weight (g)	610 ± 109	427 ± 95 *	**< 0.0001**
Body to placental weight ratio	5.72 ± 0.87	6.33 ± 1.19 *	**0.0008**
Umbilical cord diameter (mm)	12.7 ± 2.7	11.2 ± 2.3 *	**< 0.0001**
Maternal age (years)	33.1 ± 5.2	31.6 ± 5.7	0.2805
Smoking (yes/no)	11 / 70 (72 n/a)	25 / 28 (39 n/a) * †	**< 0.0001** #

Ponderal index was calculated as [100 x birth weight/length^3] (g/cm^3). Data are expressed as mean ± SD. *P*-values presented in the table are related to comparison between AGA and IUGR groups. Bold indicates significant *P*-values ($P < 0.05$). All parameters were analyzed using a Kruskal-Wallis test with Dunn's multiple comparison, excepted for smocking status. * significant difference between AGA and IUGR newborns; † significant difference between females and males. # *P*-values determined using the Fisher's exact test to compare the smoking status between mothers of AGA and IUGR neonates. n/a, not available.

Concerning the smoking status, the proportion of smoking mothers was significantly higher in IUGR males than in other groups. The latter information should however be considered with caution because the smoking status was self-reported and was not available in 31 to 47% of the medical records.

2. Smooth muscle investigations

2.1 Isolated vessel tension studies

Preliminary data showed that the non-specific PDEs inhibitor IBMX induced a dose-dependent relaxation in preconstricted UV rings (Fig. 13).

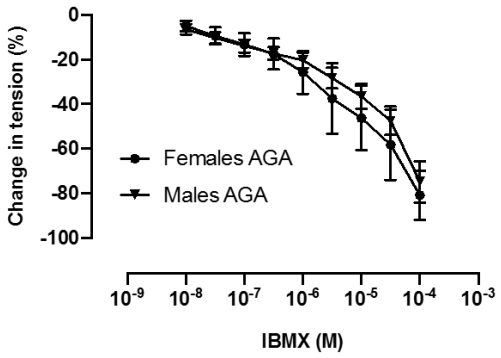

Figure 13: Relaxation induced by cumulative doses of the non-specific PDEs inhibitor IBMX on isolated umbilical veins.
Cumulative concentrations of IBMX were applied to UV rings preconstricted with 5-HT 10^{-5} M. Data are expressed as mean ± SEM of the percent of change in tension induced by IBMX (n = 5).

Dose-response curves to the NO-donor DEA/NO performed in UV rings pre-incubated with IBMX were directly compared to those obtained in absence of IBMX previously published by Peyter *et al.* in *Placenta* [84]. Such comparison was possible because experimental procedure and conditions were strictly identical between both sets of experiments. However, for a better concordance, the data published in *Placenta* [84] were re-analyzed after reclassification of patients and exclusion of those who did not reach the "2018 consensus criteria" [145].

Figures 14 and 15 present the dose-dependent relaxation induced by cumulative doses of DEA/NO, in the absence or presence of IBMX, in UV preconstricted either by 5-HT (Fig. 14) or U46619 (Fig. 15), as well as the corresponding AUC calculated for each dose-response curve.

The previous observations [84] remained valid even after reclassification of the subjects: in females, DEA/NO-induced relaxation was significantly weaker in IUGR than AGA neonates, whereas, in males, relaxant responses to DEA/NO were similar in both groups. Consistently, in females, AUC was significantly reduced in IUGR compared to AGA (Fig. 14B, Fig. 15B), whereas in males, AUC was similar in both groups (Fig. 14D, Fig. 15D).

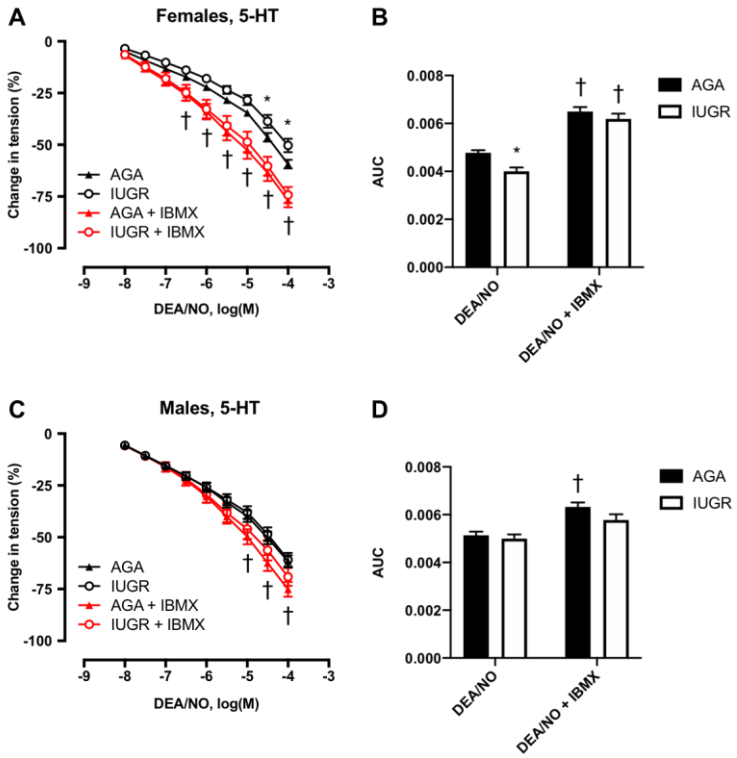

Figure 14: Relaxation induced by cumulative doses of the nitric oxide-donor DEA/NO on isolated umbilical veins preconstricted with 5-HT in the absence or presence of IBMX.
Cumulative concentrations of DEA/NO were applied to UV isolated from newborn females (A) or males (C) preconstricted with 5-HT 10^{-5} M. Data are expressed as mean ± SEM of the percent of change in tension induced by the vasodilator without IBMX (n = 36–51 in females; n = 37–50 in males) and with IBMX 10^{-4} M (n = 18–24 in females; n = 14–24 in males). Data were analyzed by two-way ANOVA. * significant difference between AGA and IUGR; † significant difference between absence and presence of IBMX, in AGA and IUGR females, but only in AGA males ($P < 0.05$). AUC was calculated for each dose-response curve of the corresponding graph (B, females; D, males). Results are expressed as mean ± SEM and were analyzed using two-way ANOVA. * significant difference between AGA and IUGR neonates; † significant difference between AUC in the presence or absence of IBMX ($P < 0.001$).

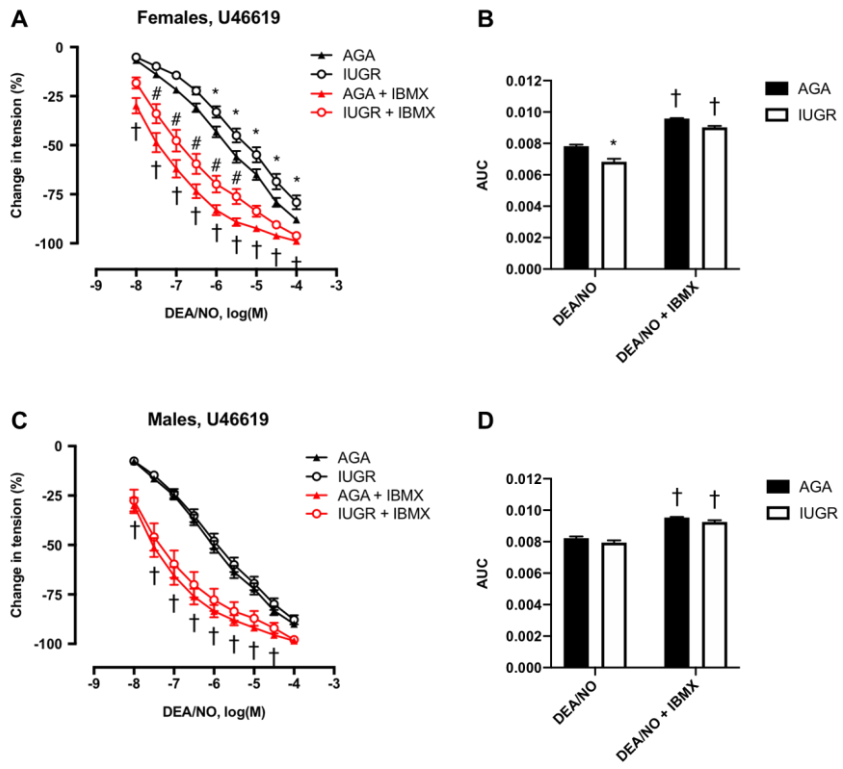

Figure 15: Relaxation induced by cumulative doses of the nitric oxide-donor DEA/NO on isolated umbilical veins preconstricted with U46619 in the absence or presence of IBMX.
Cumulative concentrations of DEA/NO were applied to UV isolated from newborn females (A) or males (C) preconstricted with U46619 10^{-6} M. Data are expressed as mean ± SEM of the percent of change in tension induced by the vasodilator without IBMX (n = 36–50 in females; n = 37–50 in males) and with IBMX 10^{-4} M (n = 18–24 in females; n = 14–24 in males). Data were analyzed by two-way ANOVA. * significant difference between AGA and IUGR; † significant difference between absence and presence of IBMX, in AGA and IUGR neonates; # significant difference between AGA and IUGR females in the presence of IBMX ($P < 0.05$). AUC was calculated for each dose-response curve of the corresponding graph (B, females; D, males). Results are expressed as mean ± SEM and were analyzed using two-way ANOVA. * significant difference between AGA and IUGR neonates; † significant difference between AUC in the presence or absence of IBMX ($P < 0.0001$).

Pre-incubation with IBMX significantly increased NO-induced relaxation in all groups (Fig. 14, Fig. 15). In female UV preconstricted with 5-HT, IBMX not only improved NO-induced relaxation, but also completely abolished the difference observed between IUGR and AGA in the absence of IBMX (Fig. 14A). In female UV preconstricted with U46619, IBMX also significantly improved relaxant response to DEA/NO in both groups (Fig. 15A); however, in UV pre-incubated with IBMX, relaxation induced by low doses of DEA/NO ($3 \cdot 10^{-8}$ to $3 \cdot 10^{-6}$ M) was significantly weaker in IUGR than in AGA females, whereas no significant difference was found for higher concentrations of DEA/NO (10^{-5} to 10^{-4} M) (Fig. 15A). AUC calculated in UV pre-incubated with IBMX were significantly increased as compared to UV without IBMX and did not show any significant difference between AGA and IUGR females (Fig. 14B, Fig. 15B). In males, relaxant responses to DEA/NO were similar in AGA and IUGR neonates, with a significant

increase in NO-induced relaxation in UV pre-incubated with IBMX compared to basal conditions (Fig. 14C, Fig. 15C). There was no difference between AUC calculated for AGA and IUGR males, either in the absence or in the presence of IBMX (Fig. 14D, Fig. 15D), and AUC was significantly higher in UV treated with IBMX compared to basal conditions (Fig. 14D, Fig. 15D).

Comparison between both sexes showed that, in absence of IBMX, AUC was significantly lower in IUGR females than IUGR males (P = 0.0003; two-way ANOVA), but was similar in AGA females and males. In UV treated with IBMX, AUC did not differ between females and males.

Table 5 shows that pre-incubation with IBMX led to a significant decrease in resting tension in all groups. However, in each separated condition, resting tension was similar in AGA and IUGR neonates. The residual tension reached in the vascular rings before addition of DEA/NO showed no significant difference between AGA and IUGR females in each condition, nor between AGA and IUGR males treated with IBMX. In contrast, residual tension was significantly lower in IUGR males than AGA preconstricted with 5-HT or U46619. Pre-incubation with IBMX did not significantly influence resting tension in all groups, excepted in AGA males preconstricted with U46619.

Table 5: Optimal resting tension and residual tension of isolated umbilical vein rings preconstricted with either 5-HT or U46619.

	- IBMX			+ IBMX		
	AGA	**IUGR**	***P*-value**	**AGA**	**IUGR**	***P*-value**
Females						
5-HT	n = 51	n = 36		n = 24	n = 18	
Resting tension (g)	0.20 ± 0.02	0.25 ± 0.04	0.4353	0.05 ± 0.02 #	0.08 ± 0.03 #	0.8964
Residual tension (g)	4.18 ± 0.16	4.04 ± 0.21	0.9506	4.12 ± 0.23	3.56 ± 0.27	0.4203
U46619	n = 50	n = 36		n = 24	n = 18	
Resting tension (g)	0.22 ± 0.02	0.30 ± 0.04	0.1226	0.06 ± 0.02 #	0.12 ± 0.03 #	0.6717
Residual tension (g)	4.00 ± 0.21	4.06 ± 0.24 †	0.9968	3.16 ± 0.21 ‡	3.34 ± 0.24	0.9717
Males						
5-HT	n = 50	n = 37		n = 24	n = 14	
Resting tension (g)	0.24 ± 0.03	0.34 ± 0.05	0.2085	0.09 ± 0.02 #	0.14 ± 0.04 #	0.9038
Residual tension (g)	4.02 ± 0.14	3.42 ± 0.19 *	**0.0400**	3.90 ± 0.21	3.13 ± 0.25	0.1214
U46619	n = 50	n = 37		n = 24	n = 14	
Resting tension (g)	0.26 ± 0.03	0.32 ± 0.04	0.5925	0.07 ± 0.01 #	0.16 ± 0.05 #	0.6313
Residual tension (g)	4.00 ± 0.16	3.28 ± 0.20 * †	**0.0151**	3.19 ± 0.16 #	2.63 ± 0.25	0.4291

The resting tension corresponds to the maximal relaxation state measured in the vascular ring. The residual tension corresponds to the tension reached in the vessel ring just before addition of DEA/NO. Data are expressed as mean ± SEM. *P*-value was calculated by two-way ANOVA. * significant difference between AGA and IUGR newborns; † significant difference between females and males; # significant difference between absence and presence of IBMX; ‡ significant difference between UV preconstricted with 5-HT or U46619 ($P < 0.05$).

Because dose-response curves in the presence of IBMX were established in UV isolated from other patients than the initial experiments performed in basal conditions (without IBMX), complementary data were obtained by testing, on UV rings from the same patient, DEA/NO-induced relaxation in the absence or presence of IBMX, as well as spontaneous relaxation (without vasodilatory agent) (Fig. 16, Fig. 17). In such conditions, pre-incubation with IBMX significantly improved DEA/NO-induced relaxation in UV of AGA and IUGR females (Fig. 16A-D, Fig. 17A-D), as well as in male UV preconstricted with U46619 (Fig. 17E–H). In male UV preconstricted with 5-HT, pre-incubation with IBMX induced a significant increase in DEA/NO-induced relaxation only in growth-restricted males (Fig. 16E–H). In all groups and conditions, spontaneous relaxation observed in the presence or absence of IBMX was significantly weaker than the corresponding DEA/NO-induced relaxant response (Fig. 16, Fig. 17). Spontaneous relaxation observed in UV preconstricted with 5-HT was similar in the presence or absence of IBMX (Fig. 16). In contrast, in UV preconstricted with U46619, spontaneous relaxation observed in vascular rings pre-incubated with IBMX was significantly increased as compared to basal conditions (Fig. 17).

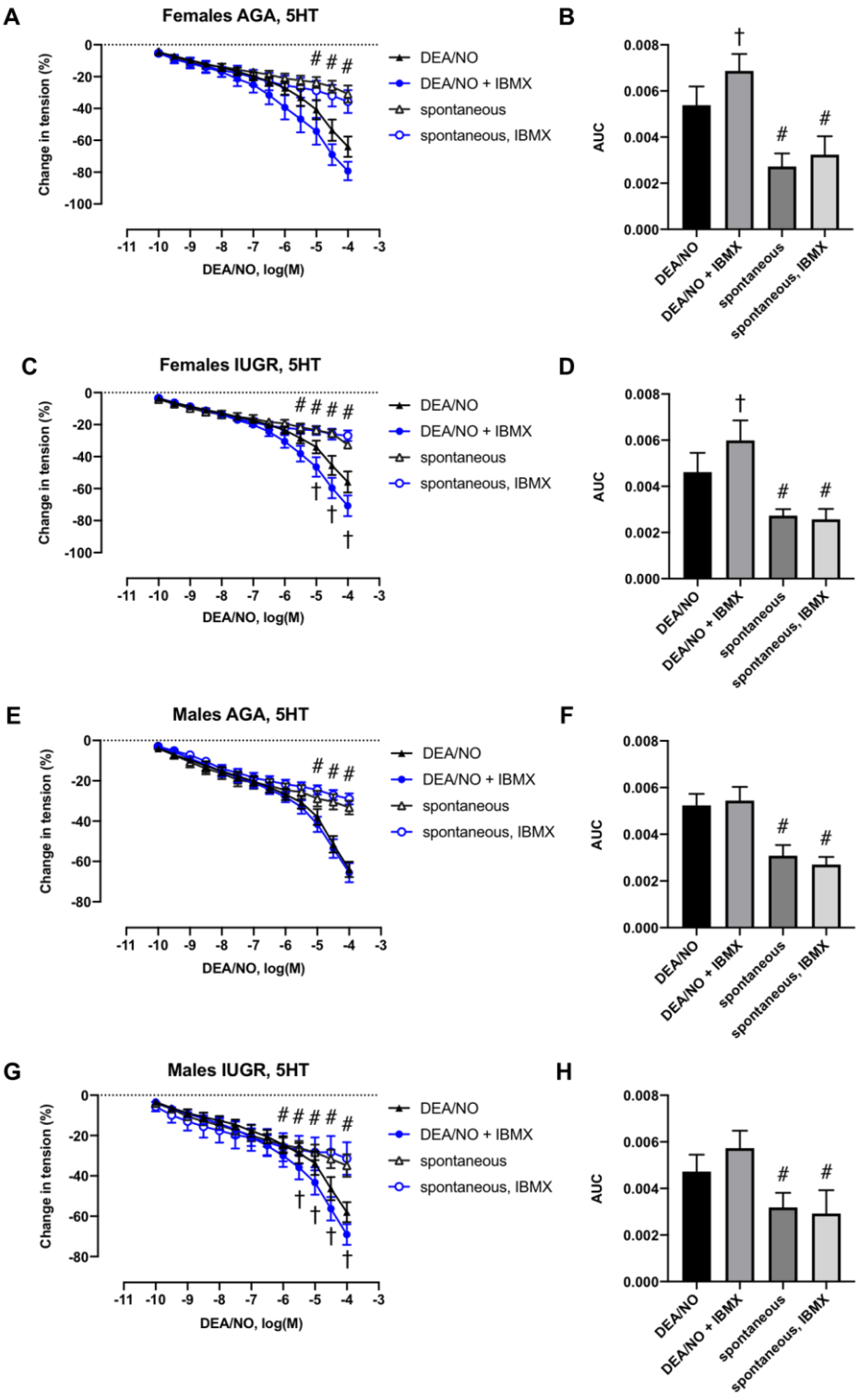

Figure 16: Spontaneous and NO-induced relaxation in isolated umbilical veins preconstricted with 5-HT in the absence or presence of IBMX.

Cumulative concentrations of DEA/NO were applied to umbilical veins isolated from AGA females (A-B), IUGR females (C-D), AGA males (E-F) or IUGR males (G-H), preconstricted with 5-HT 10^{-5} M, in the absence or presence of IBMX 10^{-4} M. Data are expressed as mean ± SEM of the percent of change in tension induced by the vasodilator (n = 5–7 in females; n = 6–7 in males). Data were analyzed by two-way ANOVA. † significant difference between DEA/NO + IBMX and DEA/NO alone; # significant difference between DEA/NO-induced relaxation and the corresponding spontaneous relaxation ($P < 0.05$). Area under the curve (AUC) was calculated for each dose-response curve of the corresponding graph. Results are expressed as mean ± SEM and were analyzed using two-way ANOVA. † significant difference between DEA/NO + IBMX and DEA/NO alone; # significant difference between DEA/NO-induced relaxation and the corresponding spontaneous relaxation ($P < 0.05$). For each group, the four experimental conditions have been tested simultaneously in vascular rings isolated from the same patient.

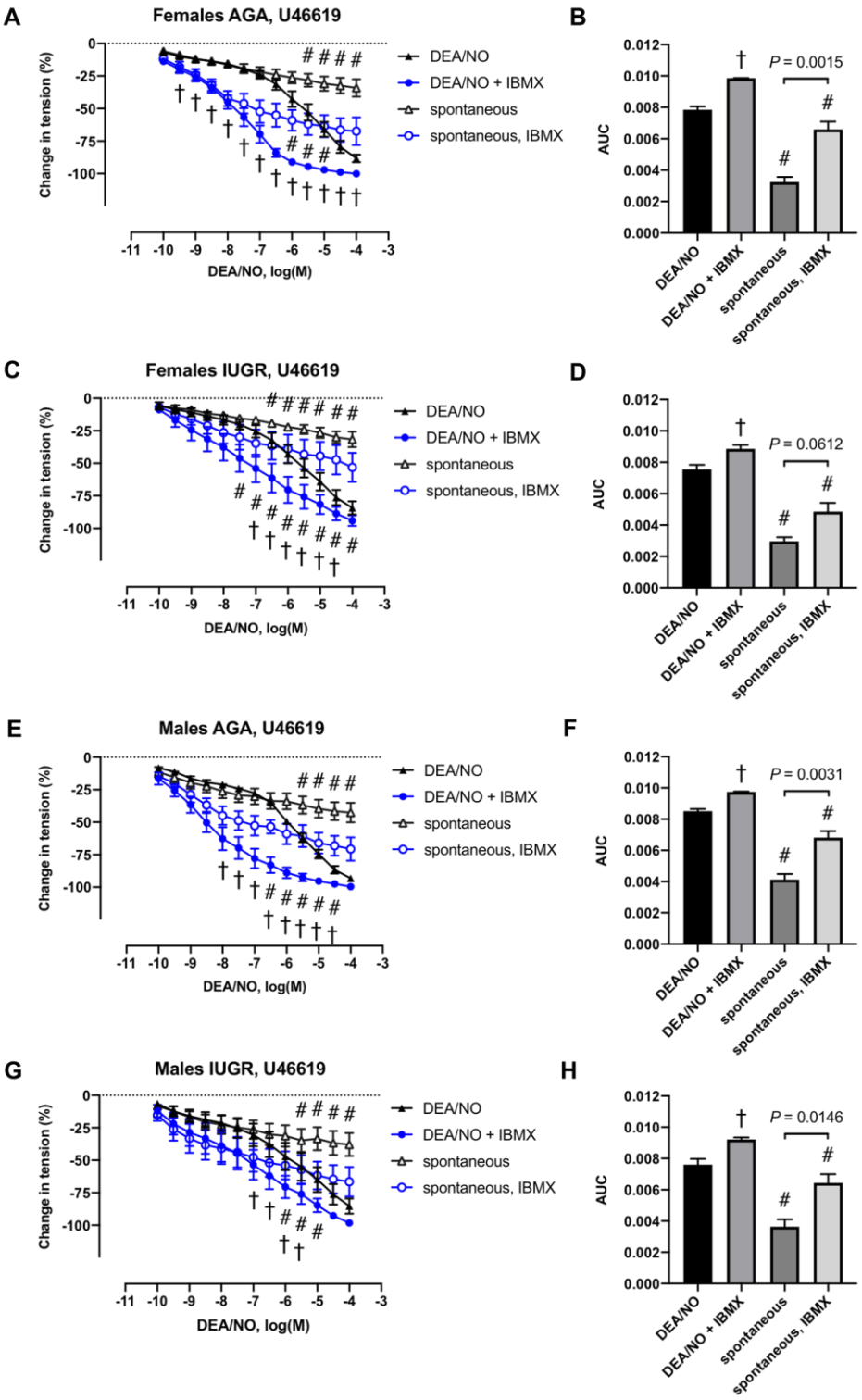

Figure 17: Spontaneous and NO-induced relaxation in isolated umbilical veins preconstricted with U46619 in the absence or presence of IBMX.

Cumulative concentrations of DEA/NO were applied to umbilical veins isolated from AGA females (A-B), IUGR females (C-D), AGA males (E-F) or IUGR males (G-H), preconstricted with U46619 10^{-6} M, in the absence or presence of IBMX 10^{-4} M. Data are expressed as mean ± SEM of the percent of change in tension induced by the vasodilator (n = 6–7). Data were analyzed by two-way ANOVA. † significant difference between DEA/NO + IBMX and DEA/NO alone; # significant difference between DEA/NO-induced relaxation and the corresponding spontaneous relaxation ($P < 0.05$). Area under the curve (AUC) was calculated for each dose-response curve of the corresponding graph. Results are expressed as mean ± SEM and were analyzed using two-way ANOVA. † significant difference between DEA/NO + IBMX and DEA/NO alone; # significant difference between DEA/NO-induced relaxation and the corresponding spontaneous relaxation ($P < 0.05$). For each group, the four experimental conditions have been tested simultaneously in vascular rings isolated from the same patient.

2.2 sGC relative protein content in umbilical vein homogenates

As displayed in Figure 18, the relative amount of sGC protein was twice as high in UV homogenates of IUGR females than in AGA. In contrast, in males, sGC protein content was similar in both groups and did not differ from AGA females (Fig.18).

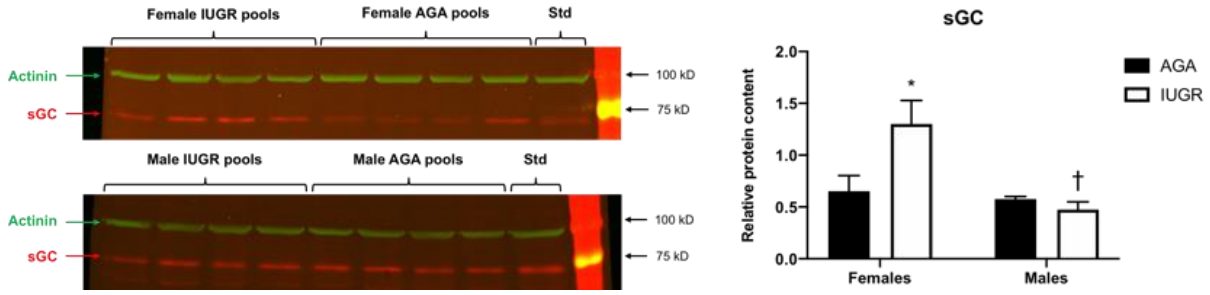

Figure 18: Relative amount of sGC protein in umbilical vein homogenates.
Western blot analysis of sGC protein in UV homogenates of AGA and IUGR newborns. For each group, samples from 40 patients were randomly distributed into 4 pools. A protein concentration of 40 µg per lane was loaded on the gel. For each pool, the target protein amount was normalized by the actinin protein content and reported to the amount measured in the "standard" sample (Std). Data are expressed as mean ± SEM (n=4 pools of 10 patients). Data were analyzed using a two-way ANOVA. * significant difference between AGA and IUGR neonates ($P < 0.05$). † significant difference between females and males ($P < 0.01$).

Similar results were obtained when performing western blots with individual samples rather than pools of patients (Fig. 19), with however less statistically significant results. In these conditions, sGC protein amount was significantly increased, by about 3 times, in IUGR females compared to AGA.

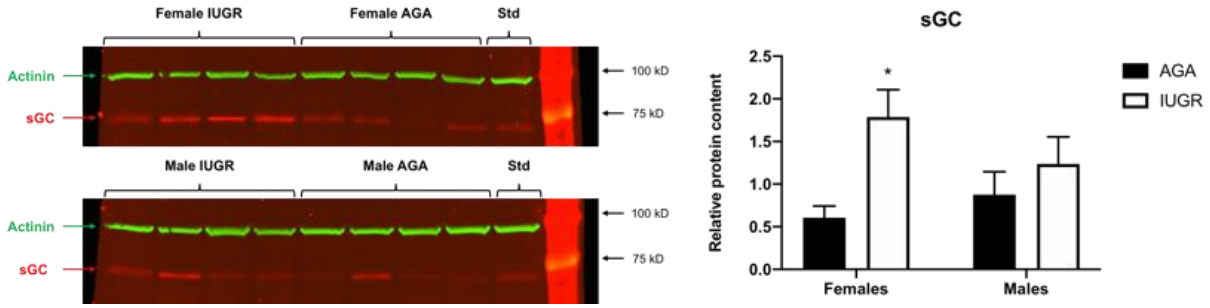

Figure 19: Relative amount of sGC protein in individual samples of umbilical vein.
Relative protein content of sGC was evaluated by western blot in UV homogenates of AGA and IUGR newborns. For each experimental group, individual samples were randomly selected among the 40 patients included in the pools analyzed in Figure 18. A protein concentration of 40 µg per lane was loaded on the gel. For each individual sample, the target protein amount was normalized by the actinin protein content and reported to the amount measured in the "standard" sample (Std). Data are expressed as mean ± SEM (n = 14–15 in females; n = 9–19 in males) and analyzed using two-way ANOVA. * significant difference between AGA and IUGR neonates ($P < 0.05$).

2.3 cGMP production in isolated umbilical veins

Figure 20 shows cGMP production measured in UV rings isolated from females (Fig. 20A) or males (Fig. 20B). Numerical data related to cGMP production in UV, expressed as pmol cGMP/mg protein/min, are summarized in Table 6. In both sexes, cGMP content measured in UV of IUGR newborns incubated with IBMX and DEA/NO was significantly greater than in basal conditions or with DEA/NO or IBMX alone (Fig. 20). In females, cGMP production measured in basal conditions, as well as in UV treated with IBMX or DEA/NO alone, did not statistically differ between AGA and IUGR neonates (Fig. 20). In the presence of IBMX and DEA/NO, however, cGMP content achieved in UV of growth-restricted females was significantly increased at about 3 as high as in AGA females (Fig. 20). In males, no significant difference was found between both groups in either condition. Between females and males, there was no significant difference, except for cGMP production measured in the presence of DEA/NO and IBMX, which was significantly higher in IUGR females than IUGR males (P = 0.0172, two-way ANOVA).

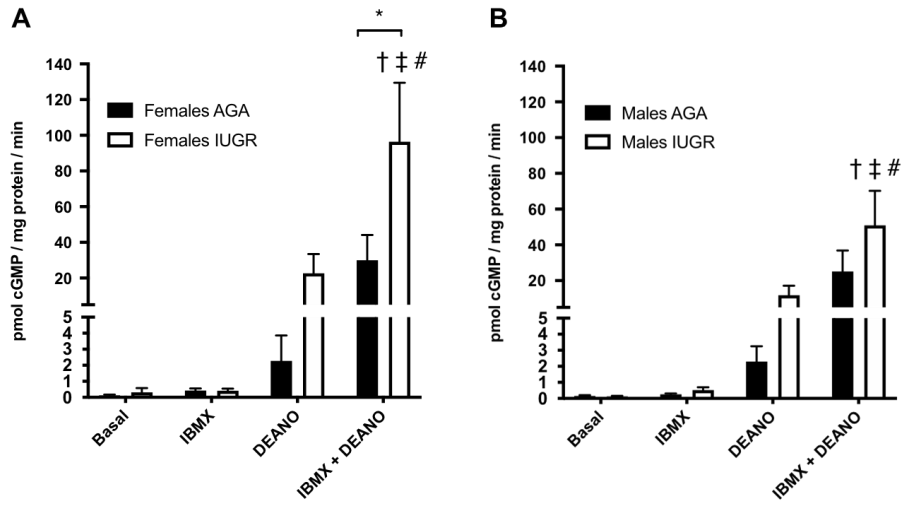

Figure 20: cGMP production in isolated umbilical veins.
cGMP production was assessed in intact UV rings isolated from females or males, in the absence or presence of IBMX 10^{-4} M and/or after stimulation by the NO donor DEA/NO 10^{-4} M. Data are expressed as mean ± SEM (n = 7–10 in females; n = 8–10 in males) of the quantity of cGMP produced, expressed as pmol cGMP/mg protein/min. Results were analyzed using two-way ANOVA. * significant difference between AGA and IUGR; † statistically different as compared to basal cGMP production; ‡ significant difference as compared to cGMP production incubated with IBMX alone; # significant difference as compared to cGMP production in the presence of DEA/NO alone ($P < 0.05$).

Table 6: cGMP production in isolated umbilical veins.

	Females			Males		
	AGA (pmol cGMP/mg protein/min)	**IUGR**	***P*-value**	**AGA** (pmol cGMP/mg protein/min)	**IUGR**	***P*-value**
	n = 10	n = 7		n = 10	n = 8	
basal	0.12 ± 0.04	0.32 ± 0.26	> 0.9999	0.16 ± 0.04	0.12 ± 0.03	> 0.9999
IBMX 10^{-4} M	0.43 ± 0.12	0.41 ± 0.14	> 0.9999	0.25 ± 0.06	0.53 ± 0.17	> 0.9999
DEA/NO 10^{-4} M	2.28 ± 1.58	22.64 ± 10.82	0.7378	2.30 ± 0.96	11.88 ± 5.25	0.8624
IBMX + DEA/NO	29.98 ± 14.16	96.39 ± 33.08 †‡# * §	**0.0011**	25.10 ± 11.77	50.94 ± 19.33 †‡# §	0.0891

Data are expressed as mean ± SEM, and were analyzed using a two-way ANOVA. *P*-values presented in the table are related to comparison between AGA and IUGR groups, and bold indicates significant *P*-values. * significant difference between AGA and IUGR; § significant difference between females and males; † significant difference as compared to basal cGMP production; ‡ significant difference as compared to cGMP production incubated with IBMX alone; # significant difference as compared to cGMP production in the presence of DEA/NO alone ($P < 0.05$).

2.4 PDEs activity in umbilical vein homogenates

Figure 21 shows IBMX-sensitive cGMP degradation measured in UV homogenates. No significant difference was observed between experimental groups.

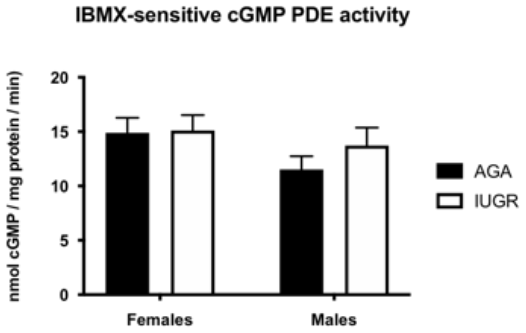

Figure 21: IBMX-sensitive cGMP phosphodiesterase activity in umbilical vein homogenates.
cGMP degradation was assessed in UV homogenates in the presence or absence of IBMX 10^{-4} M. Data are expressed as mean ± SEM (n = 6–8 in females; n = 4–8 in males) of the difference between the quantity of cGMP degraded in absence of IBMX and the quantity of cGMP degraded in the presence of IBMX. Results are expressed as nmol cGMP/mg protein/min. No significant difference was found between groups after analysis by two-way ANOVA.

Table 7 presents data related to total and IBMX-sensitive degradation of cGMP, expressed as nmol cGMP/mg protein/min. IBMX-sensitive PDEs activity represented about 32 to 37% of the total cGMP degradation capacity in UV homogenates. There was no significant difference between AGA and IUGR neonates, neither in total cGMP PDEs activity nor in IBMX-sensitive cGMP degradation.

Table 7: cGMP phosphodiesterases activity in umbilical vein homogenates.

	Females		Males	
	AGA	**IUGR**	**AGA**	**IUGR**
	n = 8	n = 6	n = 8	n = 4
Total cGMP degradation (nmol cGMP/mg protein/min)	42.39 ± 3.07	42.03 ± 4.12	36.57 ± 3.57	36.93 ± 2.67
IBMX-sensitive cGMP degradation (nmol cGMP/mg protein/min)	14.89 ± 1.40 *	15.12 ± 1.40 *	11.53 ± 1.21 *	13.72 ± 1.66 *

Data are expressed as mean ± SEM. Data were analyzed using a two-way ANOVA. * significant difference between IBMX-sensitive and total PDEs activity ($P < 0.0001$). No significant difference was found between AGA and IUGR, nor between females and males.

It should be noted that cGMP degradation was in the range of nmol cGMP/mg protein/min, whereas cGMP production was at the level of pmol cGMP/mg protein/min.

Similar observations were made regarding total and IBMX-sensitive cAMP degradation in UV homogenates, with no significant difference between groups (Table 8).

Table 8: cAMP phosphodiesterases activity in umbilical vein homogenates.

	Females		Males	
	AGA	**IUGR**	**AGA**	**IUGR**
	n = 8	n = 6	n = 8	n = 4
Total cAMP degradation (nmol cAMP/mg protein/min)	63.79 ± 2.47	65.30 ± 4.51	59.73 ± 3.31	64.14 ± 5.07
IBMX-sensitive cAMP degradation (nmol cAMP/mg protein/min)	9.42 ± 1.17 *	9.81 ± 0.94 *	9.52 ± 0.95 *	10.59 ± 1.73 *

Data are expressed as mean ± SEM. Data were analyzed by two-way ANOVA. * significant difference between IBMX-sensitive and total PDEs activity ($P < 0.0001$). No significant difference was found between AGA and IUGR, nor between females and males.

2.5 PKG relative protein content in umbilical vein homogenates

Figure 22 shows a near significant increase in PKG relative protein content in IUGR compared to AGA females ($P = 0.0565$). In males, both groups had a similar PKG protein content, which was significantly higher than in AGA females (Fig. 22).

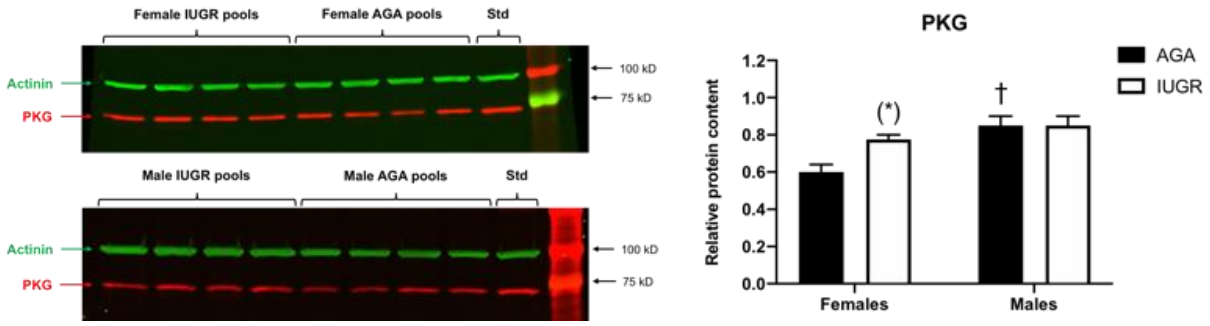

Figure 22: Relative amount of PKG protein in umbilical vein homogenates.
Relative protein content of PKG was evaluated by western blot in UV homogenates of AGA and IUGR newborns. For each experimental group, samples from 40 patients were randomly distributed into 4 pools. A protein concentration of 40 µg per lane was loaded on the gel. For each pool, the target protein amount was normalized by the actinin protein content and reported to the amount measured in the "standard" sample (Std). Data are expressed as mean ± SEM (n = 4 pools of 10 patients). Data were analyzed using two-way ANOVA. † significant difference between females and males ($P < 0.05$); (*) near significant difference between AGA and IUGR females ($P = 0.0565$).

Similar results were obtained when performing western blots with individual samples rather than pools of patients (Fig. 23), with however less statistically significant results. In these conditions, PKG protein content was significantly higher in AGA males than AGA females.

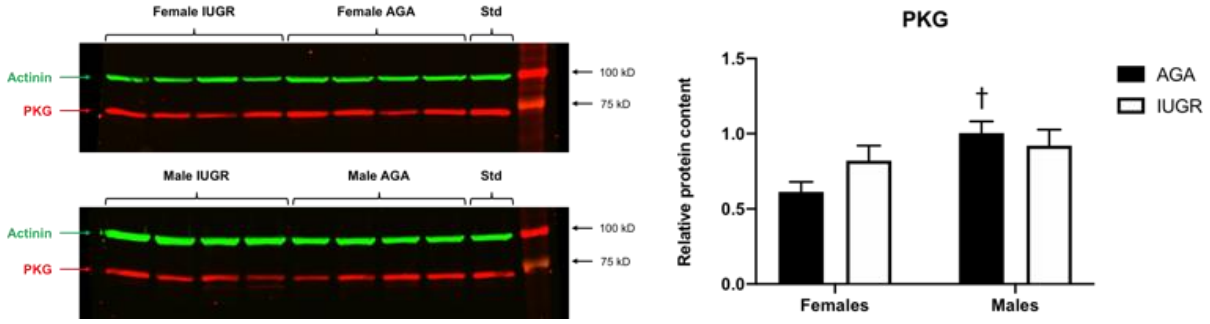

Figure 23: Relative amount of PKG protein in individual samples of umbilical vein.
Relative protein content of PKG was evaluated by western blot in UV homogenates of AGA and IUGR newborns. For each experimental group, individual samples were randomly selected among the 40 patients included in the pools analyzed in Figure 22. A protein concentration of 40 µg per lane was loaded on the gel. For each individual sample, the target protein amount was normalized by the actinin protein content and reported to the amount measured in the "standard" sample (Std). Data are expressed as mean ± SEM (n = 14–15 in females; n = 9–19 in males) and analyzed using two-way ANOVA. † significant difference between females and males ($P < 0.05$).

In UV homogenates prepared using non-denaturing conditions, there was no significant differences of relative monomers and dimers contents between groups, but the total relative amount of PKG showed a tendency to decrease in IUGR females (Fig. 24).

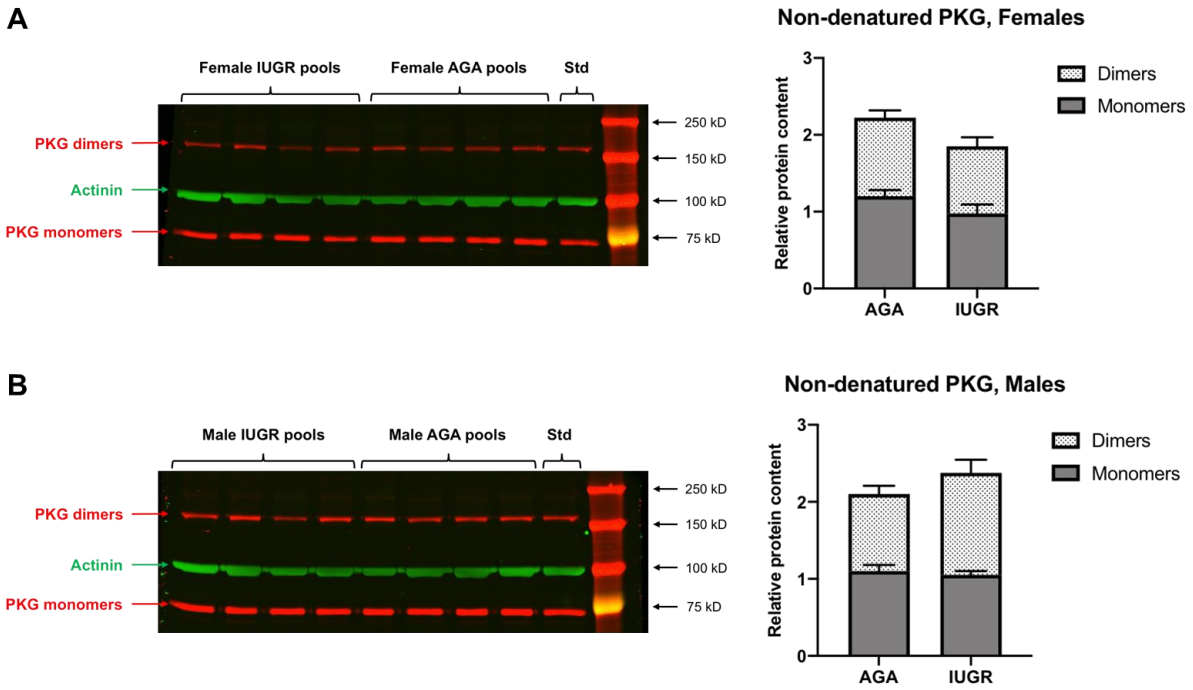

Figure 24: Relative amount of non-denatured PKG protein in umbilical vein homogenates.
Relative protein content of non-denatured PKG was evaluated by western blot in UV homogenates of AGA and IUGR female (A) and male (B) newborns. For each experimental group, samples from 12 patients were randomly distributed into 4 pools. A protein concentration of 40 µg per lane was loaded on the gel. For each pool, the target protein amount was normalized by the actinin protein content and reported to the amount measured in the non-denatured "standard" sample (Std). Data are expressed as mean ± SEM (n = 4 pools of 3 patients). No significant difference was found between groups after analysis by two-way ANOVA.

The dimers/monomers ratios tended to be higher in IUGR females and males compared to AGA, even if the difference was not statistically significant (Fig. 25).

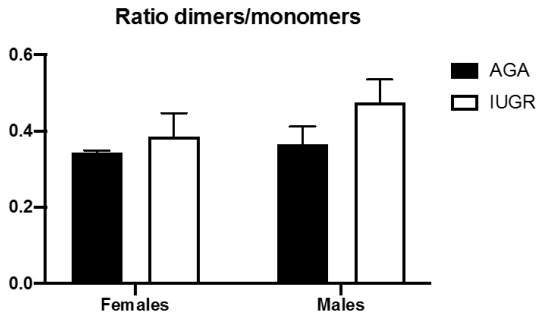

Figure 25: Ratio dimers/monomers of non-denatured PKG protein in umbilical vein homogenates.
The ratio of relative protein content of PKG dimers and monomers evaluated by western blot in Figure 24 was calculated. Data are expressed as mean ± SEM (n = 4 pools of 3 patients). No significant difference was found between groups after analysis by two-way ANOVA.

2.5.1 PKG relative protein content depending on the extraction method

Figure 26 shows the PKG relative protein content after a "classic" denaturing extraction in lysis buffer containing CHAPS or after a non-denaturing extraction without CHAPS followed by a classic extraction. Each sample was shared in two parts; the sample part 1 was extracted in denaturing conditions (S1E1D) and the sample part 2 was extracted in non-denaturing conditions (S2E1ND). Then, the pellet of the sample part 2 was re-extracted in denaturing conditions (S2E2D). For each extraction method, no difference was found between AGA and IUGR neonates (Fig. 26).

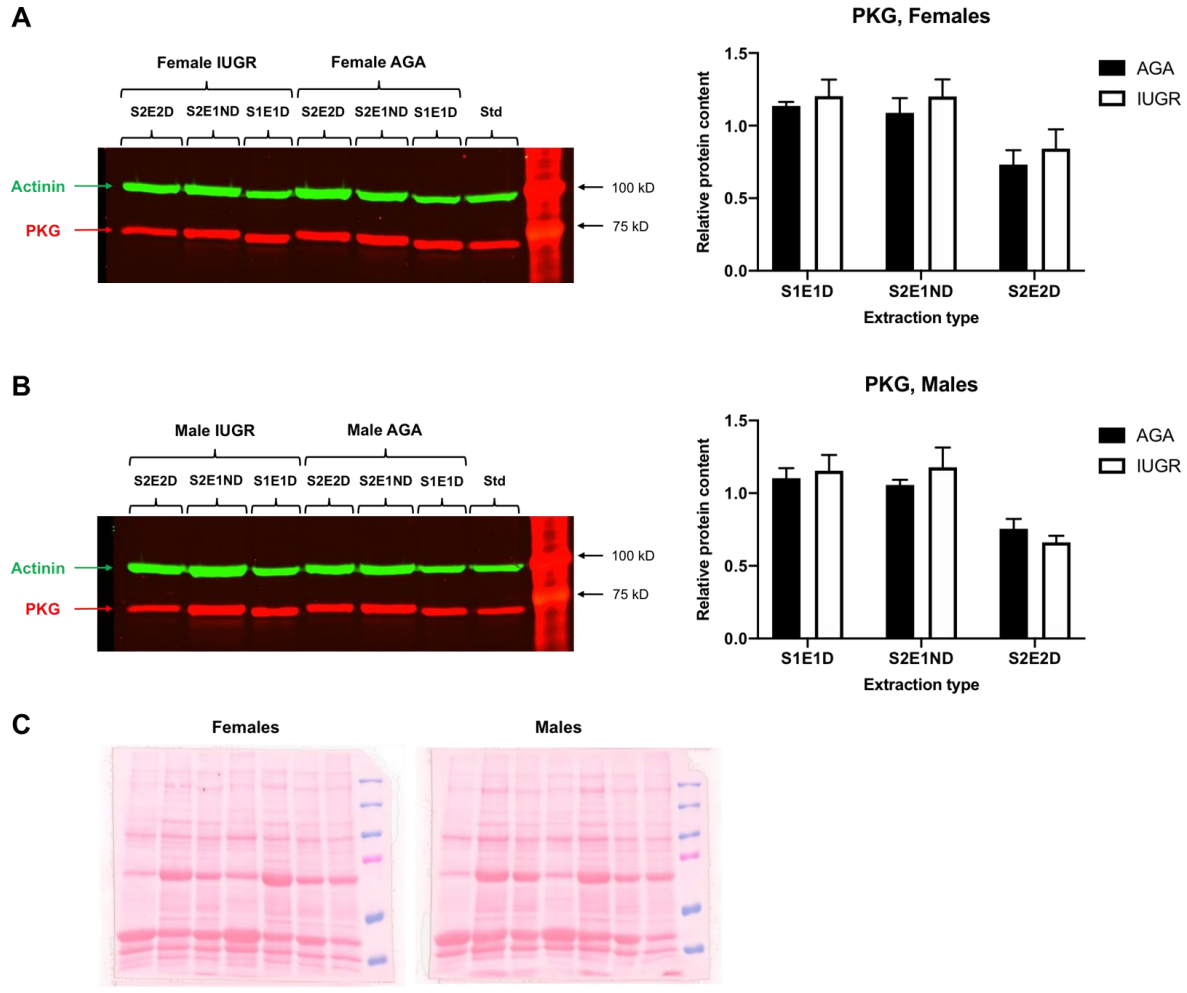

Figure 26: Relative amount of PKG protein in individual samples of umbilical vein depending on the extraction method.

S1, sample part 1. S2, sample part 2. E1, first extraction. E2, second extraction. D, denaturing extraction. ND, non-denaturing extraction. Relative protein content of PKG was evaluated by western blot in UV homogenates of AGA and IUGR female (A) and male (B) newborns. For each extraction type, a protein concentration of 40 µg was loaded on the gel. For each individual sample, the target protein amount was normalized by the total protein content visible with Ponceau coloration (C) and reported to the amount measured in the "standard" sample (Std). Data are expressed as mean ± SEM (n = 4-5 in females; n = 5 in males). No significant difference was found between groups after analysis by two-way ANOVA.

3. Endothelium investigations

3.1 eNOS relative protein content in umbilical vein homogenates

Figure 27 shows a near significant decrease of eNOS relative protein content in UV homogenates of IUGR compared to AGA males. In females, there was an inverse tendency, although eNOS relative content increase was not significant (Fig. 27B).

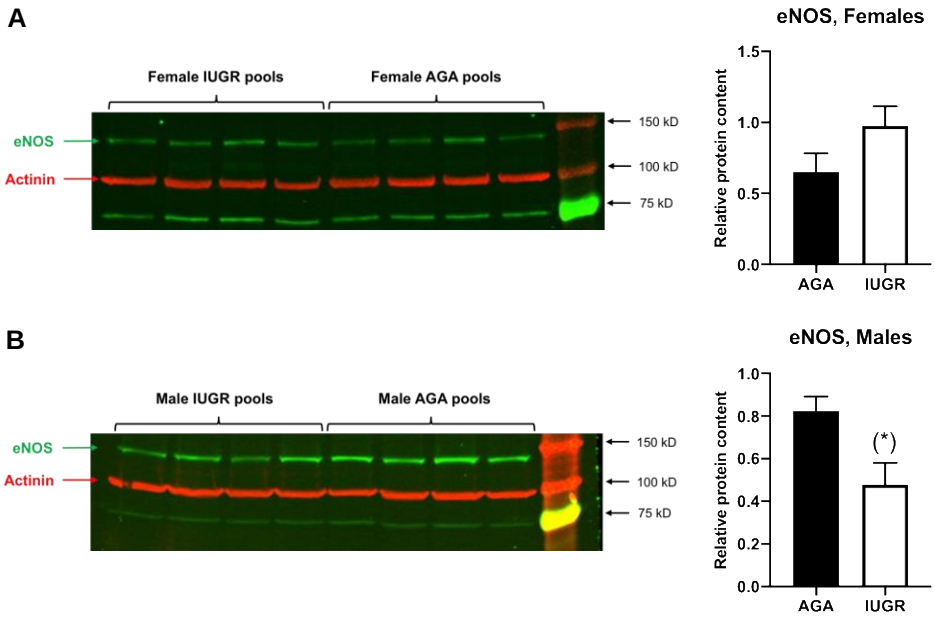

Figure 27: Relative amount of eNOS protein in umbilical vein homogenates.
Western blot analysis of eNOS protein in UV homogenates of AGA and IUGR newborns. For each group, samples from 40 patients were randomly distributed into 4 pools. A protein concentration of 80 µg per lane was loaded on the gel. For each pool, the target protein amount was normalized by the actinin protein content. Data are expressed as mean ± SEM (n=4 pools of 10 patients). Data were analyzed using a Mann-Whitney test. (*) near significant difference between AGA and IUGR females (P = 0.0571).

3.2 Antioxidant relative protein contents in umbilical vein homogenates

3.2.1 Superoxide dismutase relative protein contents

Relative protein amount of superoxide dismutase (SOD) isoforms SOD1, SOD2 and SOD3 in UV homogenates was similar between AGA and IUGR neonates (Fig. 28). However, SOD1 and

SOD3 relative contents were lower in females than in males (Fig. 28A, Fig. 28C). In contrast, SOD2 protein content did not differ between groups (Fig. 28B).

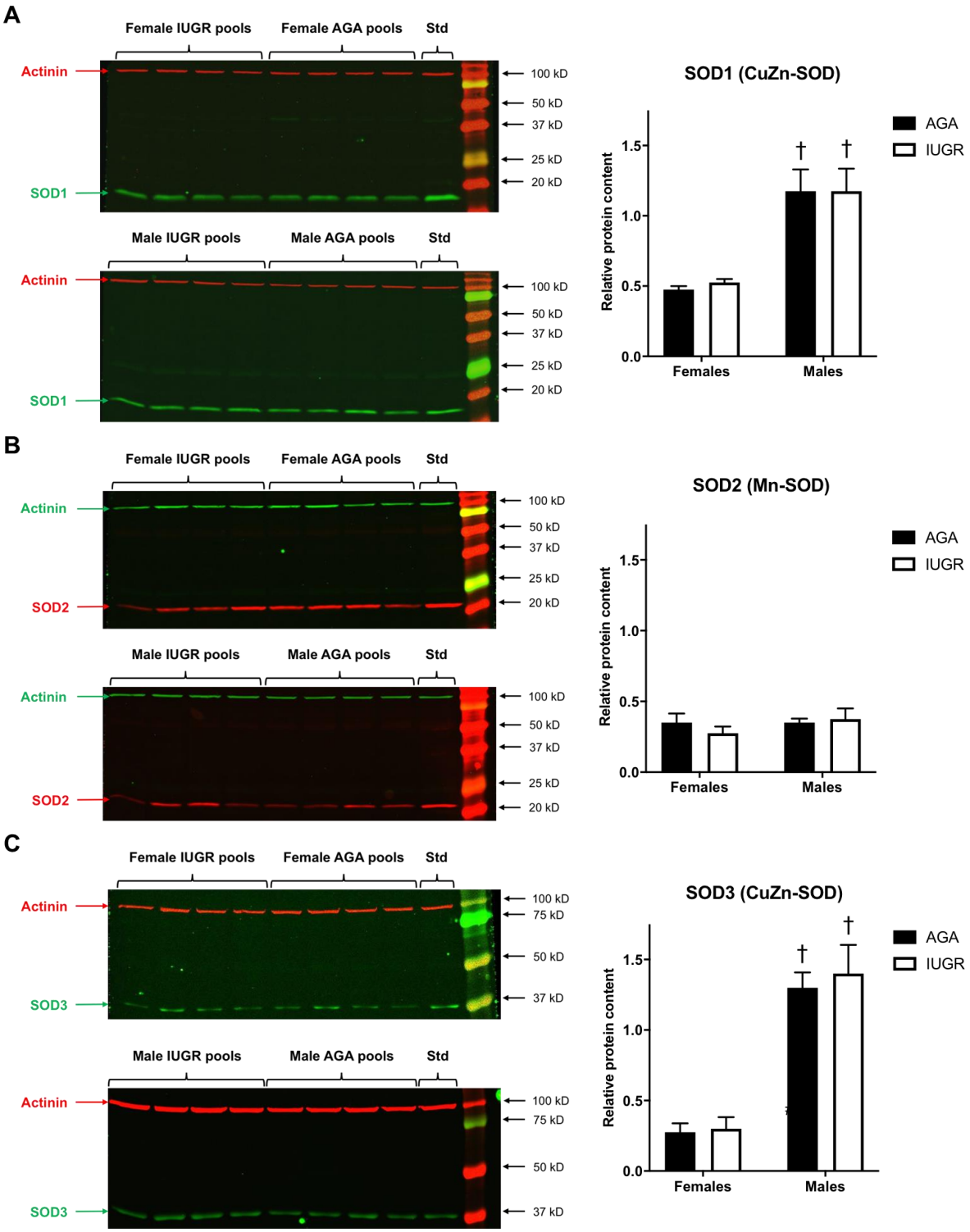

Figure 28: Relative amount of SOD1, SOD2 and SOD3 proteins in umbilical vein homogenates.
Western blot analysis of SOD isoforms in UV homogenates of AGA and IUGR newborns. For each group, samples from 40 patients were randomly distributed into 4 pools. A protein concentration of 40 µg per lane was loaded on the gel. For each pool, the target protein amount was normalized by the actinin protein content and reported to the amount measured in the "standard" sample (Std). Data are expressed as mean ± SEM (n=4 pools of 10 patients). Data were analyzed using a two-way ANOVA. † significant difference between females and males ($P < 0.01$).

3.2.2 Catalase relative protein content

Figure 29 displays that relative protein amount of catalase in UV homogenates was similar between AGA and IUGR neonates. However, there was significantly less catalase in AGA females than in the corresponding group in males. A same tendency, but no significant, was observed between IUGR females and males (Fig. 29).

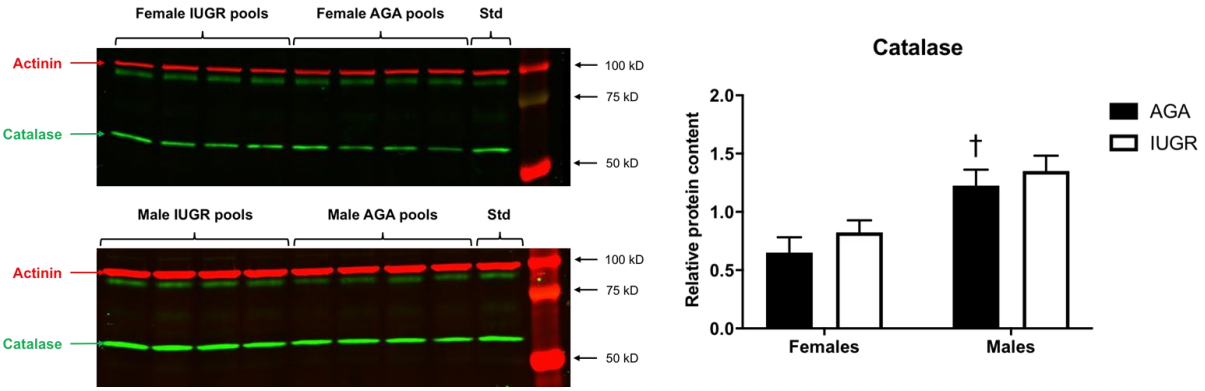

Figure 29: Relative amount of catalase protein in umbilical vein homogenates.
Western blot analysis of catalase in UV homogenates of AGA and IUGR newborns. For each group, samples from 40 patients were randomly distributed into 4 pools. A protein concentration of 40 µg per lane was loaded on the gel. For each pool, the target protein amount was normalized by the actinin protein content and reported to the amount measured in the "standard" sample (Std). Data are expressed as mean ± SEM (n=4 pools of 10 patients). Data were analyzed using a two-way ANOVA. † significant difference between females and males ($P < 0.05$).

3.3 Oxidative stress and cellular senescence

3.3.1 Superoxide anion production in umbilical vessels

In frozen umbilical cord sections, O_2^- production was observed in UV and UAs using the oxidative fluorescent dye DHE. Moreover, the origin of O_2^- production was evaluated using apocynin, an inhibitor of vascular NADPH oxidase. In each group, a significant increase of fluorescence was observed with addition of DHE compared to negative control (Fig. 30). However, no significant difference was observed between AGA and IUGR neonates. Finally, addition of apocynin induced a significant decrease of O_2^- production in UV from AGA females (Fig. 30A) and AGA and IUGR males (Fig. 30B), and in UAs from AGA females (Fig. 30C) and IUGR males (Fig. 30D). Figure 30E shows representative pictures of UV and UA sections after DHE incubation in AGA and IUGR neonates.

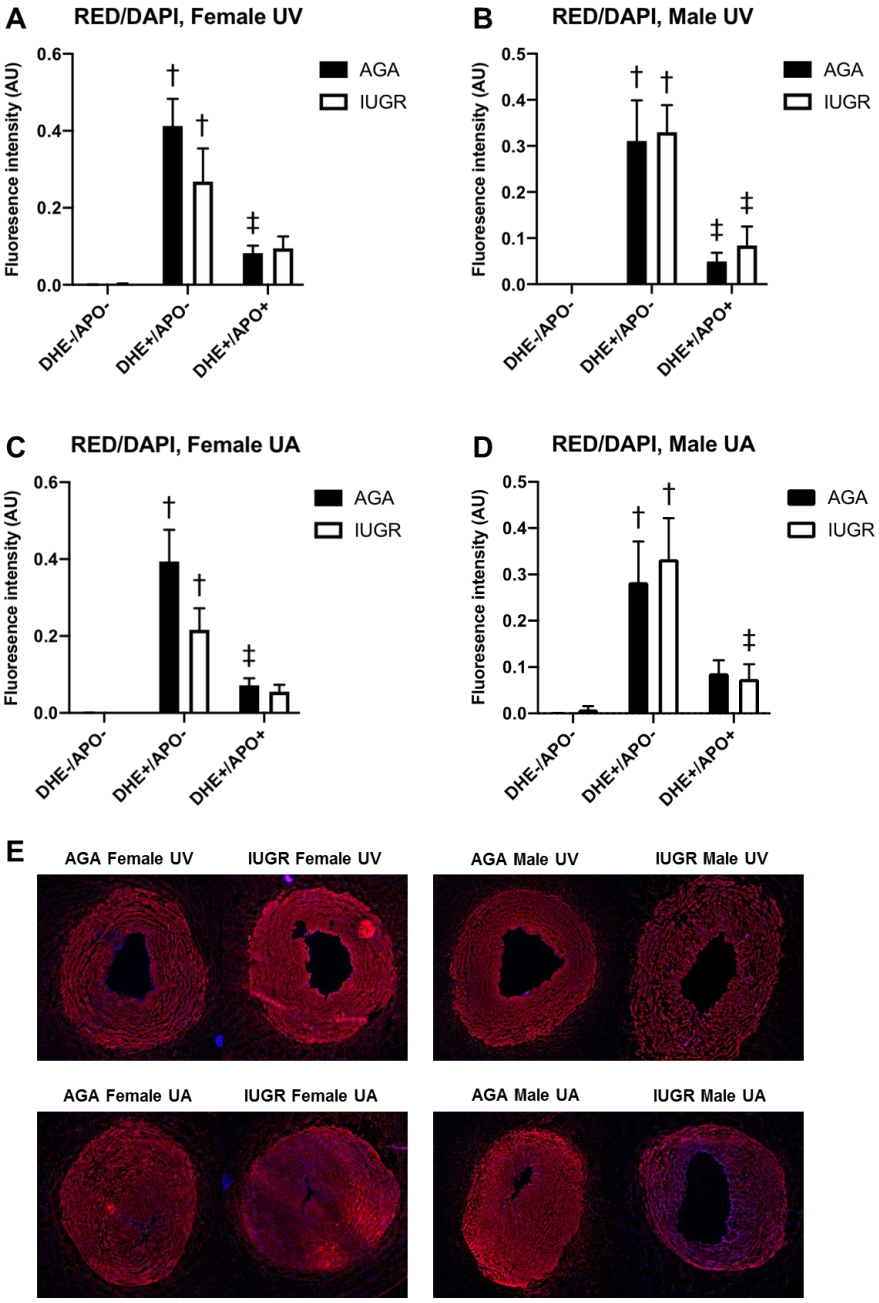

Figure 30: Superoxide anion production evaluated by DHE fluorescent dye in umbilical vessels.
Evaluation of O_2^- production in sections of umbilical cord from AGA and IUGR newborns using DHE fluorescent dye. Data are expressed as mean ± SEM (n = 6-7 in females; n = 6 in males). Data were analyzed by two-way ANOVA. † significant difference between DHE+/APO- and DHE-/APO-; ‡ significant difference between DHE+/APO+ and DHE+/APO- ($P < 0.05$).

3.3.2 Sirtuin 1 relative protein content in umbilical vein homogenates

No significant difference was found in relative protein amount of Sirtuin 1 (SIRT1) in UV homogenates between AGA and IUGR neonates, nor between females and males (Fig. 31).

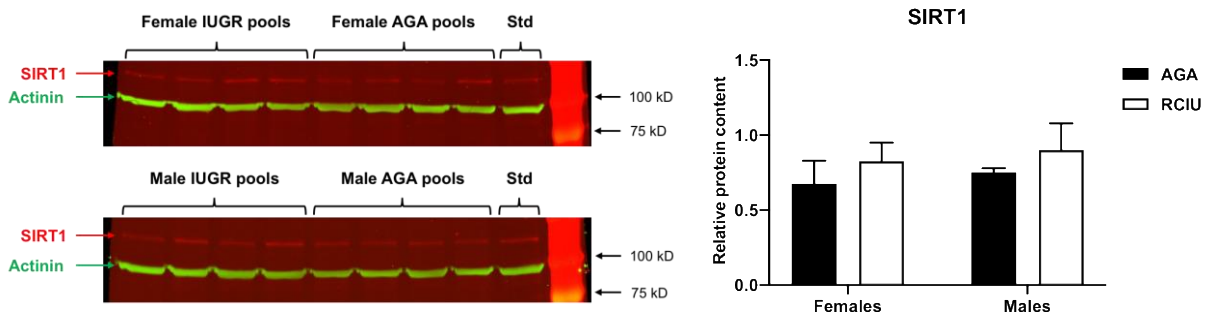

Figure 31: Relative amount of SIRT1 protein in umbilical vein homogenates.
Western blot analysis of SIRT1 protein in UV homogenates of AGA and IUGR newborns. For each group, samples from 40 patients were randomly distributed into 4 pools. A protein concentration of 80 µg per lane was loaded on the gel. For each pool, the target protein amount was normalized by the actinin protein content and reported to the amount measured in the "standard" sample (Std). Data are expressed as mean ± SEM (n=4 pools of 10 patients). No significant difference was found between groups after analysis by two-way ANOVA.

3.3.3 Stress-induced premature senescence in umbilical vein homogenates

β-galactosidase activity, a senescence marker, did not differ in UV homogenates between AGA and IUGR neonates. However, an increase was observed in IUGR females compared to IUGR males, but the difference was not statistically significant (Fig. 32).

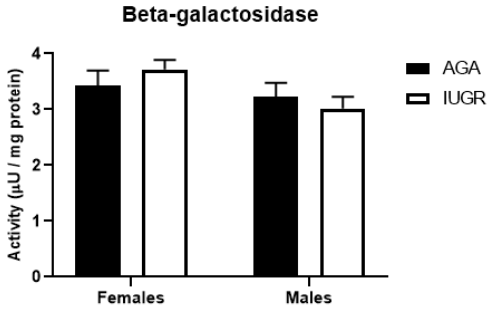

Figure 32: β-galactosidase activity in umbilical vein homogenates.
Measurement of beta-galactosidase activity in UV homogenates of AGA and IUGR newborns using a fluorometric assay kit. Data are expressed as mean ± SEM (n=5 patients) of the activity normalized by the protein content. No significant difference was found between groups after analysis by two-way ANOVA.

Discussion

Our research team previously demonstrated that IUGR is associated with structural alterations in UV of female and male neonates, and with a decreased NO-induced relaxation in female UV compared to AGA neonates [84]. The present study was designed to investigate mechanisms implicated in this sex-specific altered relaxant response to NO, in order to devise potential therapeutic interventions.

We postulated that the impaired NO-induced relaxation observed in UV of growth-restricted females could result from a down-regulation of pro-relaxant proteins and/or an up-regulation of pro-contracting proteins, resulting in an imbalance in vascular tone regulatory mechanisms.

1. Demographic data

Demographic data showed that maternal and gestational ages at delivery were homogenous between groups, avoiding two sources of bias. In contrast, fetal growth parameters (body weight, length, head circumference), along with placental weight, ponderal index and umbilical cord diameter, were significantly decreased in IUGR neonates. These observations were important to characterize our samples and confirm their classification between the AGA and IUGR study groups following the "2018 consensus criteria" [145]. However, to better characterize and separate SGA from IUGR neonates, it would be better to perform at least three US measurements to follow the fetal growth and detect the presence or not of a growth curve break. Unfortunately, such data were not available in most patient records. Indeed, a systematic screening of IUGR, with longitudinal follow-up of fetal growth and Doppler measurements, is not performed for all pregnancies, mainly because of financial considerations. Therefore, most growth-restricted fetuses are not detected before birth [141]. Given the non-negligible incidence of IUGR and its short- and long-term consequences, it would be necessary to find simple and cost-effective means to help early detection of pregnancies at risk to develop IUGR.

The body to placental weight ratio was increased in IUGR neonates, in contrast to other growth parameters. This is due to the fact that placental weight was reduced in a greater proportion (-30 to -32%) than body weight (-23 to -25%) between AGA and IUGR neonates. The one-third reduction observed in placental weight is consistent with an important contribution of placenta to the IUGR pathology. A correlation was already established between placenta and body weight at birth [84, 159].

We found a 12% decrease in the umbilical cord diameter between AGA and IUGR neonates. The umbilical cord diameter was shown to be strongly associated with placental and infant birth weight [160]. Previous studies have also established relationships between umbilical cord diameter determined by sonographic measurements and perinatal outcome [37, 161, 162]. Taken together, these observations suggest that all components of the fetoplacental unit are involved in IUGR, either as a cause or a consequence.

Finally, among the patients who filled the smoking status (53 to 69%), data showed a higher percentage of smokers in IUGR groups, with a significant difference only in male newborns. Tobacco being an important risk factor for IUGR development [122], these data seem to lead to the same conclusion, at least for males.

2. Smooth muscle investigations

We decided to focus our investigations on the NO/cGMP pathway. In the smooth muscle part of this signaling pathway, the main pro-relaxant proteins are sGC and PKG. sGC catalyzes the transformation of guanosine triphosphate (GTP) to cGMP, a second messenger able to activate, among others, PKG, leading to the vascular relaxation. At the opposite, the main counteracting components of NO-induced relaxation are PDEs, which degrade cGMP to 5'GMP. We therefore investigated the functional contribution of PDEs to the UV relaxation, by using the non-selective PDEs inhibitor IBMX. Cumulative concentrations of IBMX induced a dose-dependent relaxation in preconstricted UV rings, suggesting that PDEs directly contribute to vascular tone regulation in UV. In all groups, the vasorelaxant response to DEA/NO was significantly improved by pre-incubation with IBMX, suggesting that PDEs actively counteract NO-induced relaxation. Furthermore, when UV were pre-incubated with IBMX and preconstricted with 5-HT, the

alteration of NO-induced relaxation in UV of IUGR females was completely reversed and the difference observed between AGA and IUGR females in absence of IBMX was abolished. Such results indicate that PDEs are key elements in the regulation of UV vascular tone and that they probably contribute to the alteration of NO-induced relaxation observed in UV of IUGR females. The beneficial effect of PDEs inhibition on the relaxant response to NO suggests that PDEs could represent promising targets for therapeutic intervention.

However, a limit is due to the fact that relaxation curves in the presence of IBMX were established in UV isolated from other patients than the initial experiments performed in basal conditions (without IBMX). Some complementary experiments were therefore performed to investigate, on the same tissue, DEA/NO-induced relaxation in the absence or presence of IBMX, as well as spontaneous relaxation. In these conditions, pre-treatment with IBMX also significantly improved NO-induced relaxation in all groups, except in UV of AGA males preconstricted with 5-HT. In all groups and conditions, spontaneous relaxation was significantly weaker than the corresponding DEA/NO-induced relaxation. In UV preconstricted with 5-HT, spontaneous relaxation was similar in the presence or absence of IBMX. In contrast, when UV was preconstricted with U46619, we observed that the spontaneous relaxation in vascular rings pre-incubated with IBMX was significantly increased as compared to basal conditions. That could be explained by the fact that, in contrast to 5-HT which only has receptors on endothelial cell, U46619 interacts with receptors on endothelial cell and SMC and the resulting vasoconstriction seems to include activation of some PDEs [163-165]. Thus UV preconstricted by U46619 should be more sensitive to PDEs inhibition.

These complementary experiments were however done only on a limited number of subjects (n = 5–7) as compared to the data presented in Figures 14 and 15 (n = 15–51). Because of the high variability already observed, even if this was sufficient to test the direct effect of IBMX on DEA/NO-induced relaxation, because each vessel was its own control, this was clearly insufficient to directly compare pharmacological responses obtained in the different groups. Moreover, given that IBMX enhanced the UV sensitivity to NO, the range of DEA/NO concentrations used in these complementary experiments was adapted (10^{-10} to 10^{-4} M, instead of 10^{-8} to 10^{-4} M). Thus, a direct comparison with initial experiments was not possible. Nevertheless, these additional data confirmed that pre-incubation with IBMX could increase the

relaxant response of UV to NO, suggesting that improved relaxation observed in UV treated with IBMX compared to UV in basal conditions was really due to IBMX rather than explained by a variability between experiments performed on separate individuals.

In order to investigate molecular mechanisms implicated in the NO-induced relaxation, we analyzed by western blot specific proteins contributing to the NO/cGMP signaling pathway.
Our western blot analyses were performed using 4 pools of 10 patients for each study group to limit the influence of individual variability. To validate this approach, a part of the samples included in the pools were also tested individually. Both techniques gave similar results. The values obtained using individual samples were however more widely dispersed than those obtained using the pools. Moreover, the use of individual samples needs to perform much more experiments to reach statistically relevant results than pools, even if n is higher with individual samples, where n corresponds to the real number of patients tested, whereas with pools n corresponds only to the number of pools studied. We concluded that using pools of samples collected in many patients allows to generate accurate data in a less time-consuming and more cost-effective manner. This approach allows to highlight the main differences between groups and rapidly test a huge number of samples. The use of pools would be useful to identify a general molecular mechanism, but of course not to establish a diagnostic test, where individual values are of great importance.
Unlike to our initial expectations, western blot analyses did not show any decrease in the pro-relaxant proteins sGC and PKG in IUGR females compared to AGA, thus failing to explain the altered vasorelaxation observed in previous pharmacological experiments. Relative content of sGC was even twice higher in UV homogenates of IUGR females compared to AGA. In the same way, an increase in PKG protein content was also found in IUGR females. In contrast, in male UV, relative amount of sGC and PKG did not differ between AGA and IUGR newborns, which is consistent with pharmacological results.
It would be interesting to perform western blot analyses of PDE proteins. However, such experiments are complicated by the wide number of isoforms and the difficulty to find specific antibodies. Further investigations will nevertheless include western blot analyses of PDE1, PDE3, PDE4 and PDE5, known as major PDE isoforms in smooth muscle [166, 167].

As an increased protein level does not necessarily correlate with an increased enzymatic activity, sGC and PDEs activities were analyzed. Indeed, a low protein content can be compensated by a high activity.

The sGC enzymatic activity was evaluated by measuring the production of cGMP in isolated UV rings. cGMP synthesis measured in the present study was in a similar range than cGMP production previously reported in human pulmonary vessels in similar conditions [168].

Basal cGMP production was very low compared to NO-stimulated cGMP synthesis. sGC stimulation with DEA/NO caused an increase in cGMP content, which was significantly enhanced by pre-incubation with IBMX. These results suggest the presence of highly active PDEs. In UV incubated with IBMX and DEA/NO, cGMP content raised about 3 as high in IUGR females compared to AGA. Such data demonstrate a direct correlation between sGC protein content and cGMP production in UV of newborn females.

At the opposite, the cGMP degradation was measured in order to evaluate the PDEs activity. In UV homogenates, no significant difference was found between AGA and IUGR neonates, either in total or IBMX-sensitive cGMP PDEs activity. However, cGMP degradation measured in UV homogenates (in the range of nmol cGMP/mg protein/min) appeared to be more than 1000 times greater than cGMP production found in UV rings (in the range of pmol cGMP/mg protein/min). Such observation confirms the presence of highly active PDEs. However, IBMX-sensitive cGMP degradation represented only about 35% of the total cGMP PDEs activity. It is therefore surprising that pre-incubation with IBMX was sufficient to improve NO-induced relaxation in all groups and to reverse the alteration observed in UV of IUGR females. Indeed, IBMX-insensitive PDEs activity also greatly exceeded NO-stimulated cGMP production.

Nevertheless, sGC and PDEs activities cannot be directly compared because cGMP production was tested in intact UV rings, while cGMP degradation was measured, for technical reasons, in UV homogenates. Indeed, cGMP production was investigated in conditions close to *ex vivo* vasoreactivity, preserving tissular and subcellular organization. In contrast, tissular organization was lost in homogenates, which probably altered physiological regulation of PDEs activity. There is increasing evidence that subcellular microdomains contribute to the regulation of the NO/cGMP signaling pathway; in particular, PDEs are implicated in multimolecular regulatory complexes, called signalosomes, allowing close interactions between several

proteins, such as PDEs, PKG and sGC [169, 170]. Further investigations, using for example signalosome disruptors, could be of interest to better understand the contribution of PDEs and the role of signalosomes in the interaction between sGC, PKG and PDEs in UV.

Concerning PKG, we decided to perform western blots on UV homogenates prepared in non-denaturing conditions, because PKG was found to be more active as dimer than as monomer [171]. Although not significant, the increase observed in the dimers/monomers ratio in UV of IUGR neonates suggests that PKG could be more active in IUGR than in AGA neonates. Interestingly, western blots performed using non-denatured homogenates showed an inverse tendency as previously observed in denatured homogenates, with a lower relative PKG total amount in IUGR females than in AGA. Such data suggest that UV from IUGR females could contain a greater amount of membrane-linked PKG than AGA females, because non-denaturing conditions were performed in the absence of CHAPS, a detergent allowing to recover membrane-linked proteins. Indeed, in the absence of CHAPS in the extraction buffer, cellular membranes were not solubilized and membrane-linked PKG was not recovered, which could explain the decrease in PKG protein content between IUGR female data obtained by the two techniques. We therefore prepared new extracts from UVs isolated in additional patients from each group, either by the classical method (with CHAPS) or in non-denaturing conditions and absence of CHAPS. Although we observed no difference between AGA and IUGR neonates, this experiment revealed that a non-negligible amount of PKG was membrane-linked, as shown thanks the second extraction performed on the pellet obtained in non-denaturing conditions. As cytosolic PKG is more associated to PKG type I (PKG1) and PKG type II (PKG2) more predominantly localized at the plasma membrane [172], analysis of these two types should be done to better investigate the role of PKG in IUGR. Whether PKG1 is widely present in the vasculature to induce relaxation [173], PKG2 is normally more limited to specific cell types in bone, intestine, brain and kidney [174]. Furthermore, mammalian cells express two PKG1 isoforms, PKG1α and PKG1β, generated by alternative splicing [175]. Interestingly, PKG1α has a high sensitivity to cGMP and is activated by lower concentrations of the cGMP than the β-isoform of PKG1 [176]. Investigation of these two PKG1 isoforms could therefore provide information on the contribution of PKG to the regulation of UV in AGA and IUGR neonates.

The increase in sGC and PKG protein amounts and in sGC activity observed in IUGR females could result from compensatory mechanisms in response to the impaired NO-induced relaxation, as an attempt to improve this vasodilation. A compensatory upregulation of NO production has been described in the fetoplacental circulation in case of fetal growth restriction in humans [177]. Similar compensatory mechanisms were previously observed by Peyter *et al.* in pulmonary arteries of adult mice born in hypoxic conditions: PKG protein content and sGC activity were increased in pulmonary arteries of adult females exposed to perinatal hypoxia, whereas PDE1 contribution was enhanced, resulting in a decreased endothelium-dependent relaxation [178].

3. Endothelium investigations

The second part of this work consisted in the study of the endothelial part of the NO/cGMP relaxing pathway, with the NO bioavailability as the main point.

In the endothelial cell, NO is produced enzymatically via eNOS before diffusing into the SMC to activate sGC and the subsequent enzymatic cascade, as previously discussed. Thus, the eNOS relative protein content was analyzed by western blot in UV homogenates and appeared lower in IUGR than AGA males, whereas no significant change was found between AGA and IUGR females. Such data suggest that, although pharmacological experiments did not show any impairment of NO-induced relaxation in IUGR males compared to AGA, the decreased eNOS protein content observed in IUGR males could result in endothelial dysfunction and thus contribute to IUGR development. However, eNOS should be further studied before drawing conclusions. In particular, eNOS phosphorylation or dimerization should be investigated to evaluate potential increase or decrease in eNOS activity in case of IUGR.

Besides eNOS activity, NO bioavailability can be influenced by oxidative stress. Indeed, NO is able to react with some reactive oxygen species (ROS) such as O_2^-. ROS are detoxified, among others, by different antioxidant enzymes like SOD, catalase or glutathione peroxidase. In normal conditions, there is a balance between oxidant and antioxidant species. In pathological conditions, an imbalance often leads to a rise in the concentration of O_2^-, able to interact with

NO to form peroxynitrite, a highly toxic species. This phenomenon not only decreases NO bioavailability, but also maintains oxidative stress through peroxynitrite production. In case of overactivation of eNOS, an increased production of NO can also be responsible of an enhanced production of peroxynitrite through interaction with O_2^-, which thus is trapped by the excess of NO rather than SOD [179].

Analyses of SOD and catalase relative protein contents did not show any difference between AGA and IUGR. However, relative amounts of SOD1, SOD3 and catalase were lower in female groups compared to males. These results suggest that either females have reduced antioxidant defenses compared to males and are thus more sensitive to ROS, or males have enhanced antioxidant enzymes content because they are submitted to higher oxidative stress than females. These results could be completed by quantification of glutathione peroxidase. Moreover, analysis of the oxidant part of the balance is necessary before any conclusion.

O_2^- production was measured using the DHE fluorescent dye on frozen umbilical cord sections in order to evaluate the oxidative status. The fluorescence results from the DHE oxidation in presence of O_2^- [180]. However, such experiments did not show a significant difference in fluorescence between AGA and IUGR. Nevertheless, with a similar O_2^- production, but some decreased antioxidant defenses, females could be more affected by oxidative stress than males. However, these results were obtained in only 6 to 7 samples per group and showed an important variability; they should be therefore considered as preliminary and the number of samples should be increased to confirm them.

Among enzymatic sources for ROS production in endothelial cell, we can cite the NADPH oxidase or the uncoupled eNOS producing O_2^- instead of NO [181]. Some umbilical cord sections were then incubated with apocynin, a NADPH oxidase inhibitor, in addition to DHE. A clear decrease in red fluorescence was observed in UV and UAs after a DHE-apocynin incubation compared to DHE only, suggesting that, in all groups, a large majority of O_2^- production is due to the NADPH oxidase activity. Previous observations already showed that NADPH oxidase constituted the major enzymatic source of ROS in the vasculature [182]. To further investigate the contribution of different NADPH oxidases in O_2^- production in UV, analysis of their relative protein content should be investigated by western blot. Furthermore, to study whether the resting part of O_2^-

is due to eNOS uncoupling, similar experiments should be performed in the presence of a NOS inhibitor like NLA. In case of eNOS uncoupling, O_2^- production should be decreased by incubation with NLA.

eNOS uncoupling leads to an increased O_2^- concentration and reduced NO production. To investigate NO production, umbilical cord cryosections will be further incubated with 4,5-diaminofluorescein diacetate (DAF-2 DA), a NO fluorescent probe, to highlight a possible endothelial dysfunction [183].

Regardless the origin of O_2^-, an increase in ROS production can contribute to alter the eNOS cofactor BH_4, which, if it is limited or absent, can lead to eNOS uncoupling, thus producing O_2^- in place to NO and increasing the ROS concentration in a vicious circle [184].

Oxidative stress is a major stimulus, with other factors implicated in vascular pathologies, for the induction of endothelial cell senescence [185, 186], by acting at multiple subcellular levels [187]. It results in different pathophysiological consequences, such as decreased vasorelaxation, increased vascular inflammation or increased thrombosis [186].

SIRT1 is a protein involved in the regulation of energy metabolism, stress responses and cell survival [188]; its overexpression in endothelial cells prevents oxidative stress-induced premature senescence [189], most probably by promoting the deacetylation and consequent inactivation of p53 [190]. SIRT1 relative protein content was similar between AGA and IUGR neonates, as well as between females and males. However, some studies showed that NO may counteract senescence in the context of cellular stress, through upregulation of SIRT1 [191]. Expression of SIRT1 should be thus directly linked to NO levels.

To better investigate whether there is "stress-induced premature senescence" in IUGR UV, we investigated the senescence-associated β-galactosidase (SA-β-gal) as a marker in UV homogenates of our four study groups. However, we did not observe any difference between groups, suggesting that stress-induced premature senescence level was similar in all groups. This observation is consistent with the SIRT1 relative amounts measured in UV.

Taken together, these results are insufficient to draw precise conclusions on the contribution of endothelial alterations to the development of IUGR. Indeed, further investigations need to be

performed, such as evaluation of NO production and eNOS regulatory mechanisms like phosphorylation, dimerization or eNOS cofactors concentration. Furthermore, results about O_2^- production have to be completed. Antioxidant capacity could be also further studied. Finally, functional studies should be performed to investigate endothelium-dependent relaxation in AGA and IUGR UV.

4. Conclusion

In summary, investigations performed in the UV smooth muscle allowed to highlight a functional alteration in the relaxation of UV from IUGR females compared to AGA. This impairment of NO-induced relaxation was associated with several alterations in the NO/cGMP signaling pathway. No difference in molecular components of this pathway were found between AGA and IUGR males, which is consistent with functional investigations. Furthermore, beneficial effects of the non-specific PDEs inhibitor IBMX on NO-induced relaxation suggest that PDEs are implicated in the observed alteration and they could represent promising targets for therapeutic intervention.

In the endothelium, eNOS relative protein amount was lower in UV from IUGR than AGA males, whereas no difference was found in females. In contrast, antioxidant defenses, ROS production and stress-induced premature senescence appeared similar between AGA and IUGR neonates. However, further investigations will be necessary to better characterize the contribution of the endothelium to vascular tone regulation in UV from AGA and IUGR neonates.

Finally, our investigations highlighted many differences in UV reactivity and molecular components between females and males. We can therefore hypothesize that regulation of vasorelaxation differs between both sexes and that mechanisms implicated in the alteration of NO/cGMP pathway and thus development of IUGR are sex-specific.

References

1. Lepercq, J. and P. Boileau, *Physiology of the fetal growth.* EMC - Gynécologie-Obstétrique, 2005. **2**(3): p. 199-208.
2. *Université Virtuelle de Maïeutique Francophone UVMaF: Le développement du foetus*. Available from: http://campus.cerimes.fr/maieutique/UE-obstetrique/dev_foetus/site/html/2.html.
3. Lau, E.Y., et al., *Maternal weight gain in pregnancy and risk of obesity among offspring: a systematic review.* J Obes, 2014. **2014**: p. 524939.
4. Butte, N.F. and J.C. King, *Energy requirements during pregnancy and lactation.* Public Health Nutr, 2005. **8**(7A): p. 1010-27.
5. Viswanathan, M., et al., *Outcomes of maternal weight gain.* Evid Rep Technol Assess (Full Rep), 2008(168): p. 1-223.
6. Abrams, B., S.L. Altman, and K.E. Pickett, *Pregnancy weight gain: still controversial.* Am J Clin Nutr, 2000. **71**(5 Suppl): p. 1233S-41S.
7. Battaglia, F.C., *Placental transport and utilization of amino acids and carbohydrates.* Fed Proc, 1986. **45**(10): p. 2508-12.
8. Hytten, F. and G. Chamberlain, *Clinical physiology in obstetrics*. 2 ed. 1991, Oxford, Boston, Melbourne: Blackwell Scientific Publications.
9. Kalhan, S.C., et al., *Glucose production in pregnant women at term gestation. Sources of glucose for human fetus.* J Clin Invest, 1979. **63**(3): p. 388-94.
10. Battaglia, F.C. and G. Meschia, *Principal substrates of fetal metabolism.* Physiol Rev, 1978. **58**(2): p. 499-527.
11. Hummel, L., et al., *Maternal plasma triglycerides as a source of fetal fatty acids.* Acta Biol Med Ger, 1976. **35**(12): p. 1635-41.
12. Fowden, A.L. and A.J. Forhead, *Endocrine regulation of feto-placental growth.* Horm Res, 2009. **72**(5): p. 257-65.
13. Fowden, A.L., J. Li, and A.J. Forhead, *Glucocorticoids and the preparation for life after birth: are there long-term consequences of the life insurance?* Proc Nutr Soc, 1998. **57**(1): p. 113-22.
14. Fowden, A.L. and A.J. Forhead, *Endocrine mechanisms of intrauterine programming.* Reproduction, 2004. **127**(5): p. 515-26.
15. Fowden, A.L. and A.J. Forhead, *Hormones as epigenetic signals in developmental programming.* Exp Physiol, 2009. **94**(6): p. 607-25.
16. Jansson, T. and T.L. Powell, *Role of the placenta in fetal programming: underlying mechanisms and potential interventional approaches.* Clin Sci (Lond), 2007. **113**(1): p. 1-13.
17. Seckl, J.R., *Prenatal glucocorticoids and long-term programming.* Eur J Endocrinol, 2004. **151 Suppl 3**: p. U49-62.
18. Fowden, A.L. and A.J. Forhead, *Glucocorticoids as regulatory signals during intrauterine development.* Exp Physiol, 2015. **100**(12): p. 1477-87.
19. Barker, D.J., *Intrauterine programming of coronary heart disease and stroke.* Acta Paediatr Suppl, 1997. **423**: p. 178-82; discussion 183.
20. Barker, D.J., *Fetal origins of cardiovascular disease.* Ann Med, 1999. **31 Suppl 1**: p. 3-6.
21. Barker, D.J., *Adult consequences of fetal growth restriction.* Clin Obstet Gynecol, 2006. **49**(2): p. 270-83.
22. Barker, D.J., *In utero programming of cardiovascular disease.* Theriogenology, 2000. **53**(2): p. 555-74.
23. Joss-Moore, L.A. and R.H. Lane, *The developmental origins of adult disease.* Curr Opin Pediatr, 2009. **21**(2): p. 230-4.
24. Anderson, C.M., et al., *Placental insufficiency leads to developmental hypertension and mesenteric artery dysfunction in two generations of Sprague-Dawley rat offspring.* Biol Reprod, 2006. **74**(3): p. 538-44.
25. Vickers, M.H., *Early life nutrition, epigenetics and programming of later life disease.* Nutrients, 2014. **6**(6): p. 2165-78.

26. Burdge, G.C. and K.A. Lillycrop, *Nutrition, epigenetics, and developmental plasticity: implications for understanding human disease.* Annu Rev Nutr, 2010. **30**: p. 315-39.
27. Gluckman, P.D., et al., *Effect of in utero and early-life conditions on adult health and disease.* N Engl J Med, 2008. **359**(1): p. 61-73.
28. Gluckman, P.D., et al., *Epigenetic mechanisms that underpin metabolic and cardiovascular diseases.* Nat Rev Endocrinol, 2009. **5**(7): p. 401-8.
29. Hales, C.N. and D.J. Barker, *Type 2 (non-insulin-dependent) diabetes mellitus: the thrifty phenotype hypothesis.* Diabetologia, 1992. **35**(7): p. 595-601.
30. Kwon, E.J. and Y.J. Kim, *What is fetal programming?: a lifetime health is under the control of in utero health.* Obstet Gynecol Sci, 2017. **60**(6): p. 506-519.
31. Roseboom, T.J., et al., *Coronary heart disease after prenatal exposure to the Dutch famine, 1944-45.* Heart, 2000. **84**(6): p. 595-8.
32. Stein, A.D., et al., *Intrauterine famine exposure and body proportions at birth: the Dutch Hunger Winter.* Int J Epidemiol, 2004. **33**(4): p. 831-6.
33. Burton, G.J. and A.L. Fowden, *The placenta: a multifaceted, transient organ.* Philos Trans R Soc Lond B Biol Sci, 2015. **370**(1663): p. 20140066.
34. Lofthouse, E.M., *The accumulation of glutamate in the placental syncytiotrophoblast as a driver of membrane transport*, in *Faculty of Medicine*. 2014, University of Southampton.
35. Acharya, G., et al., *Hemodynamic aspects of normal human feto-placental (umbilical) circulation.* Acta Obstet Gynecol Scand, 2016. **95**(6): p. 672-82.
36. Tetro, N., et al., *The Placental Barrier: the Gate and the Fate in Drug Distribution.* Pharm Res, 2018. **35**(4): p. 71.
37. Di Naro, E., et al., *Umbilical cord morphology and pregnancy outcome.* Eur J Obstet Gynecol Reprod Biol, 2001. **96**(2): p. 150-7.
38. *Vita34: Umbilical cord tissue - Particularly rich in valuable stem cells*. Available from: https://www.vita34.ch/en/cord-blood/cord-tissue/.
39. Weissman, A., et al., *Sonographic measurements of the umbilical cord and vessels during normal pregnancies.* J Ultrasound Med, 1994. **13**(1): p. 11-4.
40. Persutte, W.H. and J. Hobbins, *Single umbilical artery: a clinical enigma in modern prenatal diagnosis.* Ultrasound Obstet Gynecol, 1995. **6**(3): p. 216-29.
41. Hegazy, A.A., *Anatomy and embryology of umbilicus in newborns: a review and clinical correlations.* Front Med, 2016. **10**(3): p. 271-7.
42. Moshiri, M., et al., *Comprehensive imaging review of abnormalities of the umbilical cord.* Radiographics, 2014. **34**(1): p. 179-96.
43. *Stanford Children's Health: Fetal Circulation*. Available from: https://www.stanfordchildrens.org/en/topic/default?id=fetal-circulation-90-P01790.
44. Vizza, E., et al., *The collagen skeleton of the human umbilical cord at term. A scanning electron microscopy study after 2N-NaOH maceration.* Reprod Fertil Dev, 1996. **8**(5): p. 885-94.
45. Takechi, K., Y. Kuwabara, and M. Mizuno, *Ultrastructural and immunohistochemical studies of Wharton's jelly umbilical cord cells.* Placenta, 1993. **14**(2): p. 235-45.
46. Strong, T.H., Jr., J.P. Elliott, and T.G. Radin, *Non-coiled umbilical blood vessels: a new marker for the fetus at risk.* Obstet Gynecol, 1993. **81**(3): p. 409-11.
47. Baergen, R.N., *Umbilical Cord Pathology.* Surg Pathol Clin, 2013. **6**(1): p. 61-85.
48. Ismail, K.I., et al., *Abnormal placental cord insertion and adverse pregnancy outcomes: a systematic review and meta-analysis.* Syst Rev, 2017. **6**(1): p. 242.
49. Fleischer, A.C., et al., *Fleischer's Sonography in Obstetrics and Gynecology*. 2017, OH, United States: McGraw-Hill Education.
50. Fox, S.B. and T.Y. Khong, *Lack of innervation of human umbilical cord. An immunohistological and histochemical study.* Placenta, 1990. **11**(1): p. 59-62.
51. Thompson, R.S. and B.J. Trudinger, *Doppler waveform pulsatility index and resistance, pressure and flow in the umbilical placental circulation: an investigation using a mathematical model.* Ultrasound Med Biol, 1990. **16**(5): p. 449-58.
52. Lackman, F., et al., *Fetal umbilical cord oxygen values and birth to placental weight ratio in relation to size at birth.* Am J Obstet Gynecol, 2001. **185**(3): p. 674-82.
53. Wareing, M., *Oxygen sensitivity, potassium channels, and regulation of placental vascular tone.* Microcirculation, 2014. **21**(1): p. 58-66.

54. Ghimire, K., et al., *Nitric oxide: what's new to NO?* Am J Physiol Cell Physiol, 2017. **312**(3): p. C254-C262.
55. Stuehr, D.J., et al., *Update on mechanism and catalytic regulation in the NO synthases.* J Biol Chem, 2004. **279**(35): p. 36167-70.
56. Erez, A., et al., *Requirement of argininosuccinate lyase for systemic nitric oxide production.* Nat Med, 2011. **17**(12): p. 1619-26.
57. Stuehr, D.J., *Enzymes of the L-arginine to nitric oxide pathway.* J Nutr, 2004. **134**(10 Suppl): p. 2748S-2751S; discussion 2765S-2767S.
58. Katusic, Z.S., L.V. d'Uscio, and K.A. Nath, *Vascular protection by tetrahydrobiopterin: progress and therapeutic prospects.* Trends Pharmacol Sci, 2009. **30**(1): p. 48-54.
59. Scotland, R.S., et al., *Functional reconstitution of endothelial nitric oxide synthase reveals the importance of serine 1179 in endothelium-dependent vasomotion.* Circ Res, 2002. **90**(8): p. 904-10.
60. Fleming, I., et al., *Phosphorylation of Thr(495) regulates Ca(2+)/calmodulin-dependent endothelial nitric oxide synthase activity.* Circ Res, 2001. **88**(11): p. E68-75.
61. Behrendt, D. and P. Ganz, *Endothelial function. From vascular biology to clinical applications.* Am J Cardiol, 2002. **90**(10C): p. 40L-48L.
62. *Integrative therapeutics: Nitric Oxide Synthesis: an overview*. Available from: https://www.integrativepro.com/Resources/Integrative-Blog/2014/Nitric-Oxide-Synthesis-An-Overview.
63. Lincoln, T.M., et al., *cGMP signaling through cAMP- and cGMP-dependent protein kinases.* Adv Pharmacol, 1995. **34**: p. 305-22.
64. Sausbier, M., et al., *Mechanisms of NO/cGMP-dependent vasorelaxation.* Circ Res, 2000. **87**(9): p. 825-30.
65. Shimizu-Albergine, M., et al., *Individual cerebellar Purkinje cells express different cGMP phosphodiesterases (PDEs): in vivo phosphorylation of cGMP-specific PDE (PDE5) as an indicator of cGMP-dependent protein kinase (PKG) activation.* J Neurosci, 2003. **23**(16): p. 6452-9.
66. Tegeder, I., et al., *Reduced inflammatory hyperalgesia with preservation of acute thermal nociception in mice lacking cGMP-dependent protein kinase I.* Proc Natl Acad Sci U S A, 2004. **101**(9): p. 3253-7.
67. Hofmann, F., et al., *cGMP regulated protein kinases (cGK).* Handb Exp Pharmacol, 2009(191): p. 137-62.
68. Agostino, P.V., S.A. Plano, and D.A. Golombek, *Sildenafil accelerates reentrainment of circadian rhythms after advancing light schedules.* Proc Natl Acad Sci U S A, 2007. **104**(23): p. 9834-9.
69. Francis, S.H., et al., *cGMP-dependent protein kinases and cGMP phosphodiesterases in nitric oxide and cGMP action.* Pharmacol Rev, 2010. **62**(3): p. 525-63.
70. Burton, G.J., et al., *Rheological and physiological consequences of conversion of the maternal spiral arteries for uteroplacental blood flow during human pregnancy.* Placenta, 2009. **30**(6): p. 473-82.
71. Ferrazzi, E., et al., *Temporal sequence of abnormal Doppler changes in the peripheral and central circulatory systems of the severely growth-restricted fetus.* Ultrasound Obstet Gynecol, 2002. **19**(2): p. 140-6.
72. Levytska, K., et al., *Placental Pathology in Relation to Uterine Artery Doppler Findings in Pregnancies with Severe Intrauterine Growth Restriction and Abnormal Umbilical Artery Doppler Changes.* Am J Perinatol, 2017. **34**(5): p. 451-457.
73. Huang, P.L., *eNOS, metabolic syndrome and cardiovascular disease.* Trends Endocrinol Metab, 2009. **20**(6): p. 295-302.
74. Alp, N.J. and K.M. Channon, *Regulation of endothelial nitric oxide synthase by tetrahydrobiopterin in vascular disease.* Arterioscler Thromb Vasc Biol, 2004. **24**(3): p. 413-20.
75. Kuzkaya, N., et al., *Interactions of peroxynitrite, tetrahydrobiopterin, ascorbic acid, and thiols: implications for uncoupling endothelial nitric-oxide synthase.* J Biol Chem, 2003. **278**(25): p. 22546-54.
76. Achan, V., et al., *Asymmetric dimethylarginine causes hypertension and cardiac dysfunction in humans and is actively metabolized by dimethylarginine dimethylaminohydrolase.* Arterioscler Thromb Vasc Biol, 2003. **23**(8): p. 1455-9.

77. Kietadisorn, R., R.P. Juni, and A.L. Moens, *Tackling endothelial dysfunction by modulating NOS uncoupling: new insights into its pathogenesis and therapeutic possibilities.* Am J Physiol Endocrinol Metab, 2012. **302**(5): p. E481-95.
78. Bachetti, T., et al., *Arginase pathway in human endothelial cells in pathophysiological conditions.* J Mol Cell Cardiol, 2004. **37**(2): p. 515-23.
79. Xu, W., et al., *Increased arginase II and decreased NO synthesis in endothelial cells of patients with pulmonary arterial hypertension.* FASEB J, 2004. **18**(14): p. 1746-8.
80. Morris, N.H., B.M. Eaton, and G. Dekker, *Nitric oxide, the endothelium, pregnancy and pre-eclampsia.* Br J Obstet Gynaecol, 1996. **103**(1): p. 4-15.
81. Becker, R.M., et al., *Reduced serum amino acid concentrations in infants with necrotizing enterocolitis.* J Pediatr, 2000. **137**(6): p. 785-93.
82. Casanello, P. and L. Sobrevia, *Intrauterine growth retardation is associated with reduced activity and expression of the cationic amino acid transport systems y+/hCAT-1 and y+/hCAT-2B and lower activity of nitric oxide synthase in human umbilical vein endothelial cells.* Circ Res, 2002. **91**(2): p. 127-34.
83. Chen, J., et al., *Effect of L-arginine and sildenafil citrate on intrauterine growth restriction fetuses: a meta-analysis.* BMC Pregnancy Childbirth, 2016. **16**: p. 225.
84. Peyter, A.C., et al., *Intrauterine growth restriction is associated with structural alterations in human umbilical cord and decreased nitric oxide-induced relaxation of umbilical vein.* Placenta, 2014. **35**(11): p. 891-9.
85. Gilbert, J.S. and M.J. Nijland, *Sex differences in the developmental origins of hypertension and cardiorenal disease.* Am J Physiol Regul Integr Comp Physiol, 2008. **295**(6): p. R1941-52.
86. Pels, A., et al., *Maternal Sildenafil vs Placebo in Pregnant Women With Severe Early-Onset Fetal Growth Restriction: A Randomized Clinical Trial.* JAMA Netw Open, 2020. **3**(6): p. e205323.
87. Sclowitz, I.K. and S. Santos Ida, *[Risk factors for repetition of low birth weight, intrauterine growth retardation, and prematurity in subsequent pregnancies: a systematic review].* Cad Saude Publica, 2006. **22**(6): p. 1129-36.
88. Nardozza, L.M., et al., *Fetal growth restriction: current knowledge.* Arch Gynecol Obstet, 2017. **295**(5): p. 1061-1077.
89. Sharma, D., et al., *Intrauterine growth restriction - part 1.* J Matern Fetal Neonatal Med, 2016. **29**(24): p. 3977-87.
90. Froen, J.F., et al., *Restricted fetal growth in sudden intrauterine unexplained death.* Acta Obstet Gynecol Scand, 2004. **83**(9): p. 801-7.
91. American College of, O., B.-O. Gynecologists' Committee on Practice, and f.-F. the Society, *ACOG Practice Bulletin No. 204: Fetal Growth Restriction.* Obstet Gynecol, 2019. **133**(2): p. e97-e109.
92. *ACOG Practice Bulletin - Clinical Management Guidelines for Obstetrician-Gynecologists - Number 13, February 2000.* Obstetrics and Gynecology, 2000. **95**(2): p. 1-7.
93. Kiserud, T., et al., *The World Health Organization fetal growth charts: concept, findings, interpretation, and application.* Am J Obstet Gynecol, 2018. **218**(2S): p. S619-S629.
94. Gluckman, P.D., et al., *Fetal growth in late gestation--a constrained pattern of growth.* Acta Paediatr Scand Suppl, 1990. **367**: p. 105-10.
95. Wollmann, H.A., *Intrauterine growth restriction: definition and etiology.* Horm Res, 1998. **49 Suppl 2**: p. 1-6.
96. Bernstein, P.S. and M.Y. Divon, *Etiologies of fetal growth restriction.* Clin Obstet Gynecol, 1997. **40**(4): p. 723-9.
97. Snijders, R.J., et al., *Fetal growth retardation: associated malformations and chromosomal abnormalities.* Am J Obstet Gynecol, 1993. **168**(2): p. 547-55.
98. Hendrix, N. and V. Berghella, *Non-placental causes of intrauterine growth restriction.* Semin Perinatol, 2008. **32**(3): p. 161-5.
99. Wallenstein, M.B., et al., *Fetal congenital heart disease and intrauterine growth restriction: a retrospective cohort study.* J Matern Fetal Neonatal Med, 2012. **25**(6): p. 662-5.
100. Balayla, J. and H.A. Abenhaim, *Incidence, predictors and outcomes of congenital diaphragmatic hernia: a population-based study of 32 million births in the United States.* J Matern Fetal Neonatal Med, 2014. **27**(14): p. 1438-44.
101. Priyadarshi, A., et al., *Transient Neonatal Diabetes Mellitus followed by recurrent asymptomatic hypoglycaemia: a case report.* BMC Pediatr, 2015. **15**: p. 200.

102. Lewi, L., et al., *Clinical outcome and placental characteristics of monochorionic diamniotic twin pairs with early- and late-onset discordant growth.* Am J Obstet Gynecol, 2008. **199**(5): p. 511 e1-7.
103. Heinonen, S., P. Taipale, and S. Saarikoski, *Weights of placentae from small-for-gestational age infants revisited.* Placenta, 2001. **22**(5): p. 399-404.
104. Zygmunt, M., *Placental circulation: Clinical significance.* Early Pregnancy, 2001. **5**(1): p. 72-3.
105. Djakovic, A., et al., *[Severe foetal growth retardation in a patient with uterus bicornis, velamentous insertion and partial placental abruption in the 26th week of gestation--a case report].* Z Geburtshilfe Neonatol, 2007. **211**(4): p. 169-73.
106. Silver, K.L., et al., *Complement driven innate immune response to malaria: fuelling severe malarial diseases.* Cell Microbiol, 2010. **12**(8): p. 1036-45.
107. Langer, H.F., et al., *Complement-mediated inhibition of neovascularization reveals a point of convergence between innate immunity and angiogenesis.* Blood, 2010. **116**(22): p. 4395-403.
108. Conroy, A.L., et al., *Complement activation and the resulting placental vascular insufficiency drives fetal growth restriction associated with placental malaria.* Cell Host Microbe, 2013. **13**(2): p. 215-26.
109. Wilkins-Haug, L., B. Quade, and C.C. Morton, *Confined placental mosaicism as a risk factor among newborns with fetal growth restriction.* Prenat Diagn, 2006. **26**(5): p. 428-32.
110. Szentpeteri, I., et al., *Placental gene expression patterns of endoglin (CD105) in intrauterine growth restriction.* J Matern Fetal Neonatal Med, 2014. **27**(4): p. 350-4.
111. Strobino, D.M., et al., *Mechanisms for maternal age differences in birth weight.* Am J Epidemiol, 1995. **142**(5): p. 504-14.
112. Albouy-Llaty, M., et al., *Influence of fetal and parental factors on intrauterine growth measurements: results of the EDEN mother-child cohort.* Ultrasound Obstet Gynecol, 2011. **38**(6): p. 673-80.
113. Cogswell, M.E. and R. Yip, *The influence of fetal and maternal factors on the distribution of birthweight.* Semin Perinatol, 1995. **19**(3): p. 222-40.
114. Galan, H.L., et al., *Reduction of subcutaneous mass, but not lean mass, in normal fetuses in Denver, Colorado.* Am J Obstet Gynecol, 2001. **185**(4): p. 839-44.
115. Timmermans, S., et al., *The Mediterranean diet and fetal size parameters: the Generation R Study.* Br J Nutr, 2012. **108**(8): p. 1399-409.
116. Knudsen, V.K., et al., *Major dietary patterns in pregnancy and fetal growth.* Eur J Clin Nutr, 2008. **62**(4): p. 463-70.
117. Han, Z., et al., *Maternal underweight and the risk of preterm birth and low birth weight: a systematic review and meta-analyses.* Int J Epidemiol, 2011. **40**(1): p. 65-101.
118. Nohr, E.A., et al., *Combined associations of prepregnancy body mass index and gestational weight gain with the outcome of pregnancy.* Am J Clin Nutr, 2008. **87**(6): p. 1750-9.
119. Abenhaim, H.A., et al., *Effect of prepregnancy body mass index categories on obstetrical and neonatal outcomes.* Arch Gynecol Obstet, 2007. **275**(1): p. 39-43.
120. Radulescu, L., et al., *The implications and consequences of maternal obesity on fetal intrauterine growth restriction.* J Med Life, 2013. **6**(3): p. 292-8.
121. Mayer, C. and K.S. Joseph, *Fetal growth: a review of terms, concepts and issues relevant to obstetrics.* Ultrasound Obstet Gynecol, 2013. **41**(2): p. 136-45.
122. Andres, R.L. and M.C. Day, *Perinatal complications associated with maternal tobacco use.* Semin Neonatol, 2000. **5**(3): p. 231-41.
123. Haddon, W., Jr., R.E. Nesbitt, and R. Garcia, *Smoking and pregnancy: carbon monoxide in blood during gestation and at term.* Obstet Gynecol, 1961. **18**: p. 262-7.
124. Goel, P., et al., *Effects of passive smoking on outcome in pregnancy.* J Postgrad Med, 2004. **50**(1): p. 12-6.
125. Norsa'adah, B. and O. Salinah, *The Effect of Second-Hand Smoke Exposure during Pregnancy on the Newborn Weight in Malaysia.* Malays J Med Sci, 2014. **21**(2): p. 44-53.
126. Lundsberg, L.S., M.B. Bracken, and A.F. Saftlas, *Low-to-moderate gestational alcohol use and intrauterine growth retardation, low birthweight, and preterm delivery.* Ann Epidemiol, 1997. **7**(7): p. 498-508.
127. Yang, Q., et al., *A case-control study of maternal alcohol consumption and intrauterine growth retardation.* Ann Epidemiol, 2001. **11**(7): p. 497-503.

128. Zuckerman, B., et al., *Effects of Maternal Marijuana and Cocaine Use on Fetal Growth.* New England Journal of Medicine, 1989. **320**(12): p. 762-768.
129. Ladhani, N.N.N., et al., *Prenatal amphetamine exposure and birth outcomes: a systematic review and metaanalysis.* American Journal of Obstetrics and Gynecology, 2011. **205**(3).
130. Wen, S.W., et al., *Maternal exposure to folic acid antagonists and placenta-mediated adverse pregnancy outcomes.* Canadian Medical Association Journal, 2008. **179**(12): p. 1263-1268.
131. Lopez, M., et al., *Risk of intrauterine growth restriction among HIV-infected pregnant women: a cohort study.* European Journal of Clinical Microbiology & Infectious Diseases, 2015. **34**(2): p. 223-230.
132. Huang, Q.T., et al., *Maternal HCV infection is associated with intrauterine fetal growth disturbance: A meta-analysis of observational studies.* Medicine, 2016. **95**(35).
133. Murki, S. and D. Sharma, *Intrauterine Growth Retardation - A Review Article.* Journal of Neonatal Biology, 2014. **3**(3).
134. Lewis, A.J., E. Austin, and M. Galbally, *Prenatal maternal mental health and fetal growth restriction: a systematic review.* Journal of Developmental Origins of Health and Disease, 2016. **7**(4): p. 416-428.
135. Ding, X.X., et al., *Maternal anxiety during pregnancy and adverse birth outcomes: A systematic review and meta-analysis of prospective cohort studies.* Journal of Affective Disorders, 2014. **159**: p. 103-110.
136. Grote, N.K., et al., *A Meta-analysis of Depression During Pregnancy and the Risk of Preterm Birth, Low Birth Weight, and Intrauterine Growth Restriction.* Archives of General Psychiatry, 2010. **67**(10): p. 1012-1024.
137. Zhu, B.P., et al., *Effect of the interval between pregnancies on perinatal outcomes.* New England Journal of Medicine, 1999. **340**(8): p. 589-594.
138. Schieve, L.A., et al., *Low and very low birth weight in infants conceived with use of assisted reproductive technology.* New England Journal of Medicine, 2002. **346**(10): p. 731-737.
139. Krampl, E., *Pregnancy at high altitude.* Ultrasound in Obstetrics & Gynecology, 2002. **19**(6): p. 535-539.
140. Illanes, S. and P. Soothill, *Management of fetal growth restriction.* Semin Fetal Neonatal Med, 2004. **9**(5): p. 395-401.
141. Monier, I., et al., *Poor effectiveness of antenatal detection of fetal growth restriction and consequences for obstetric management and neonatal outcomes: a French national study.* Bjog-an International Journal of Obstetrics and Gynaecology, 2015. **122**(4): p. 518-527.
142. Lausman, A., J. Kingdom, and C. Maternal Fetal Medicine, *Intrauterine growth restriction: screening, diagnosis, and management.* J Obstet Gynaecol Can, 2013. **35**(8): p. 741-748.
143. Publications, A., *ACOG Publications: September 2019 (vol 134, pg 653, 2019).* Obstetrics and Gynecology, 2019. **134**(5): p. 1121-1121.
144. Monier, I., et al., *Does the Presence of Risk Factors for Fetal Growth Restriction Increase the Probability of Antenatal Detection? A French National Study.* Paediatric and Perinatal Epidemiology, 2016. **30**(1): p. 46-55.
145. Beune, I.M., et al., *Consensus Based Definition of Growth Restriction in the Newborn.* Journal of Pediatrics, 2018. **196**: p. 71-+.
146. Longo, S., et al., *Short-term and long-term sequelae in intrauterine growth retardation (IUGR).* Journal of Maternal-Fetal & Neonatal Medicine, 2013. **26**(3): p. 222-225.
147. Rosenberg, A., *The IUGR newborn.* Seminars in Perinatology, 2008. **32**(3): p. 219-224.
148. Hediger, M.L., et al., *Growth and fatness at three to six years of age of children born small- or large-for-gestational age.* Pediatrics, 1999. **104**(3): p. art. no.-e33.
149. Hediger, M.L., et al., *Growth of Infants and Young Children Born Small or Large for Gestational Age - Findings from the Third National Health and Nutrition Examination Survey.* Archives of Pediatrics & Adolescent Medicine, 1998. **152**(12): p. 1225-1231.
150. Karlberg, J. and K. Albertssonwikland, *Growth in Full-Term Small-for-Gestational-Age Infants - from Birth to Final Height.* Pediatric Research, 1995. **38**(5): p. 733-739.
151. Allen, M.C., *Developmental outcome and followup of the small for gestational age infant.* Semin Perinatol, 1984. **8**(2): p. 123-56.
152. Guellec, I., et al., *Neurologic Outcomes at School Age in Very Preterm Infants Born With Severe or Mild Growth Restriction.* Pediatrics, 2011. **127**(4): p. E883-E891.

153. Morsing, E., et al., *Cognitive Function After Intrauterine Growth Restriction and Very Preterm Birth.* Pediatrics, 2011. **127**(4): p. E874-E882.
154. Kutschera, J., et al., *Small for gestational age - Somatic, neurological and cognitive development until adulthood.* Zeitschrift Fur Geburtshilfe Und Neonatologie, 2002. **206**(2): p. 65-71.
155. Matharu, K. and S.E. Ozanne, *The Fetal Origns of Disease and Associations With Low Birthweight.* NeoReviews, 2004. **5**(12).
156. Barker, D.J.P., *The origins of the developmental origins theory.* Journal of Internal Medicine, 2007. **261**(5): p. 412-417.
157. Sharma, D., et al., *Intrauterine growth restriction - part 2.* Journal of Maternal-Fetal & Neonatal Medicine, 2016. **29**(24): p. 4037-4048.
158. Voigt, M., et al., *Analyse des Neugeborenenkollektivs der Bundesrepublik Deutschland.* Geburtshilfe Frauenheilkd, 2006. **66**(10): p. 956-970.
159. Pathak, S., et al., *Placental weight, digitally derived placental dimensions at term and their relationship to birth weight.* J Matern Fetal Neonatal Med, 2010. **23**(10): p. 1176-82.
160. Proctor, L.K., et al., *Umbilical cord diameter percentile curves and their correlation to birth weight and placental pathology.* Placenta, 2013. **34**(1): p. 62-6.
161. Ghezzi, F., et al., *Sonographic umbilical vessel morphometry and perinatal outcome of fetuses with a lean umbilical cord.* J Clin Ultrasound, 2005. **33**(1): p. 18-23.
162. Raio, L., et al., *Umbilical cord morphologic characteristics and umbilical artery Doppler parameters in intrauterine growth-restricted fetuses.* Journal of Ultrasound in Medicine, 2003. **22**(12): p. 1341-1347.
163. Liu, C.Q., et al., *Prostanoid TP receptor-mediated impairment of cyclic AMP-dependent vasorelaxation is reversed by phosphodiesterase inhibitors.* Eur J Pharmacol, 2010. **632**(1-3): p. 45-51.
164. Liu, C.Q., et al., *Thromboxane prostanoid receptor activation impairs endothelial nitric oxide-dependent vasorelaxations: the role of Rho kinase.* Biochem Pharmacol, 2009. **78**(4): p. 374-81.
165. Ozen, G., et al., *Mechanism of thromboxane receptor-induced vasoconstriction in human saphenous vein.* Prostaglandins Other Lipid Mediat, 2020. **151**: p. 106476.
166. Omori, K. and J. Kotera, *Overview of PDEs and their regulation.* Circ Res, 2007. **100**(3): p. 309-27.
167. Rybalkin, S.D., et al., *Cyclic GMP phosphodiesterases and regulation of smooth muscle function.* Circ Res, 2003. **93**(4): p. 280-91.
168. Pussard, G., et al., *Endothelin-1 modulates cyclic GMP production and relaxation in human pulmonary vessels.* J Pharmacol Exp Ther, 1995. **274**(2): p. 969-75.
169. Maurice, D.H., et al., *Advances in targeting cyclic nucleotide phosphodiesterases.* Nat Rev Drug Discov, 2014. **13**(4): p. 290-314.
170. Ahmad, F., et al., *Cyclic nucleotide phosphodiesterases: important signaling modulators and therapeutic targets.* Oral Dis, 2015. **21**(1): p. e25-50.
171. Burgoyne, J.R., et al., *Cysteine redox sensor in PKGIa enables oxidant-induced activation.* Science, 2007. **317**(5843): p. 1393-7.
172. Rangaswami, H., et al., *Type II cGMP-dependent protein kinase mediates osteoblast mechanotransduction.* J Biol Chem, 2009. **284**(22): p. 14796-808.
173. Rainer, P.P. and D.A. Kass, *Old dog, new tricks: novel cardiac targets and stress regulation by protein kinase G.* Cardiovasc Res, 2016. **111**(2): p. 154-62.
174. Vaandrager, A.B., B.M. Hogema, and H.R. de Jonge, *Molecular properties and biological functions of cGMP-dependent protein kinase II.* Front Biosci, 2005. **10**: p. 2150-64.
175. Hofmann, F., et al., *Function of cGMP-dependent protein kinases as revealed by gene deletion.* Physiol Rev, 2006. **86**(1): p. 1-23.
176. Ruth, P., et al., *Identification of the amino acid sequences responsible for high affinity activation of cGMP kinase Ialpha.* J Biol Chem, 1997. **272**(16): p. 10522-8.
177. Pisaneschi, S., et al., *Compensatory feto-placental upregulation of the nitric oxide system during fetal growth restriction.* PLoS One, 2012. **7**(9): p. e45294.
178. Peyter, A.C., et al., *Muscarinic receptor M1 and phosphodiesterase 1 are key determinants in pulmonary vascular dysfunction following perinatal hypoxia in mice.* Am J Physiol Lung Cell Mol Physiol, 2008. **295**(1): p. L201-13.
179. Radi, R., *Oxygen radicals, nitric oxide, and peroxynitrite: Redox pathways in molecular medicine.* Proc Natl Acad Sci U S A, 2018. **115**(23): p. 5839-5848.

180. Chen, J., S.C. Rogers, and M. Kavdia, *Analysis of kinetics of dihydroethidium fluorescence with superoxide using xanthine oxidase and hypoxanthine assay.* Ann Biomed Eng, 2013. **41**(2): p. 327-37.
181. Pellegrin, M., et al., *Endothelial dysfunction and cardiovascular risk. Exercise protects endothelial function and prevents cardiovascular disease.* Science & Sports, 2009. **24**(2): p. 63-73.
182. Marques, J., et al., *Implications of NADPH oxidase 5 in vascular diseases.* Int J Biochem Cell Biol, 2020. **128**: p. 105851.
183. Zhou, X. and P. He, *Improved measurements of intracellular nitric oxide in intact microvessels using 4,5-diaminofluorescein diacetate.* Am J Physiol Heart Circ Physiol, 2011. **301**(1): p. H108-14.
184. Goncalves, D.A., et al., *Imbalance between nitric oxide and superoxide anion induced by uncoupled nitric oxide synthase contributes to human melanoma development.* International Journal of Biochemistry & Cell Biology, 2019. **115**.
185. Muller, F.L., et al., *Trends in oxidative aging theories.* Free Radic Biol Med, 2007. **43**(4): p. 477-503.
186. Erusalimsky, J.D., *Vascular endothelial senescence: from mechanisms to pathophysiology.* J Appl Physiol (1985), 2009. **106**(1): p. 326-32.
187. Erusalimsky, J.D. and D.J. Kurz, *Endothelial cell senescence.* Handb Exp Pharmacol, 2006(176 Pt 2): p. 213-48.
188. Haigis, M.C. and L.P. Guarente, *Mammalian sirtuins--emerging roles in physiology, aging, and calorie restriction.* Genes Dev, 2006. **20**(21): p. 2913-21.
189. Ota, H., et al., *Sirt1 modulates premature senescence-like phenotype in human endothelial cells.* J Mol Cell Cardiol, 2007. **43**(5): p. 571-9.
190. Luo, J., et al., *Negative control of p53 by Sir2alpha promotes cell survival under stress.* Cell, 2001. **107**(2): p. 137-48.
191. Ota, H., et al., *Cilostazol inhibits oxidative stress-induced premature senescence via upregulation of Sirt1 in human endothelial cells.* Arterioscler Thromb Vasc Biol, 2008. **28**(9): p. 1634-9.

Annex

Placenta 93 (2020) 83–93

Contents lists available at ScienceDirect

Placenta

journal homepage: http://www.elsevier.com/locate/placenta

Intrauterine growth restriction is associated with sex-specific alterations in the nitric oxide/cyclic GMP relaxing pathway in the human umbilical vein

Manon Beaumann [a], Flavien Delhaes [a], Steeve Menétrey [a], Sébastien Joye [c], Yvan Vial [b], David Baud [b], Jacquier Goetschmann Magaly [c], Jean-François Tolsa [a,c,1], Anne-Christine Peyter [a,*,1]

[a] Neonatal Research Laboratory, Clinic of Neonatology, Department Woman-Mother-Child, Centre Hospitalier Universitaire Vaudois and University of Lausanne, 1011, Lausanne, Switzerland
[b] Clinic of Gynecology and Obstetrics, Department Woman-Mother-Child, Centre Hospitalier Universitaire Vaudois and University of Lausanne, 1011, Lausanne, Switzerland
[c] Clinic of Neonatology, Department Woman-Mother-Child, Centre Hospitalier Universitaire Vaudois and University of Lausanne, 1011, Lausanne, Switzerland

ARTICLE INFO

Keywords:
Intrauterine growth restriction
Human umbilical vein
Vasodilation
Nitric oxide
Cyclic guanosine monophosphate
Phosphodiesterases

ABSTRACT

Introduction: Intrauterine growth restriction (IUGR) is a leading cause of perinatal mortality and morbidity, and is linked to an increased risk to develop chronic diseases in adulthood. We previously demonstrated that IUGR is associated, in female neonates, with a decreased nitric oxide (NO)-induced relaxation of the umbilical vein (UV). The present study aimed to investigate the contribution of the smooth muscle components of the NO/cyclic GMP (cGMP) pathway to this alteration.

Methods: UVs were collected in growth-restricted or appropriate for gestational age (AGA) human term newborns. Soluble guanylyl cyclase (sGC) and cGMP-dependent protein kinase (PKG) were studied by Western blot, cGMP production by ELISA and cyclic nucleotide phosphodiesterases (PDEs) activity using a colorimetric assay. Contribution of PDEs was evaluated using the non-specific PDEs inhibitor 3-isobutyl-1-methylxanthine (IBMX) in isolated vessel tension studies.

Results: NO-induced relaxation was reduced in IUGR females despite increased sGC protein and activity, and some increase in PKG protein compared to AGA. In males, no significant difference was observed between both groups. In the presence of IBMX, NO-stimulated cGMP production was significantly higher in IUGR than AGA females. Pre-incubation with IBMX significantly improved NO-induced relaxation in all groups and abolished the difference between IUGR and AGA females.

Conclusion: IUGR is associated with sex-specific alterations in the UV's smooth muscle. The impaired NO-induced relaxation observed in growth-restricted females is linked to an imbalance in the NO/cGMP pathway. The beneficial effects of IBMX suggest that PDEs are implicated in such alteration and they could represent promising targets for therapeutic intervention.

1. Introduction

Intrauterine growth restriction (IUGR) is a common complication, affecting approximately 8% of all pregnancies. IUGR can be defined as a failure of the fetus to achieve its full, genetically determined growth potential, resulting in a body weight below the 10th percentile (P10) at birth. It is the second leading cause of perinatal mortality, after prematurity. IUGR is associated with short- and long-term adverse outcome [1,2]. Growth-restricted fetuses are at increased risk of stillbirth and perinatal complications such as fetal distress or asphyxia [2,3]. Moreover, because adverse events occurring during the perinatal period may influence the developmental programming of the fetus, IUGR is

* Corresponding author. Neonatal Research Laboratory, Clinic of Neonatology, Department Woman-Mother-Child, Centre Hospitalier Universitaire Vaudois, Rue du Bugnon 27, 1011, Lausanne, Switzerland.
E-mail addresses: Manon.Beaumann@chuv.ch (M. Beaumann), fdelhaes@uwo.ca (F. Delhaes), Steeve.Menetrey@chuv.ch (S. Menétrey), Sebastien.Joye@chuv.ch (S. Joye), Yvan.Vial@chuv.ch (Y. Vial), David.Baud@chuv.ch (D. Baud), magaly.goetschmann@gmail.com (J.G. Magaly), Jean-Francois.Tolsa@chuv.ch (J.-F. Tolsa), Anne-Christine.Peyter@chuv.ch (A.-C. Peyter).
[1] These authors contributed equally to this work.

https://doi.org/10.1016/j.placenta.2020.02.014
Received 30 April 2019; Received in revised form 18 February 2020; Accepted 19 February 2020
Available online 25 February 2020

associated with a higher incidence of chronic diseases in adulthood, like cardiovascular disorders, metabolic syndrome, or non-insulin-dependent diabetes mellitus [1,4,5].

The mechanisms implicated in the development of IUGR remain poorly understood, despite identification of some maternal risk factors, like maternal diseases (e.g. systemic arterial hypertension, lupus, renal insufficiency), malnutrition, mother's stress, strenuous work, as well as tobacco, alcohol and drug abuse [6]. There is currently no efficient way to prevent or treat IUGR, but only preventive approaches to reduce risk factors [7]. Identifying high-risk pregnancies is key in order to prevent or alleviate the consequences of IUGR [8] and remains a challenge [9]. Prenatal screening of impaired fetal growth is based on ultrasonographic biometrical measurements, completed by *in utero* Doppler velocimetry of some relevant vessels, like uterine artery, umbilical arteries (UAs), fetal middle cerebral arteries and ductus venosus [8–10]. Some maternal blood biomarkers, such as placental growth factor [11], are currently under investigation to combine with ultrasound [9]. Clinical management of IUGR is mainly based on careful monitoring of fetal growth and biophysical profile. Premature delivery is often the only issue when fetal adaptation is overwhelmed, contributing to further increased risk of perinatal mortality and morbidity. A better understanding of the mechanisms implicated in the development of IUGR, as well as in the fetal programming of adult diseases, is necessary to develop novel strategies to prevent or limit IUGR and its adverse consequences.

Fetal growth is primarily determined by nutrient availability. IUGR is associated with a reduced oxygen and nutrient supply across the placenta [12,13]. Placental insufficiency is associated with a decrease in fetal-maternal exchanges and is recognized as a major cause of IUGR [14]. Therefore, an interdisciplinary approach to investigate placenta disorders can help in diagnosis and management of fetal growth restriction [15]. Placental insufficiency induces several adaptive mechanisms in the fetus, including modifications in fetal circulation, metabolism and endocrinology [14,16,17], thus contributing to the developmental origins of adult diseases [18,19].

We previously demonstrated that IUGR was associated with an important reduction in placental weight, as well as structural and functional alterations in the umbilical cord [20]. In particular, umbilical cord diameter was thinner in growth-restricted neonates than in appropriate for gestational age (AGA) controls [20]. Total cross-section and smooth muscle areas were significantly smaller in the umbilical vein (UV) of growth-restricted than AGA newborns, whereas no difference was found in UAs morphometry [20], as already observed [21]. We also found that nitric oxide (NO)-induced relaxation was altered in the UV of growth-restricted females as compared to AGA controls, whereas in males relaxant response to NO was similar in both groups [20]. In UAs, we did not observe any difference in NO-induced relaxation between IUGR and AGA neonates (unpublished data). Although UAs are classically investigated in fetal growth monitoring, several Doppler ultrasound studies also demonstrated an impaired UV blood flow in IUGR [16, 22–24]. Because UV is the unique vessel to carry the fresh oxygenated and nutrient-rich blood from the placenta to the fetus, it could represent a potential target for therapeutic interventions to improve the circulation from the placenta to the fetus. In contrast, UAs, conducting the deoxygenated blood containing metabolic waste from the fetus to the placenta, probably reflect mainly adaptive responses of the fetus to the altered blood/oxygen/nutrients supply. Impaired blood flow within the umbilical cord could have important consequences for the fetus and may be associated with IUGR or worsen it.

Umbilical circulation is regulated by numerous vasoactive factors, in particular by the NO-cyclic guanosine monophosphate (cGMP) signaling pathway [25], which plays a crucial role in the cardiovascular system [26]. NO is a gaseous molecule endogenously produced in the endothelium by the endothelial NO synthase (eNOS). It diffuses into the smooth muscle, where it stimulates the soluble guanylyl cyclase (sGC), leading to synthesis of cGMP. In turn, cGMP activates, among others, the cGMP-dependent protein kinase (PKG), leading to vasorelaxation [27, 28]. Intracellular levels of cGMP are tightly controlled by cyclic nucleotide phosphodiesterases (PDEs) catalyzing the hydrolysis of cGMP to the non-active form 5′-GMP. So far, 11 structurally related but functionally distinct mammalian PDE gene families (PDE1 to PDE11) have been identified based on substrate affinity, selectivity, and regulatory mechanisms [29,30], leading to synthesis of close to 100 PDE isoenzymes by alternative splicing or transcriptional processing [31]. In vascular smooth muscle, the major isoforms regulating vascular tone are PDE1, PDE3, PDE4 and PDE5 [32]. Furthermore, these PDEs seem implicated in the development of chronic diseases [33]. However, the contribution of PDEs to the regulation of umbilical circulation and to the development of IUGR is unknown.

The present study was designed to investigate mechanisms contributing to the impaired NO-induced relaxation we described previously in UV of growth-restricted females [20]. Our investigations were focused on the smooth muscle part of the NO/cGMP pathway. We demonstrated that the sex-specific impairment of NO-induced relaxation is associated with an imbalance in the NO/cGMP pathway. Our results also highlighted beneficial effects of the non-specific PDEs inhibitor 3-isobutyl-1--methylxanthine (IBMX), suggesting that PDEs could represent promising targets for further therapeutic intervention.

2. Methods

2.1. Patients – inclusion/exclusion criteria and classification

The present study was approved by the ethical committee of the Faculty of Biology and Medicine of the University of Lausanne (protocol number 134/08). This was a direct continuation of our previous work [20].

Data presented in this manuscript were obtained using biological samples from patients already included in our previous study [20] and from new patients. Umbilical cords were collected in 535 newborns delivered at the Maternity of the University Hospital CHUV in Lausanne (Switzerland) between June 2009 and December 2019. Samples collection, processing, inclusion and exclusion criteria were exactly as previously described [20].

Inclusion criteria were term (≥37 accomplished weeks of gestation) singleton pregnancies. Exclusion criteria were neonates with a birth weight (BW) >P90, fetal abnormalities, genetic syndromes, single UA, mothers presenting with HIV, hepatitis A, B or C, and preeclampsia.

Newborns were dichotomized into two categories, based on body weight at birth: "IUGR" and "AGA". Samples were assigned to the "AGA" group when BW was between P10 and P90, and to the "IUGR" group when BW was <P10. The percentile classification was determined using a growth centile calculator, which consisted on an Excel file using a formula based on data extracted from growth charts endorsed by the Swiss Society of Pediatrics [34]. When available, prenatal data (e.g. estimated fetal weight) were used to determine whether a growth curve break occurred, namely a significant change in percentiles, in order to distinguish "IUGR" from constitutive "Small for Gestational Age" [35]. Male and female neonates were studied separately.

However, since prenatal growth follow-up or other parameters like ultrasound/Doppler measurements were not available for all patients, our subjects were retroactively reclassified according to the criteria of the "Consensus Based Definition of Growth Restriction in the Newborn" published in The Journal of Pediatrics (2018) [36]. This allowed a more rigorous postnatal classification of our patients. Subjects who did not reach these criteria were excluded from the initial groups. Details are presented in Supplementary Table 1.

All data included in the present report therefore correspond to those obtained in the 467 patients reaching the criteria of the "2018 clinical consensus" [36]. Even isolated vessel tension studies data already published in *Placenta* [20] were re-analyzed after reclassification of the subjects.

2.2. Samples collection

The proximal part (close to the fetus) of the umbilical cord was collected at delivery and used within 24 h. A 10–15 cm segment was cut as close as possible to the fetus and kept, until dissection, at 4 °C in deoxygenated modified Krebs-Ringer solution (118.3 mM NaCl, 4.7 mM KCl, 2.5 mM $CaCl_2$, 1.2 mM $MgSO_4$, 1.2 mM KH_2PO_4, 25.0 mM $NaHCO_3$, and 11.1 mM glucose), prepared by bubbling with 21% O_2 and 5% CO_2, balanced with nitrogen, during about 30 min [20]. Before dissection, the diameter of the collected cord segment was measured at three different places, using a digital caliper, to calculate the average umbilical cord diameter for each patient.

For technical reasons, it was not possible to perform all types of experiments on each umbilical cord. In particular, all experiments requiring freshly isolated vessels (organ bath experiments, cGMP production and PDEs activity) were performed on different patients. In contrast, homogenates analyzed by Western blot were prepared with frozen UV segments dissected from umbilical cords used for the experiments mentioned above. However, we checked that each subset of samples used for the various experiments was representative of the entire population included in this study. In particular, we verified that the growth parameters were significantly reduced in IUGR compared to AGA neonates used for each type of experiments. Supplementary Fig. 1 shows the distribution of BW of patients used for each type of experiments compared to all patients included in the present study for each experimental group.

2.3. Isolated vessel tension experiments

UV reactivity was investigated as previously described [20]. Briefly, UV was dissected, cut into small rings (4–5 mm length) and placed into vertical organ chambers filled with 10 ml modified Krebs-Ringer solution, bubbled with 21% O_2–5% CO_2, and maintained at 37.5 °C. A 2 g stretch tension was applied to each vessel ring, followed by 20-min equilibration before washing. Stretch/equilibration/wash steps were repeated still three times, in order to get the vessels to their optimal resting tension. After equilibration, N^G-nitro-L-arginine (NLA, 10^{-4} M) and indomethacin (10^{-5} M) were added in order to exclude possible interference of endogenous NO and prostanoids. IBMX (10^{-4} M), a non-specific inhibitor of PDEs, was also added to investigate the contribution of PDEs in NO-induced relaxation. Vascular rings were then pre-contracted with serotonin (5-HT, 10^{-5} M) or an analogue of thromboxan A_2 (U46619, 10^{-6} M), before relaxant response to cumulative doses of the NO-donor 2-(*N*,*N*-Diethylamino)-diazenolate-2-oxide (DEA/NO, 10^{-8} to 10^{-4} M) was tested. Change in tension induced by DEA/NO was expressed as percent of the initial contraction induced by the vasoconstrictor. Area under the curve (AUC) was calculated for each relaxation curve using Prism 8.0.

An additional set of experiments was performed to investigate simultaneously, in vascular rings isolated from the same UV, the relaxation induced by DEA/NO (10^{-10} to 10^{-4} M) in the presence or absence of IBMX, as well as spontaneous relaxation observed in the absence of the relaxing agent.

2.4. Western blot

The relative amounts of sGC and PKG in UV homogenates were investigated by Western blot. Flash-frozen UV were crushed in a cryogenic mortar, homogenized in lysis buffer {50 mM HEPES, 1 mM EDTA, 1 mM EGTA, 10% glycerol, 1 mM DTT, 5 μg/ml pepstatin, 3 μg/ml aprotinin, 10 μg/ml leupeptin, 0.1 mM 4-(2-aminoethyl)benzenesulfonyl fluoride hydrochloride (AEBSF), 1 mM sodium vanadate, 50 mM sodium fluoride, and 20 mM 3-[(3cholamidopropyl)dimethylammonio]-1-propanesulfonate (CHAPS)}, and centrifuged for 10 min at 3′000 g at 4 °C. Supernatant protein concentration was quantified using a BCA protein assay kit (Pierce). Samples were diluted in Laemmli buffer, to reach a concentration of 40 μg per lane, and were heated for 5 min at 95 °C before loading on a 7.5% polyacrylamide gel. Proteins were fractioned by SDS-PAGE (1 h 35 min, 0.05 A) and transferred to a nitrocellulose membrane (overnight, 30 V, 4 °C). After a 30-min blocking in casein solution (Vector) at room temperature (RT), membranes were immunoblotted (overnight, 4 °C, or 1 h, RT) using specific antibodies targeted against sGC (1:10′000, Abcam), PKG (1:1′000, Stressgen) or actinin (1:250, Sigma), diluted in casein solution containing 0.1% Tween. Blots were then incubated with an anti-mouse or anti-rabbit antibody (LICOR) diluted 1:10′000 in casein solution (1 h, RT). Target proteins were visualized using an Odyssey Infrared Imaging System (LICOR). The amount of each specific protein was quantified using ImageJ software and normalized to actinin content.

For each experimental group, samples from 40 patients were randomly distributed into 4 pools, in order to limit the influence of individual variability on the results. To allow comparison between the different membranes and between groups, the specific protein content measured in each pool was reported to the amount measured in a "standard" sample, constituted of proteins extracted from 6 additional patients (3 AGA males and 3 AGA females), which were not included in the pools.

Some experiments were also performed using individual samples rather than pools of patients. For that purpose, individual patients were randomly selected in each pool in order to investigate sGC and PKG protein content. To allow comparison between the different membranes and groups, the target protein content measured in each sample was reported to the amount measured in the same "standard" sample as for experiments using pools of patients.

2.5. cGMP production in isolated UV

UV were dissected as for organ bath experiments and incubated in modified Krebs-Ringer solution (37.5 °C, bubbled with 21% O_2–5% CO_2). All measurements were performed in the presence of indomethacin (10^{-5} M) and NLA (10^{-4} M), such as in isolated vessel tension studies. Several conditions were tested at the same time on vascular rings from the same UV. IBMX (10^{-4} M) was used to prevent the degradation of cGMP. After a 20-min equilibration period, DEA/NO (10^{-4} M) was added in the bath. After a 4-min incubation, UV rings were quickly frozen in liquid nitrogen. Vascular rings were crushed in a cryogenic mortar and homogenized in 0.1 N HCl. The cGMP content was quantified in homogenates using the direct cGMP ELISA Kit (Enzo Life Sciences) according to the manufacturer's instructions. This is a colorimetric competitive immunoassay, with an optional acetylation protocol to increase the sensitivity. Samples with high cGMP content (vessel rings treated with DEA/NO ± IBMX) were processed using the classical protocol, whereas samples with low cGMP content (vessel rings in basal conditions or treated with IBMX alone) were tested using the acetylation protocol. Results obtained by both protocols can be compared because in each procedure cGMP concentration in samples is calculated based on an appropriate standard curve. For each sample, cGMP content was normalized by the corresponding protein content, quantified using the BCA protein assay kit, and expressed as pmol cGMP/mg protein/min.

2.6. PDEs activity in UV homogenates

The PDEs activity was quantified in UV homogenates using a cyclic nucleotide phosphodiesterase assay kit (Enzo Life Sciences) according to the manufacturer's instructions. Briefly, flash-frozen vein segments were crushed in a cryogenic mortar, and 450 mg was mixed with 1 ml Assay Buffer containing 20 mM CHAPS using a tissue grinder. Homogenates were then sonicated and centrifuged for 10 min at 3′000 g at 4 °C. A buffer exchange was performed using Pierce™ Protein Concentrators PES, 3K MWCO, 0.5 ml, in order to remove excess free phosphate, which interferes with the BIOMOL® GREEN reagent of the kit. cGMP degradation was tested in the absence or presence of IBMX 10^{-4} M. Enzymatic

reaction was performed during 20 min at 30 °C in Assay buffer containing 0.5 mM $MgCl_2$, 0.2 mM $CaCl_2$ and 2 μM calmodulin. For each sample, total and IBMX-sensitive PDEs activity were normalized by the corresponding protein content, quantified using the BCA protein assay kit, and expressed as nmol cGMP/mg protein/min.

2.7. Data analyses

Statistical analyses were performed using Prism 8.0 (GraphPad Software). The test used to analyze each type of experiment is specified in figure/table legends. The differences were considered statistically significant when $P < 0.05$.

3. Results

3.1. Demographic data

Table 1 displays maternal and neonatal characteristics of each group. Gestational age and maternal age at delivery were similar in all groups. As expected, body weight, length and head circumference at birth were significantly reduced in growth-restricted neonates compared to AGA controls. Ponderal index, placental weight and umbilical cord diameter were also significantly lower in IUGR than AGA newborns, whereas the body to placental weight ratio was significantly increased. Finally, the proportion of smoking mothers was significantly higher in IUGR males than in other groups. The latter information should however be considered with caution because the smoking status was self-reported and was not available in 26–43% of the medical records.

Table 1
Demographic data related to patients included in the present study.

	Females		*P*-value
	AGA	IUGR	
Number of patients included	151	90	
Gestational age (weeks)	39.5 ± 1.0	39.4 ± 1.1	>0.9999
Birth weight (g)	3308 ± 303	2565 ± 262 *	< **0.0001**
Length (cm)	49.0 ± 1.6	46.5 ± 2.0 *	< **0.0001**
Head circumference (cm)	34.5 ± 1.1 †	32.7 ± 1.1 *	< **0.0001**
Ponderal index (g/cm^3)	2.82 ± 0.23	2.56 ± 0.28 *	< **0.0001**
Placental weight (g)	617 ± 119	420 ± 84 *	< **0.0001**
Body to placental weight ratio	5.52 ± 0.92	6.29 ± 1.14 *	< **0.0001**
Umbilical cord diameter (mm)	12.0 ± 2.1	10.7 ± 2.1 *	< **0.0001**
Maternal age (years)	31.9 ± 5.3	31.4 ± 5.3	>0.9999
Smoking (yes/no)	15/71 (65 n/a)	17/50 (23 n/a) †	0.2381 #
	Males		***P*-value**
	AGA	**IUGR**	
Number of patients included	143	83	
Gestational age (weeks)	39.5 ± 1.0	39.2 ± 1.2	>0.9999
Birth weight (g)	3440 ± 303	2605 ± 299 *	< **0.0001**
Length (cm)	49.8 ± 1.7	46.8 ± 1.9 *	< **0.0001**
Head circumference (cm)	35.1 ± 1.0 †	33.0 ± 1.3 *	< **0.0001**
Ponderal index (g/cm^3)	2.77 ± 0.22	2.54 ± 0.22 *	< **0.0001**
Placental weight (g)	610 ± 109	427 ± 95 *	< **0.0001**
Body to placental weight ratio	5.72 ± 0.87	6.33 ± 1.20 *	**0.0008**
Umbilical cord diameter (mm)	12.8 ± 2.8	11.3 ± 2.3 *	< **0.0001**
Maternal age (years)	33.2 ± 5.2	31.3 ± 5.7	0.0875
Smoking (yes/no)	11/70 (62 n/a)	25/28 (30 n/a) * †	< **0.0001** #

AGA, appropriate for gestational age neonates; IUGR, growth-restricted newborns; n/a, not available.
Ponderal index was calculated as [100 x birth weight/length^3] (g/cm^3). Data are expressed as mean ± SD. *P*-values presented in the table are related to comparison between AGA and IUGR groups. Bold indicates significant *P*-values ($P < 0.05$). All parameters were analyzed using a Kruskal-Wallis test with Dunn's multiple comparison, excepted for smocking status. * significant difference between AGA and IUGR newborns; † significant difference between females and males. # *P*-values determined using the Fisher's exact test to compare the smoking status between mothers of AGA and IUGR neonates.

3.2. Western blotting analyses

Fig. 1 presents data obtained by Western blot analysis of sGC and PKG protein content in UV homogenates of 40 patients/group randomly distributed into 4 pools/group. The relative amount of sGC protein was twice as high in IUGR females than in AGA (Fig. 1A). In contrast, in males, sGC protein level was similar in both groups and did not differ from AGA females (Fig. 1A). Fig. 1B shows a near significant increase in PKG relative protein content in IUGR compared to AGA females ($P = 0.0565$). In males, both groups had a similar PKG protein content, which was significantly higher than in AGA females.

Similar results were obtained when performing western blots with individual samples rather than pools of patients (Supplementary Fig. 2), with however less statistically significant results. In these conditions, sGC protein amount was significantly increased, by about 3 times, in IUGR females compared to AGA, and PKG protein content was significantly higher in AGA males than AGA females.

3.3. Isolated vessel tension studies

Preliminary data showed that the non-specific PDEs inhibitor IBMX induced a dose-dependent relaxation in pre-constricted UV rings (Supplementary Fig. 3).

Dose-response curves to the NO-donor DEA/NO performed in UV rings pre-incubated with IBMX were directly compared to those obtained in absence of IBMX we previously published in *Placenta* [20]. Such comparison was possible because experimental procedure and conditions were strictly identical between both sets of experiments. However, for a better concordance, the data published in Ref. [20] were re-analyzed after reclassification of patients and exclusion of those who did not reach the "2018 consensus criteria" [36].

Figs. 2 and 3 display the dose-dependent relaxation induced by cumulative doses of DEA/NO, in the absence or presence of IBMX, in UV pre-constricted either by 5-HT (Fig. 2) or U46619 (Fig. 3), as well as the corresponding AUC calculated for each dose-response curve. Our previous observations [20] remained valid even after reclassification of the subjects: in females, DEA/NO-induced relaxation was significantly weaker in IUGR than AGA neonates, whereas, in males, relaxant responses to DEA/NO were similar in both groups. Consistently, in females, AUC was significantly reduced in IUGR compared to AGA (Figs. 2 and 3 B), whereas in males, AUC was similar in both groups (Figs. 2 and 3 D).

Pre-incubation with IBMX significantly increased NO-induced relaxation in all groups (Figs. 2 and 3). In female UV pre-contracted with 5-HT, IBMX not only improved NO-induced relaxation, but also completely abolished the difference observed between IUGR and AGA in the absence of IBMX (Fig. 2A). In female UV pre-constricted with U46619, IBMX also significantly improved relaxant response to DEA/NO in both groups (Fig. 3A); however, in UV pre-incubated with IBMX, relaxation induced by low doses of DEA/NO ($3 \cdot 10^{-8}$ to $3 \cdot 10^{-6}$ M) was significantly weaker in IUGR than in AGA females, whereas no significant difference was found for higher concentrations of DEA/NO (10^{-5} to 10^{-4} M) (Fig. 3A). AUC calculated in UV pre-incubated with IBMX were significantly increased as compared to UV without IBMX and did not show any significant difference between IUGR and AGA females (Figs. 2 and 3 B).

In males, relaxant responses to DEA/NO were similar in IUGR and AGA neonates, with a significant increase in NO-induced relaxation in UV pre-incubated with IBMX compared to basal conditions (Figs. 2 and 3 C). There was no difference between AUC calculated for IUGR and AGA

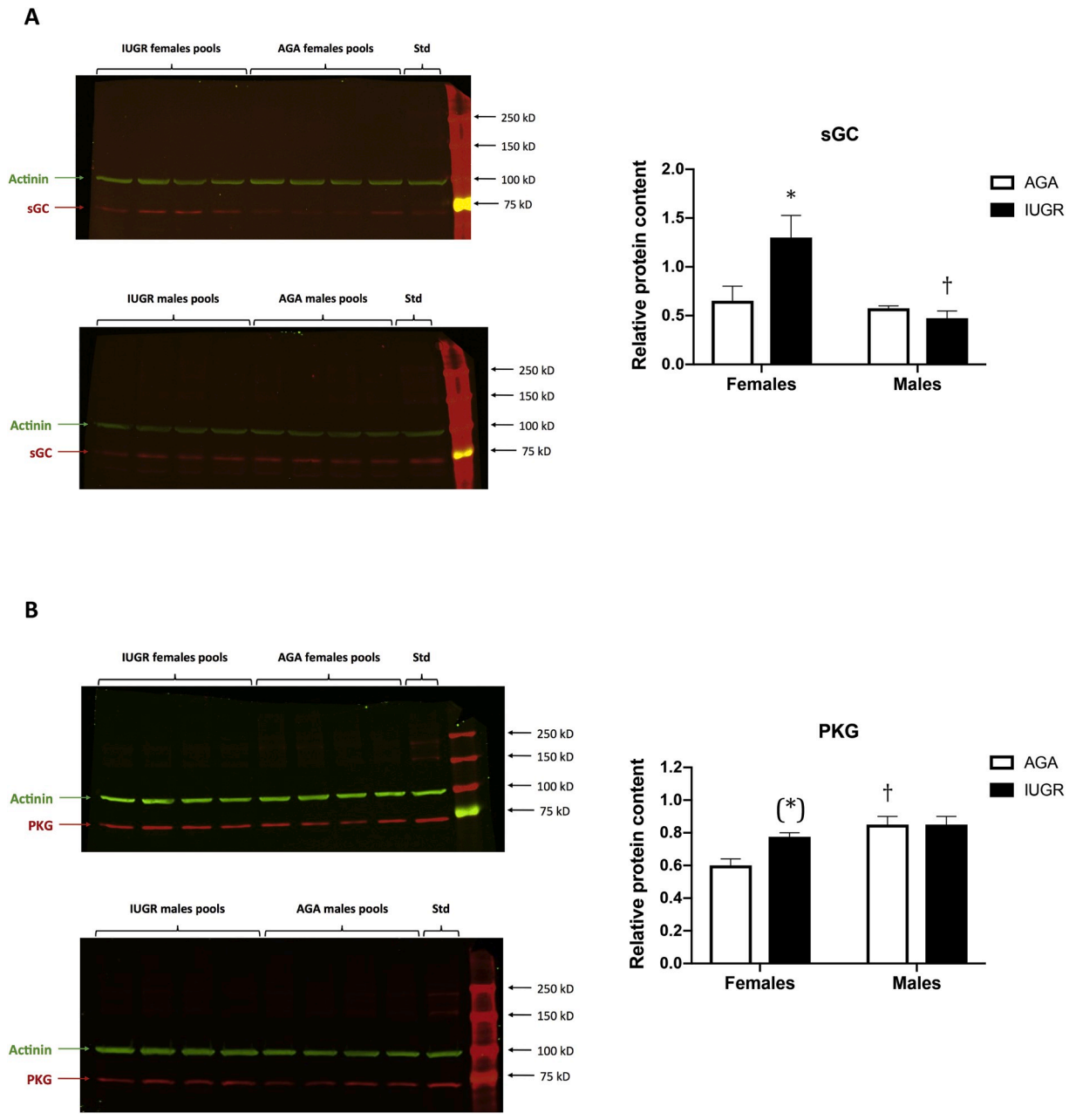

Fig. 1. Relative amounts of sGC and PKG proteins in human umbilical vein. AGA, appropriate for gestational age neonates; IUGR, growth-restricted newborns; Std, "standard" sample. Representative blots are presented for each protein. Relative protein content of sGC (A) or PKG (B) was evaluated by Western blot in umbilical vein homogenates of AGA and IUGR newborns. For each experimental group, samples from 40 patients were randomly distributed into 4 pools. For each pool, the target protein amount was normalized by the actinin protein content and reported to the amount measured in the "standard" sample. Data are expressed as mean + SEM (n = 4 pools of 10 patients). Data were analyzed using *two-way ANOVA*. * significant difference between IUGR and AGA neonates; † statistical difference between males and females ($P < 0.05$); (*) near significant difference between IUGR and AGA females ($P = 0.0565$).

males, either in the absence or in the presence of IBMX (Figs. 2 and 3 D), and AUC was significantly higher in UV treated with IBMX compared to basal conditions (Figs. 2 and 3 D).

Comparison between both sexes showed that, in absence of IBMX, AUC was significantly lower in IUGR females than IUGR males ($P = 0.0003$; *two-way ANOVA*), but was similar in AGA males and females. In UV treated with IBMX, AUC did not differ between males and females.

Because dose-response curves in the presence of IBMX were established in UV isolated from other patients than the initial experiments performed in basal conditions (without IBMX), complementary data were obtained by testing, on UV rings from the same patient, DEA/NO-induced relaxation in the absence or presence of IBMX, as well as spontaneous relaxation (without vasodilatory agent) (Supplementary Fig. 4 and Fig. 5). In such conditions, pre-incubation with IBMX significantly improved DEA/NO-induced relaxation in UV of AGA and IUGR females (Suppl. Fig.4-5 A-D), as well as in male UV pre-contracted with U46619 (Suppl. Fig. 5 E–H). In male UV pre-constricted with 5-HT, pre-incubation with IBMX induced a significant increase in DEA/NO-induced relaxation only in growth-restricted males (Suppl. Fig. 4 E–H). In all groups and conditions, spontaneous relaxation observed in the presence or absence of IBMX was significantly weaker than the corresponding DEA/NO-induced relaxant response (Supplementary Fig. 4 and Fig. 5). Spontaneous relaxation observed in UV pre-contracted with 5-HT was similar in the presence or absence of IBMX

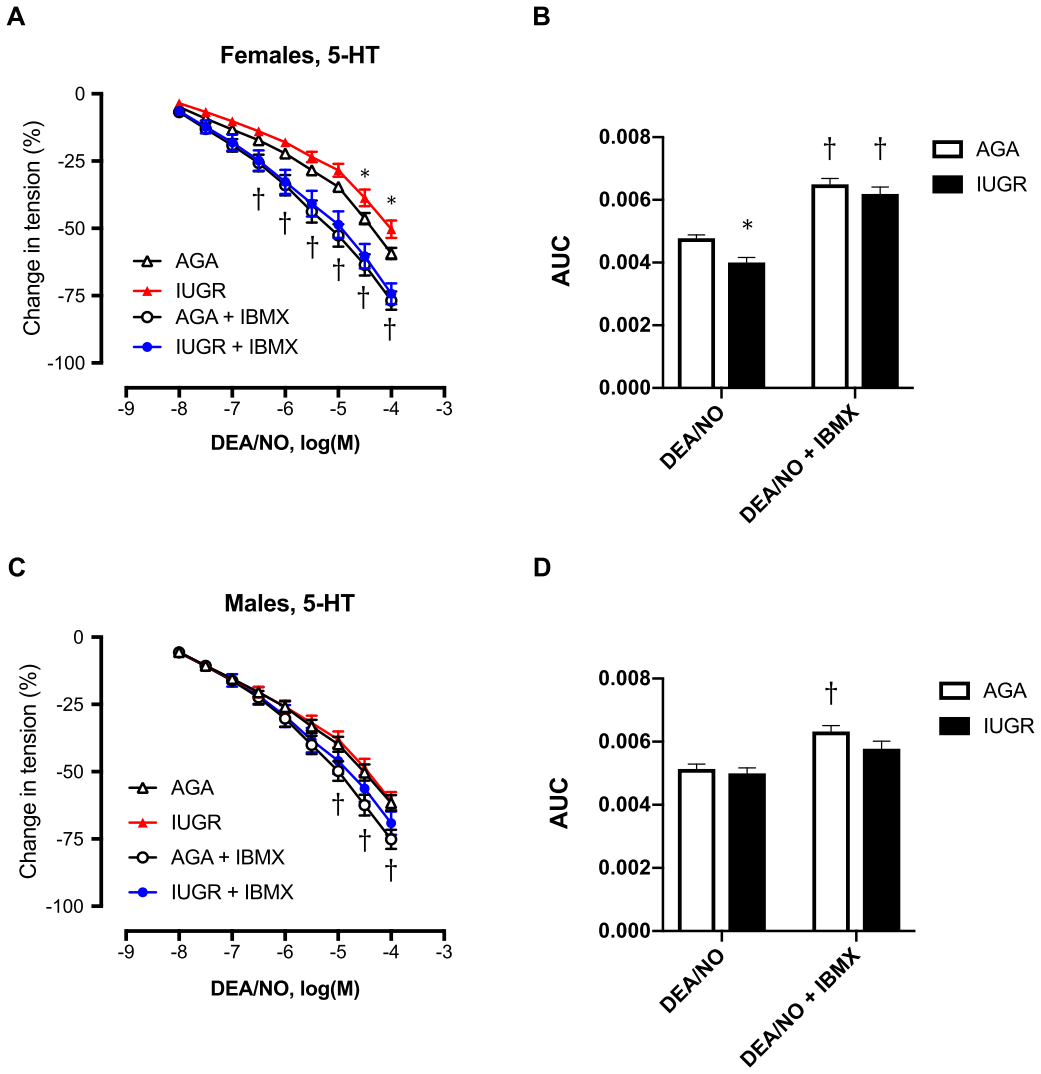

Fig. 2. Relaxation induced by cumulative doses of the nitric oxide-donor DEA/NO on isolated umbilical veins pre-contracted with 5-HT in the absence or presence of IBMX. AGA, appropriate for gestational age neonates; IUGR, growth-restricted newborns. Cumulative concentrations of DEA/NO were applied to UV isolated from newborn females (A) or males (C) pre-contracted with 5-HT 10^{-5} M. Data are expressed as mean ± SEM of the percent of change in tension induced by the vasodilator *without IBMX* (n = 36–51 in females; n = 37–50 in males) and *with IBMX* 10^{-4} *M* (n = 18–24 in females; n = 14–24 in males). Data were analyzed by *two-way ANOVA*. * statistical difference between AGA and IUGR; † significant difference between absence and presence of IBMX, in IUGR and AGA females, but only in AGA males ($P < 0.05$). Dose-response curves obtained in absence of IBMX previously published in *Placenta* (Peyter et al., 2014) were re-analyzed after reclassification of patients according to the "Consensus Based Definition of Growth Restriction in the Newborn" (Beune et al., 2018). Area under the curve (AUC) was calculated for each dose-response curve of the corresponding graph (B, females; D, males). Results are expressed as mean + SEM and were analyzed using *two-way ANOVA*. * significant difference between IUGR and AGA neonates; † statistical difference between AUC in the presence or absence of IBMX ($P < 0.001$).

(Supplementary Fig. 4). In contrast, in UV pre-contracted with U46619, spontaneous relaxation observed in vascular rings pre-incubated with IBMX was significantly increased as compared to basal conditions (Supplementary Fig. 5).

3.4. cGMP production in isolated UV

Fig. 4 shows cGMP production measured in UV rings isolated from females (Fig. 4A) or males (Fig. 4B). Numerical data related to cGMP production in UV, expressed as pmol cGMP/mg protein/min, are summarized in Supplementary Table 2. In both sexes, cGMP content measured in UV of growth-restricted newborns incubated with IBMX and DEA/NO was significantly greater than in basal conditions or with DEA/NO or IBMX alone (Fig. 4). In females, cGMP production measured in basal conditions, as well as in UV treated with IBMX or DEA/NO alone, did not statistically differ between IUGR and AGA neonates (Fig. 4). In the presence of IBMX and DEA/NO, however, cGMP content achieved in UV of growth-restricted females was significantly increased at about 3 as high as in AGA females (Fig. 4). In males, no significant difference was found between both groups in either condition. Between males and females, there was no significant difference, except for cGMP production measured in the presence of DEA/NO and IBMX, which was significantly higher in IUGR females than IUGR males ($P = 0.0172$, *two-way ANOVA*).

3.5. PDEs activity in UV homogenates

Fig. 5 shows IBMX-sensitive cGMP degradation measured in UV homogenates. No significant difference was observed between experimental groups. Supplementary Table 3 presents data related to total and IBMX-sensitive degradation of cGMP, expressed as nmol cGMP/mg protein/min. IBMX-sensitive PDEs activity represented about 32–37% of

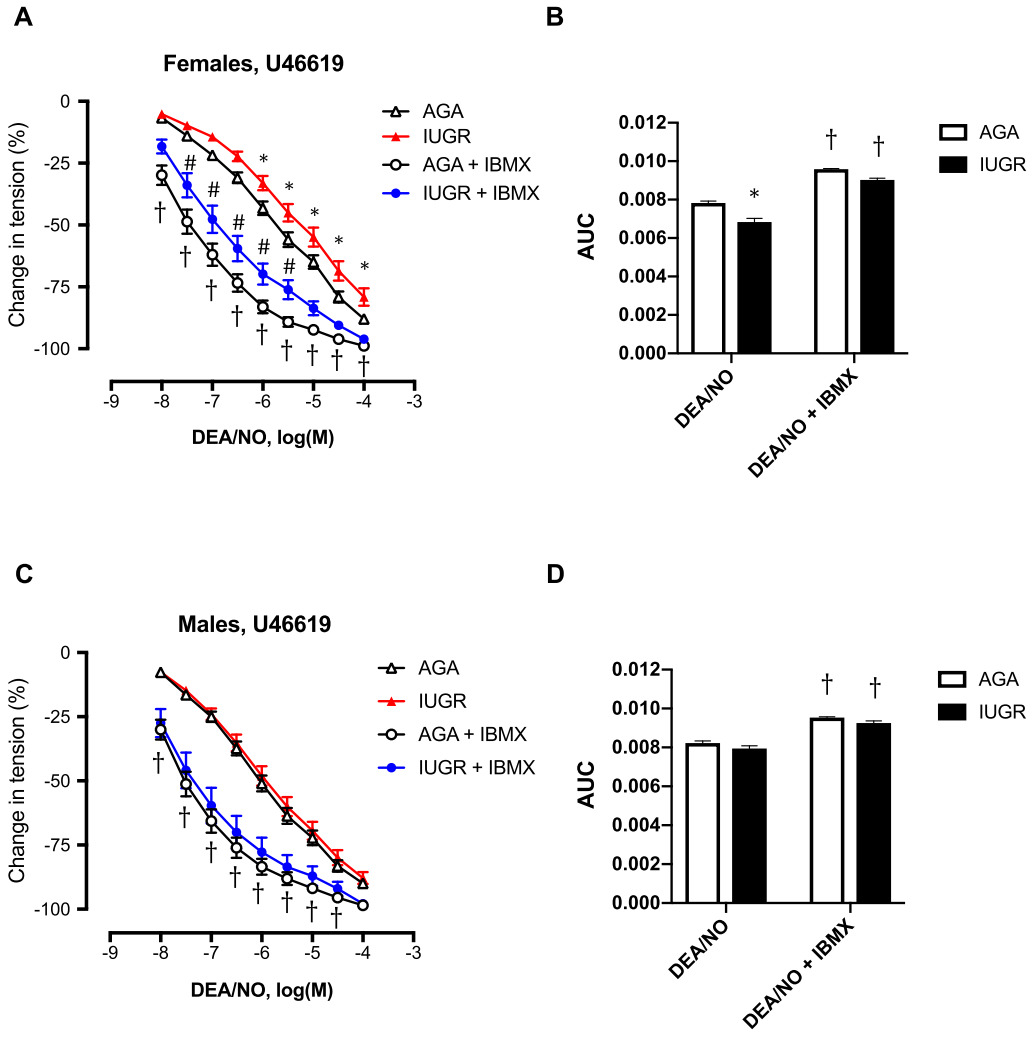

Fig. 3. Relaxation induced by cumulative doses of the nitric oxide-donor DEA/NO on isolated umbilical veins pre-contracted with U46619 in the absence or presence of IBMX. AGA, appropriate for gestational age neonates; IUGR, growth-restricted newborns. Cumulative concentrations of DEA/NO were applied to UV isolated from newborn females (A) or males (C) pre-contracted with U46619 10^{-6} M. Data are expressed as mean ± SEM of the percent of change in tension induced by the vasodilator *without IBMX* (n = 36–50 in females; n = 37–50 in males) and *with IBMX* 10^{-4} *M* (n = 18–24 in females; n = 14–24 in males). Data were analyzed by *two-way ANOVA*. * statistical difference between AGA and IUGR; † significant difference between absence and presence of IBMX, in IUGR and AGA neonates; # significant difference between IUGR and AGA females in the presence of IBMX ($P < 0.05$). Dose-response curves obtained in absence of IBMX previously published in *Placenta* (Peyter et al., 2014) were re-analyzed after reclassification of patients according to the "Consensus Based Definition of Growth Restriction in the Newborn" (Beune et al., 2018). Area under the curve (AUC) was calculated for each dose-response curve of the corresponding graph (B, females; D, males). Results are expressed as mean + SEM and were analyzed using *two-way ANOVA*. * significant difference between IUGR and AGA neonates; † statistical difference between AUC in the presence or absence of IBMX ($P < 0.0001$).

the total cGMP degradation capacity in UV homogenates. There was no significant difference between IUGR and AGA neonates, neither in total cGMP PDEs activity nor in IBMX-sensitive cGMP degradation.

It should be noted that cGMP degradation was in the range of nmol cGMP/mg protein/min, whereas cGMP production was at the level of pmol cGMP/mg protein/min.

4. Discussion

We previously demonstrated that IUGR is associated with structural alterations in UV of male and female neonates, and with a decreased NO-induced relaxation in female UV [20]. The present study was designed to investigate mechanisms implicated in this sex-specific altered relaxant response to NO, in order to potentially target corrective interventions. Experiments were focused on identification of alterations in the smooth muscle part of the NO/cGMP signaling pathway.

We postulated that the impaired NO-induced relaxation observed in UV of growth-restricted females could result from a down-regulation of pro-relaxant proteins and/or an up-regulation of pro-contracting proteins, resulting in an imbalance in vascular tone regulatory mechanisms.

However, Western blot analyses did not show any decrease in the pro-relaxant proteins sGC and PKG in growth-restricted females. In contrast, relative amount of sGC was twice as high in UV homogenates of IUGR females compared to AGA, which is in contradiction with our initial expectations. Similarly, some increase in PKG protein content was also found in IUGR females. However, an increased protein level does not necessarily correlate with an increased enzymatic activity. In contrast, in male UV, relative amount of sGC and PKG did not differ between IUGR and AGA newborns, which is consistent with pharmacological results.

Our Western blot analyses were performed using 4 pools of 10 patients for each group in order to limit the influence of individual

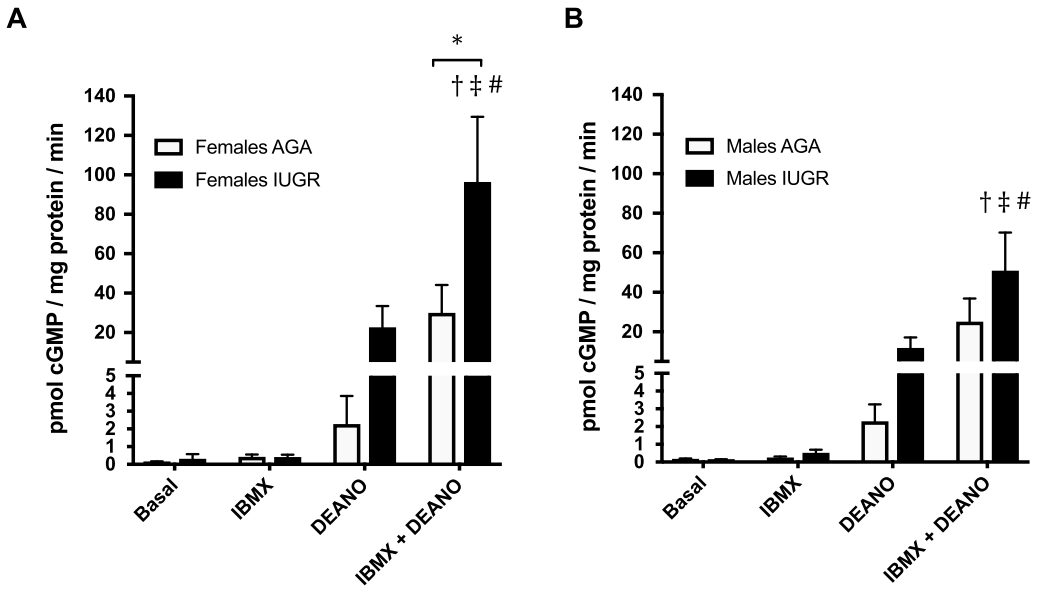

Fig. 4. cGMP production in isolated umbilical veins. AGA, appropriate for gestational age neonates; IUGR, growth-restricted newborns. cGMP production was assessed in intact UV rings isolated from females (A) or males (B), in the absence or presence of IBMX 10^{-4} M and/or after stimulation by the NO donor DEA/NO 10^{-4} M. Data are expressed as mean + SEM (n = 6–10 in females; n = 8–10 in males) of the quantity of cGMP produced, expressed as picomoles cGMP per milligram of protein per minute. Results were analyzed using *two-way ANOVA*. * significant difference between AGA and IUGR; † statistically different as compared to basal cGMP production; ‡ significant difference as compared to cGMP production incubated with IBMX alone; # significant difference as compared to cGMP production in the presence of DEA/NO alone ($P < 0.05$).

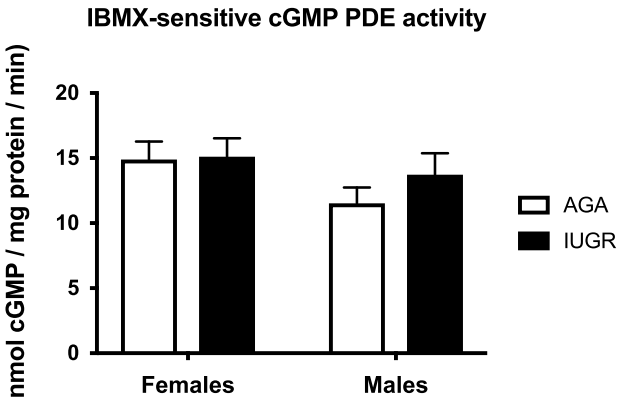

Fig. 5. IBMX-sensitive cGMP phosphodiesterase activity in umbilical vein homogenates. AGA, appropriate for gestational age neonates; IUGR, growth-restricted newborns. cGMP degradation was assessed in UV homogenates in the presence or absence of IBMX 10^{-4} M. Data are expressed as mean + SEM (n = 6–8 in females; n = 4–8 in males) of the difference between the quantity of cGMP degraded in absence of IBMX and the quantity of cGMP degraded in the presence of IBMX. Results are expressed as nanomoles cGMP per milligram of protein per minute. No significant difference was found between groups after analysis by *two-way ANOVA*.

variability on the results. To validate this approach, a part of the samples included in the pools were also tested individually. Both techniques led to similar results. The values obtained using individual samples were however more widely dispersed than those obtained by using the pools. Moreover, the use of individual samples needs to perform much more experiments to reach statistically relevant results than pools, even if *n* is higher with individual samples, where *n* corresponds to the real number of patients tested, whereas with pools *n* corresponds only to the number of pools studied. We concluded that using pools of samples collected in many patients allows to generate accurate data in a less time-consuming and more cost-effective manner. This approach has the advantage to highlight the main differences between groups, because it allows to test rapidly a huge number of samples. The use of pools would be useful to identify a general molecular mechanism, but of course not to establish a diagnostic test, where individual values are of great importance.

In smooth muscle cell, the main counteracting components of NO-induced relaxation are PDEs. We therefore investigated the functional contribution of PDEs to the relaxant response of UV to NO, by using the non-selective PDEs inhibitor IBMX. Cumulative concentrations of IBMX induced a dose-dependent relaxation in pre-constricted UV rings, suggesting that PDEs directly contribute to vascular tone regulation in UV. In all groups, the vasorelaxant response to DEA/NO was significantly improved by pre-incubation with IBMX. Moreover, pre-treatment with IBMX completely reversed the alteration of NO-induced relaxation in UV of IUGR females pre-contracted with 5-HT. Such results indicate that PDEs are key elements in the regulation of UV vascular tone and that they probably contribute to the alteration of NO-induced relaxation observed in UV of growth-restricted females. The beneficial effect of PDEs inhibition on the relaxant response to NO suggests that PDEs could represent promising targets for therapeutic intervention.

However, the fact that relaxation curves in the presence of IBMX were established in UV isolated from other patients than the initial experiments performed in basal conditions (without IBMX) constitutes a limit. Some complementary experiments were therefore performed to investigate, on the same tissue, DEA/NO-induced relaxation in the absence or presence of IBMX, as well as spontaneous relaxation. In such conditions, pre-treatment with IBMX also significantly improved NO-induced relaxation in all groups, except in UV of AGA males pre-constricted with 5-HT. In all groups and conditions, spontaneous relaxation was significantly weaker than the corresponding DEA/NO-induced relaxation. In UV pre-contracted with 5-HT, spontaneous relaxation was similar in the presence or absence of IBMX. In contrast, in UV pre-constricted with U46619, spontaneous relaxation observed in vascular rings pre-incubated with IBMX was significantly increased as compared to basal conditions.

These complementary experiments were however done only on a limited number of subjects (n = 5–7) as compared to the data presented in Figs. 2 and 3 (n = 15–51). This was sufficient to test the direct effect of IBMX on DEA/NO-induced relaxation, because each vessel was its own control, but was clearly insufficient to compare pharmacological responses obtained in the different groups, because of the high variability already observed in our previous study. Moreover, given that IBMX enhanced the UV sensitivity to NO, the range of DEA/NO concentrations used in these complementary experiments was adapted (10^{-10} to 10^{-4} M, instead of 10^{-8} to 10^{-4} M). Thus, a direct comparison with initial experiments was not possible. Nevertheless, these additional data confirmed that pre-incubation with IBMX was able to increase the relaxant response of UV to NO, suggesting that improved relaxation observed in UV treated with IBMX compared to UV in basal conditions was really due to IBMX rather than variability between experiments.

The contribution of PDEs to cGMP homeostasis was then investigated in isolated UV rings. cGMP synthesis measured in the present study was in a similar range than cGMP production previously reported in human pulmonary vessels in similar conditions [37]. Basal cGMP production was very low as compared to NO-stimulated cGMP synthesis. sGC stimulation with DEA/NO led to an increase in cGMP content, which was significantly enhanced by pre-incubation with IBMX. These results suggest the presence of highly active PDEs. In UV incubated with IBMX and DEA/NO, cGMP content raised about 3 as high in IUGR females compared to AGA. Such data demonstrate a direct correlation between sGC protein content and cGMP production in UV of newborn females.

Finally, cGMP degradation was measured in UV homogenates. No significant difference was found between IUGR and AGA neonates, either in total or IBMX-sensitive cGMP PDEs activity. However, cGMP degradation measured in UV homogenates (in the range of nmol cGMP/mg protein/min) appeared to be more than 1000 times greater than cGMP production found in UV rings (in the range of pmol cGMP/mg protein/min). Such observation confirms the presence of highly active PDEs. However, IBMX-sensitive cGMP degradation represented only about 35% of the total cGMP PDEs activity. It is therefore surprising that pre-incubation with IBMX was sufficient to improve NO-induced relaxation in all groups and to reverse the alteration observed in UV of growth-restricted females. Indeed, IBMX-insensitive PDEs activity also greatly exceeded NO-stimulated cGMP production.

Nevertheless, sGC and PDEs activities cannot be directly compared because cGMP production was tested in intact UV rings, whereas cGMP degradation was measured, for technical reasons, in UV homogenates. Indeed, cGMP production was investigated in conditions close to *ex vivo* vasoreactivity, preserving tissular and subcellular organization. In contrast, tissular organization was lost in homogenates, which probably altered physiological regulation of PDEs activity. There is increasing evidence that subcellular microdomains contribute to the regulation of the NO/cGMP signaling pathway; in particular, PDEs are implicated in multimolecular regulatory complexes, called signalosomes, allowing close interactions between several proteins, such as PDEs, PKG and sGC [31,33]. Further investigations, using for example signalosome disruptors, could be of interest to better understand the contribution of PDEs.

In UV of IUGR females, PDEs inhibition likely allows to take advantage of the increased sGC activity, probably contributing to the beneficial effect of IBMX on NO-induced relaxation. This observation could be of therapeutic interest. PDEs represent good candidates for therapeutic intervention, because some PDEs inhibitors are already used in humans to treat several pathologies, including erectile dysfunction, pulmonary hypertension or chronic obstructive pulmonary disease [31,38] The most famous is the PDE5 inhibitor sildenafil, extensively tested in human and animal studies to treat several disorders. Recently, a multicenter clinical trial using sildenafil in IUGR complicated pregnancies was however suddenly interrupted because of post-natal deaths in the treated group [39–41]. Although a clear correlation has not yet been established between the treatment and the observed adverse effects, it should be noted that published effects of sildenafil on fetal growth, in human or animal studies, remains controversial [42]. Moreover, a clear implication of the PDE5 isoform has not been demonstrated in fetal growth restriction. It would be therefore necessary to extensively investigate the contribution of all PDE gene families to the regulation of umbilical circulation in order to devise isoform-specific therapeutic interventions, to avoid side-effects.

Another limitation of our study was linked to the characterization of the collected samples. Indeed, an important part of pregnant women giving birth in our hospital was followed up outside, thus limiting access to medical data, like longitudinal fetal growth or Doppler measurements. Therefore, our patients were retroactively reclassified according to the recently published "Consensus Based Definition of Growth Restriction in the Newborn" [36]. These criteria allowed a more rigorous postnatal classification of our subjects, even those included in our previous report, thus contributing to strengthen the present study.

In summary, the present study identified several alterations in the smooth muscle part of the NO/cGMP pathway in UV of IUGR compared to AGA females, with no significant difference between IUGR and AGA males. To our knowledge, this is the first report showing an association between IUGR and alterations in smooth muscle components of the NO/cGMP relaxing pathway in human UV, with a sexual dimorphism, raising the importance of also studying vascular smooth muscle alterations in IUGR complications.

The increased sGC protein amount and activity and PKG protein content observed in growth-restricted females could result from compensatory mechanisms in response to the impaired NO-induced relaxation, as an attempt to improve this vasodilation. Compensatory upregulation of NO production has been described in the feto-placental circulation in case of fetal growth restriction in humans [43]. We also previously observed similar compensatory mechanisms in pulmonary arteries of adult mice born in hypoxic conditions: PKG protein content and sGC activity were increased in pulmonary arteries of adult females exposed to perinatal hypoxia, whereas PDE1 contribution was enhanced, resulting in a decreased endothelium-dependent relaxation [44].

The enhancement of pro-relaxant proteins seemed counterbalanced by highly active PDEs. Moreover, although the increase in sGC protein content was found to correlate with a similar increase in cGMP production, PKG activity and its regulatory mechanisms remain to be further investigated. Indeed, a downregulated PKG activity cannot be excluded, despite the modest increase in PKG protein. Moreover, other cGMP or PKG targets, like potassium channels, could be implicated and would need attention.

The present study was focused on the smooth muscle part of the NO/cGMP relaxing pathway. Smooth muscle relaxation was directly stimulated by an exogenous NO-donor, when endogenous NO production by endothelium was avoided using the NOS inhibitor NLA. However, interactions between endothelium and smooth muscle are essential in blood vessel function, and an alteration may contribute to the development of pathologic processes [45]. Further investigation of potential alterations in the endothelium of UV in growth-restricted neonates will therefore be necessary.

Our data suggest that alterations occurring in the umbilical circulation in case of IUGR differ between males and females. NO-induced relaxation was reduced only in IUGR females, whereas no alteration was found in males. Moreover, relaxant response to NO was weaker in UV of IUGR females than IUGR males. In contrast, sGC protein and activity was significantly higher in IUGR females than IUGR males. Another difference was the higher proportion of smoking mothers in IUGR males than in IUGR females, even if this information should be considered with caution. It is possible that, whereas NO-mediated relaxation is impaired in females, males display alterations in the endothelium-dependent relaxation or vasoconstrictive mechanisms. Such differences could be linked to epigenetic processes. The observed sexual dimorphism needs to be further investigated, even in AGA

neonates, because regulatory mechanisms of umbilical circulation remain poorly understood. Indeed, a sexual dimorphism seemed also present in UV of AGA neonates, as suggested by the higher PKG protein amount in males than females. In particular, it would be of interest to study the effects of sex hormones, because they were found to directly influence vascular tone [46]. Further investigations would lead to a better understanding of the umbilical circulation regulation and finally to identification of sex-specific interventions to prevent or treat IUGR and its consequences. As consequence of the observed sexual dimorphism, it would be necessary to carefully identify sex-specific UV regulation and modifications occurring in IUGR, in order to devise either sex-specific treatments or combined therapeutic interventions without side-effects depending on the fetal sex.

The originality of the present research is the focus on human umbilical vessels, whereas most studies have investigated the placental contribution to IUGR. Our assumption was that, even if placental alterations could be corrected, this would be relatively inefficient if umbilical circulation is impaired. Although UAs are classically investigated in clinical diagnosis and monitoring of fetal growth restriction, UV would need special attention. Indeed, UV is the unique vessel to ensure blood supply to the fetus and could therefore represent a potential target for therapeutic interventions to improve the circulation from the placenta to the fetus. UAs, as direct prolongation of fetal iliac arteries, probably reflect mainly adaptive responses of the fetus to the alteration of blood/oxygen/nutrients supply. The present report was focused on UV, because we found an altered NO-induced relaxation in UV and not in UAs. However, it will be necessary to further investigate UAs, in order to better understand the regulation of umbilical circulation, but also to be sure that proposed interventions to improve blood flow in UV would not have adverse effects on UAs.

In conclusion, the present study displayed sex-specific alterations in the smooth muscle part of the NO/cGMP pathway in UV, which are in accordance with the sex-specific impairment of NO-induced relaxation we described previously [20]. Such alterations could disrupt placental-fetal circulation and then contribute to IUGR. Inhibition of PDEs could be a potential therapeutic strategy to improve placental-fetal blood flow. Evaluation of additional approaches to modulate NO/cGMP pathway could also be of interest [47]. Further investigation of endothelial function will be necessary for a complete understanding of UV regulation in physiological and pathological conditions, in order to devise appropriate interventions against IUGR.

Funding

This work was supported by the Swiss National Foundation (grant number 32003B_138491) and by the W. and E. Grand d'Hauteville Foundation For Academic Biomedical and Nursing Research.

Declaration of competing interest

The authors declare that there is no conflict of interests regarding the publication of this manuscript.

Acknowledgments

We are grateful to the team of midwives of the Clinic of Gynecology and Obstetrics of the Department Woman-Mother-Child at the Centre Hospitalier Universitaire Vaudois in Lausanne for their active collaboration in umbilical cords harvesting.

Abbreviations

5-HT	serotonin
AGA	appropriate for gestational age
AUC	area under the curve
BW	birth weight
cGMP	cyclic guanosine monophosphate
DEA/NO	2-(*N*,*N*-DiEthylAmino)-diazenolate-2-Oxide
IBMX	3-IsoButyl-1-MethylXanthine
IUGR	intrauterine growth restriction
NLA	nitro-L-arginine
NO	nitric oxide
PDE	phosphodiesterase
PKG	cGMP-dependent protein kinase
RT	room temperature
sGC	soluble guanylyl cyclase
U46619	thromboxane A2 analog
UA	umbilical artery
UV	umbilical vein

Appendix A. Supplementary data

Supplementary data to this article can be found online at https://doi.org/10.1016/j.placenta.2020.02.014.

References

[1] D.J. Barker, Adult consequences of fetal growth restriction, Clin. Obstet. Gynecol. 49 (2) (2006) 270–283.
[2] P.D. Gluckman, M.A. Hanson, Living with the past: evolution, development, and patterns of disease, Science 305 (2004) 1733–1736.
[3] M. Kaijser, A.K. Bonamy, O. Akre, S. Cnattingius, F. Granath, M. Norman, A. Ekbom, Perinatal risk factors for ischemic heart disease: disentangling the roles of birth weight and preterm birth, Circulation 117 (3) (2008) 405–410.
[4] L.A. Joss-Moore, R.H. Lane, The developmental origins of adult disease, Curr. Opin. Pediatr. 21 (2) (2009) 230–234.
[5] C. Yzydorczyk, J.B. Armengaud, A.C. Peyter, H. Chehade, F. Cachat, C. Juvet, B. Siddeek, S. Simoncini, F. Sabatier, F. Dignat-George, D. Mitanchez, U. Simeoni, Endothelial dysfunction in individuals born after fetal growth restriction: cardiovascular and renal consequences and preventive approaches, J. Dev. Orig. Health Dis. 8 (4) (2017) 448–464.
[6] A. Romo, R. Carceller, J. Tobajas, Intrauterine growth retardation (IUGR): epidemiology and etiology, Pediatr. Endocrinol. Rev. 6 (Suppl 3) (2009) 332–336.
[7] A. Nawathe, A.L. David, Prophylaxis and treatment of foetal growth restriction, Best practice & research, Clin. Obstetr. Gynaecol. 49 (2018) 66–78.
[8] E. Platz, R. Newman, Diagnosis of IUGR: traditional biometry, Semin. Perinatol. 32 (3) (2008) 140–147.
[9] M.C. Audette, J.C. Kingdom, Screening for fetal growth restriction and placental insufficiency, Semin. Fetal Neonatal Med. 23 (2) (2018) 119–125.
[10] F. Figueras, E. Gratacos, An integrated approach to fetal growth restriction, Best practice & research, Clin. Obstetr. Gynaecol. 38 (2017) 48–58.
[11] S.J. Benton, L.M. McCowan, A.E. Heazell, D. Grynspan, J.A. Hutcheon, C. Senger, O. Burke, Y. Chan, J.E. Harding, J. Yockell-Lelievre, Y. Hu, L.C. Chappell, M. J. Griffin, A.H. Shennan, L.A. Magee, A. Gruslin, P. von Dadelszen, Placental growth factor as a marker of fetal growth restriction caused by placental dysfunction, Placenta 42 (2016) 1–8.
[12] A.M. Marconi, C.L. Paolini, Nutrient transport across the intrauterine growth-restricted placenta, Semin. Perinatol. 32 (2008) 178–181.
[13] I. Cetin, G. Alvino, Intrauterine growth restriction: implications for placental metabolism and transport. A review, Placenta 30 (Suppl A) (2009) S77–S82.
[14] M.G. Neerhof, L.G. Thaete, The fetal response to chronic placental insufficiency, Semin. Perinatol. 32 (2008) 201–205.
[15] J.C. Kingdom, M.C. Audette, S.R. Hobson, R.C. Windrim, E. Morgen, A placenta clinic approach to the diagnosis and management of fetal growth restriction, Am. J. Obstet. Gynecol. 218 (2S) (2018) S803–S817.
[16] K. Marsal, Physiological adaptation of the growth-restricted fetus, Best practice & research, Clin. Obstetr. Gynaecol. 49 (2018) 37–52.
[17] T. Van Mieghem, R. Hodges, E. Jaeggi, G. Ryan, Functional echocardiography in the fetus with non-cardiac disease, Prenat. Diagn. 34 (1) (2014) 23–32.
[18] J.N. Cheong, M.E. Wlodek, K.M. Moritz, J.S. Cuffe, Programming of maternal and offspring disease: impact of growth restriction, fetal sex and transmission across generations, J. Physiol. 594 (17) (2016) 4727–4740.
[19] F. Crispi, J. Miranda, E. Gratacos, Long-term cardiovascular consequences of fetal growth restriction: biology, clinical implications, and opportunities for prevention of adult disease, Am. J. Obstet. Gynecol. 218 (2S) (2018) S869–S879.
[20] A.C. Peyter, F. Delhaes, D. Baud, Y. Vial, G. Diaceri, S. Menetrey, P. Hohlfeld, J. F. Tolsa, Intrauterine growth restriction is associated with structural alterations in human umbilical cord and decreased nitric oxide-induced relaxation of umbilical vein, Placenta 35 (11) (2014) 891–899.
[21] J.F. Bruch, O. Sibony, K. Benali, J.C. Challier, P. Blot, C. Nessmann, Computerized microscope morphometry of umbilical vessels from pregnancies with intrauterine growth retardation and abnormal umbilical artery Doppler, Hum. Pathol. 28 (10) (1997) 1139–1145.
[22] E. Ferrazzi, S. Rigano, M. Bozzo, M. Bellotti, N. Giovannini, H. Galan, F. C. Battaglia, Umbilical vein blood flow in growth-restricted fetuses, Ultrasound Obstet. Gynecol. 16 (5) (2000) 432–438.

[23] S. Rigano, M. Bozzo, E. Ferrazzi, M. Bellotti, F.C. Battaglia, H.L. Galan, Early and persistent reduction in umbilical vein blood flow in the growth-restricted fetus: a longitudinal study, Am. J. Obstet. Gynecol. 185 (4) (2001) 834–838.
[24] N.M. AbdelMaboud, H.H. Elsaid, Role of venous Doppler evaluation of intrauterine growth retardation, Egypt J. Radiol. Nucl. M 46 (1) (2015) 167–174.
[25] S.L. Adamson, L. Myatt, B.M.P. Byrne, Regulation of umbilical blood flow, in: R. A. Polin, W.W. Fox (Eds.), Fetal and Neonatal Physiology, Saunders, Philadelphia, 1998, pp. 977–989.
[26] Y. Zhao, P.M. Vanhoutte, S.W. Leung, Vascular nitric oxide: beyond eNOS, J. Pharmacol. Sci. 129 (2) (2015) 83–94.
[27] A. Smolenski, A.M. Burkhardt, M. Eigenthaler, E. Butt, S. Gambaryan, S. M. Lohmann, U. Walter, Functional analysis of cGMP-dependent protein kinases I and II as mediators of NO/cGMP effects, Naunyn-Schmiedeberg's Arch. Pharmacol. 358 (1) (1998) 134–139.
[28] M. Morgado, E. Cairrao, A.J. Santos-Silva, I. Verde, Cyclic nucleotide-dependent relaxation pathways in vascular smooth muscle, Cell. Mol. Life Sci. 69 (2) (2012) 247–266.
[29] J.B. Polson, S.J. Strada, Cyclic nucleotide phosphodiesterases and vascular smooth muscle, Annu. Rev. Pharmacol. Toxicol. 36 (7) (1996) 403–427.
[30] A.T. Bender, J.A. Beavo, Cyclic nucleotide phosphodiesterases: molecular regulation to clinical use, Pharmacol. Rev. 58 (3) (2006) 488–520.
[31] D.H. Maurice, H. Ke, F. Ahmad, Y. Wang, J. Chung, V.C. Manganiello, Advances in targeting cyclic nucleotide phosphodiesterases, Nat. Rev. Drug Discov. 13 (4) (2014) 290–314.
[32] K. Omori, J. Kotera, Overview of PDEs and their regulation, Circ. Res. 100 (3) (2007) 309–327.
[33] F. Ahmad, T. Murata, K. Shimizu, E. Degerman, D. Maurice, V. Manganiello, Cyclic nucleotide phosphodiesterases: important signaling modulators and therapeutic targets, Oral Dis. 21 (1) (2015) e25–50.
[34] M. Voigt, C. Fusch, D. Olbertz, K. Hartmann, N. Rochow, C. Renken, et al., Analyse des Neugeborenenkollectivs des Bundesrepublik Deutschland - 12. Mitteilung: vorstellung engmaschiger Perzentilwerte (-kurven) für die Körpermasse Neugeborener, Geburtshilfe Frauenheilkd 66 (2006) 956–970.
[35] E.D. Barker, F.M. McAuliffe, F. Alderdice, J. Unterscheider, S. Daly, M.P. Geary, M. M. Kennelly, K. O'Donoghue, A. Hunter, J.J. Morrison, G. Burke, P. Dicker, E. C. Tully, F.D. Malone, The role of growth trajectories in classifying fetal growth restriction, Obstet. Gynecol. 122 (2013) 248–254.
[36] I.M. Beune, F.H. Bloomfield, W. Ganzevoort, N.D. Embleton, P.J. Rozance, A.G. van Wassenaer-Leemhuis, K. Wynia, S.J. Gordijn, Consensus based definition of growth restriction in the newborn, J. Pediatr. 196 (2018) 71–76 e1.
[37] G. Pussard, J.P. Gascard, I. Gorenne, C. Labat, X. Norel, E. Dulmet, C. Brink, Endothelin-1 modulates cyclic GMP production and relaxation in human pulmonary vessels, J. Pharmacol. Exp. Therapeut. 274 (2) (1995) 969–975.
[38] T. Keravis, C. Lugnier, Cyclic nucleotide phosphodiesterase (PDE) isozymes as targets of the intracellular signalling network: benefits of PDE inhibitors in various diseases and perspectives for future therapeutic developments, Br. J. Pharmacol. 165 (5) (2012) 1288–1305.
[39] F. Figueras, Sildenafil therapy in early-onset fetal growth restriction: waiting for the individual patient data meta-analysis, BJOG 126 (8) (2019) 1007.
[40] N. Lombardi, G. Crescioli, A. Bettiol, C. Ravaldi, A. Vannacci, Perinatal deaths after sildenafil treatment of fetal growth restriction raise the issue of safety in randomised clinical trials, Pharmacoepidemiol. Drug Saf. 28 (4) (2019) 437–438.
[41] A. Pels, J.C. Jakobsen, W. Ganzevoort, C.A. Naaktgeboren, W. Onland, A.G. van Wassenaer-Leemhuis, C. Gluud, Detailed statistical analysis plan for the Dutch STRIDER (Sildenafil TheRapy in Dismal prognosis Early-onset fetal growth Restriction) randomised clinical trial on sildenafil versus placebo for pregnant women with severe early onset fetal growth restriction, Trials 20 (1) (2019) 42.
[42] K.M. Groom, A.L. David, The role of aspirin, heparin, and other interventions in the prevention and treatment of fetal growth restriction, Am. J. Obstet. Gynecol. 218 (2S) (2018) S829–S840.
[43] S. Pisaneschi, F.A. Strigini, A.M. Sanchez, S. Begliuomini, E. Casarosa, A. Ripoli, P. Ghirri, A. Boldrini, B. Fink, A.R. Genazzani, F. Coceani, T. Simoncini, Compensatory feto-placental upregulation of the nitric oxide system during fetal growth restriction, PloS One 7 (9) (2012), e45294.
[44] A.C. Peyter, V. Muehlethaler, L. Liaudet, M. Marino, S. Di Bernardo, G. Diaceri, J. F. Tolsa, Muscarinic receptor M1 and phosphodiesterase 1 are key determinants in pulmonary vascular dysfunction following perinatal hypoxia in mice, Am. J. Physiol. Lung Cell Mol. Physiol. 295 (1) (2008) L201–L213.
[45] G. Yetik-Anacak, J.D. Catravas, Nitric oxide and the endothelium: history and impact on cardiovascular disease, Vasc. Pharmacol. 45 (5) (2006) 268–276.
[46] J.M. Orshal, R.A. Khalil, Gender, sex hormones, and vascular tone, Am. J. Physiol. Regul. Integr. Comp. Physiol. 286 (2) (2004) R233–R249.
[47] J.R. Kraehling, W.C. Sessa, Contemporary approaches to modulating the nitric oxide-cGMP pathway in cardiovascular disease, Circ. Res. 120 (7) (2017) 1174–1182.

Supplementary data

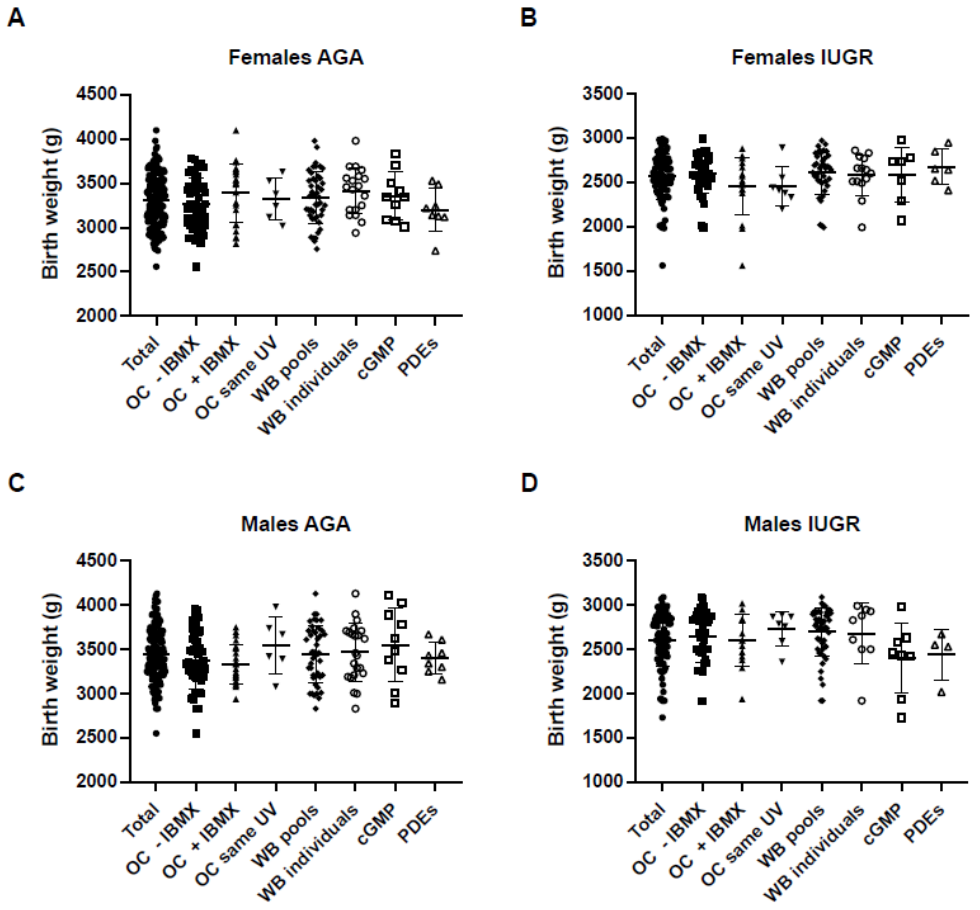

Supplementary Figure 1. Distribution of birth weight in subsets of patients used, for each experimental group, in the different experiments.

AGA, appropriate for gestational age neonates; IUGR, growth-restricted newborns; OC, organ chambers; WB, Western blot. Dot plots show the distribution of birth weight in subsets of patients used for each type of experiments compared to all patients included in the present study ("Total") for each experimental group. "OC - IBMX", isolated vessel tension studies in absence of IBMX; "OC + IBMX", isolated vessel tension studies in umbilical vein pre-incubated with IBMX; "OC same UV", isolated vessel tension studies testing NO-induced relaxation in absence or presence of IBMX on umbilical vein isolated from the same patient; "WB pools", WB using pools of patients; "WB individuals", WB performed with individual samples; "cGMP", sGC activity quantification; "PDEs", PDEs activity measurement.

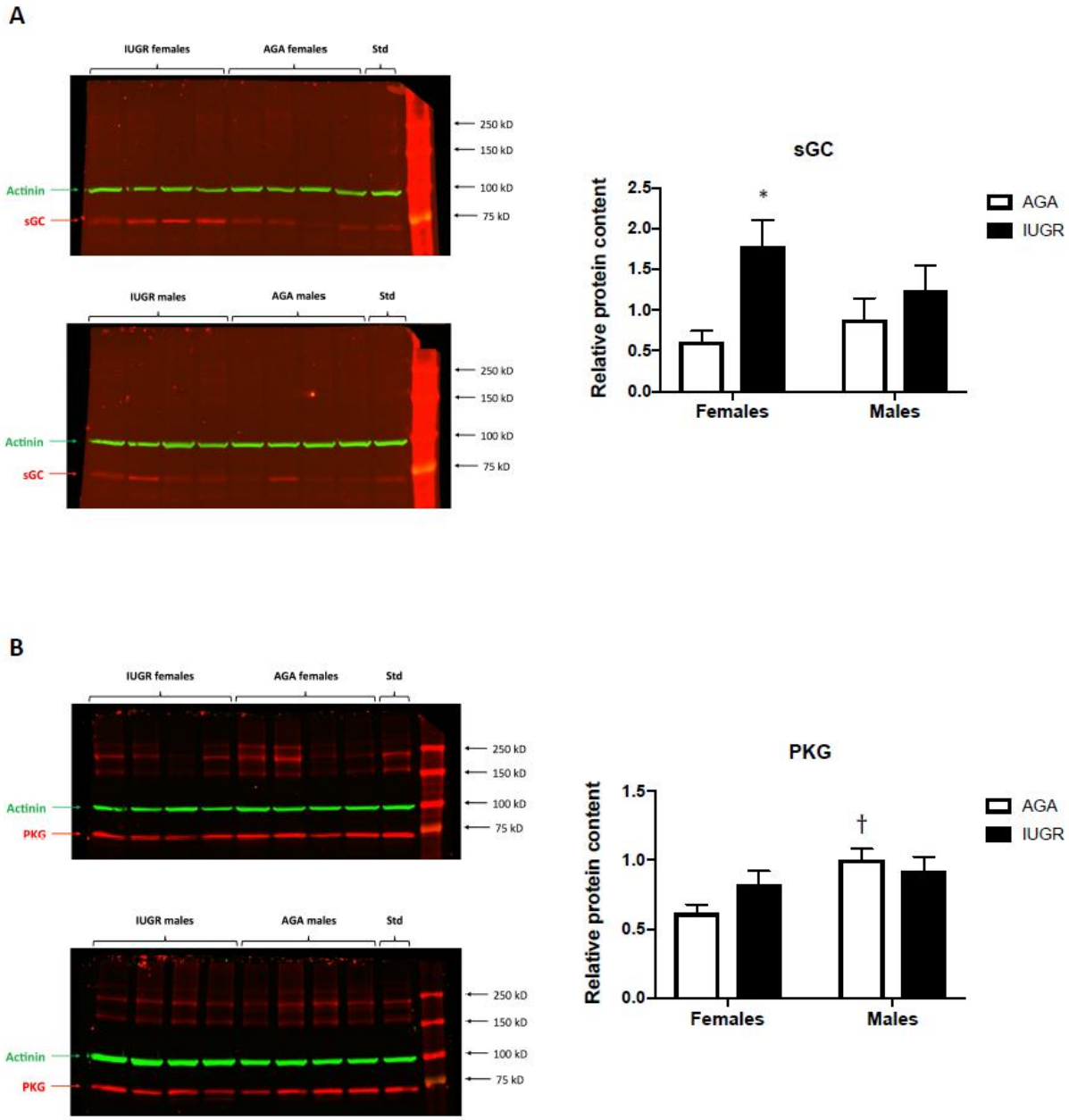

Supplementary Figure 2. Relative amounts of sGC and PKG proteins in individual samples of human umbilical vein.

AGA, appropriate for gestational age neonates; IUGR, growth-restricted newborns; Std, "standard" sample. Representative blots are presented for each protein. Relative protein content of sGC (A) or PKG (B) was evaluated by western blot in umbilical vein homogenates of AGA and IUGR newborns. For each experimental group, individual samples were randomly selected among the 40 patients included in the pools analyzed in Figure 1. For each individual sample, the target protein amount was normalized by the actinin protein content and reported to the amount measured in the "standard" sample. Data are expressed as mean + SEM (n=14-15 in females; n=9-19 in males) and analyzed using two-way ANOVA. * significant difference between IUGR and AGA neonates; † statistical difference between males and females ($P < 0.05$).

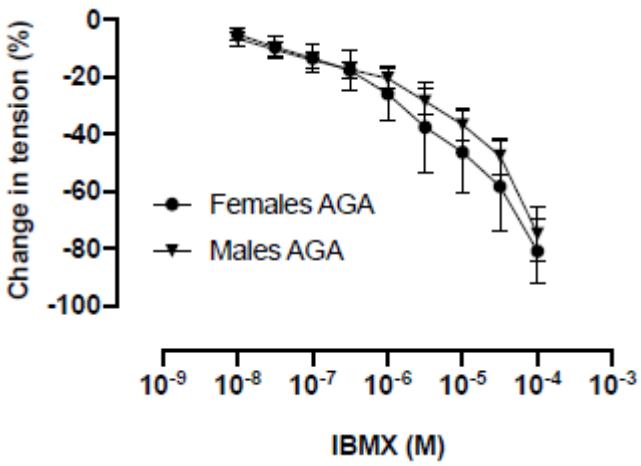

Supplementary Figure 3. Relaxation induced by cumulative doses of the non-specific PDEs inhibitor IBMX on isolated umbilical veins.

AGA, appropriate for gestational age newborns. Cumulative concentrations of IBMX were applied to umbilical vein rings pre-contracted with 5-HT 10-5 M. Data are expressed as mean ± SEM of the percent of change in tension induced by IBMX (n=5).

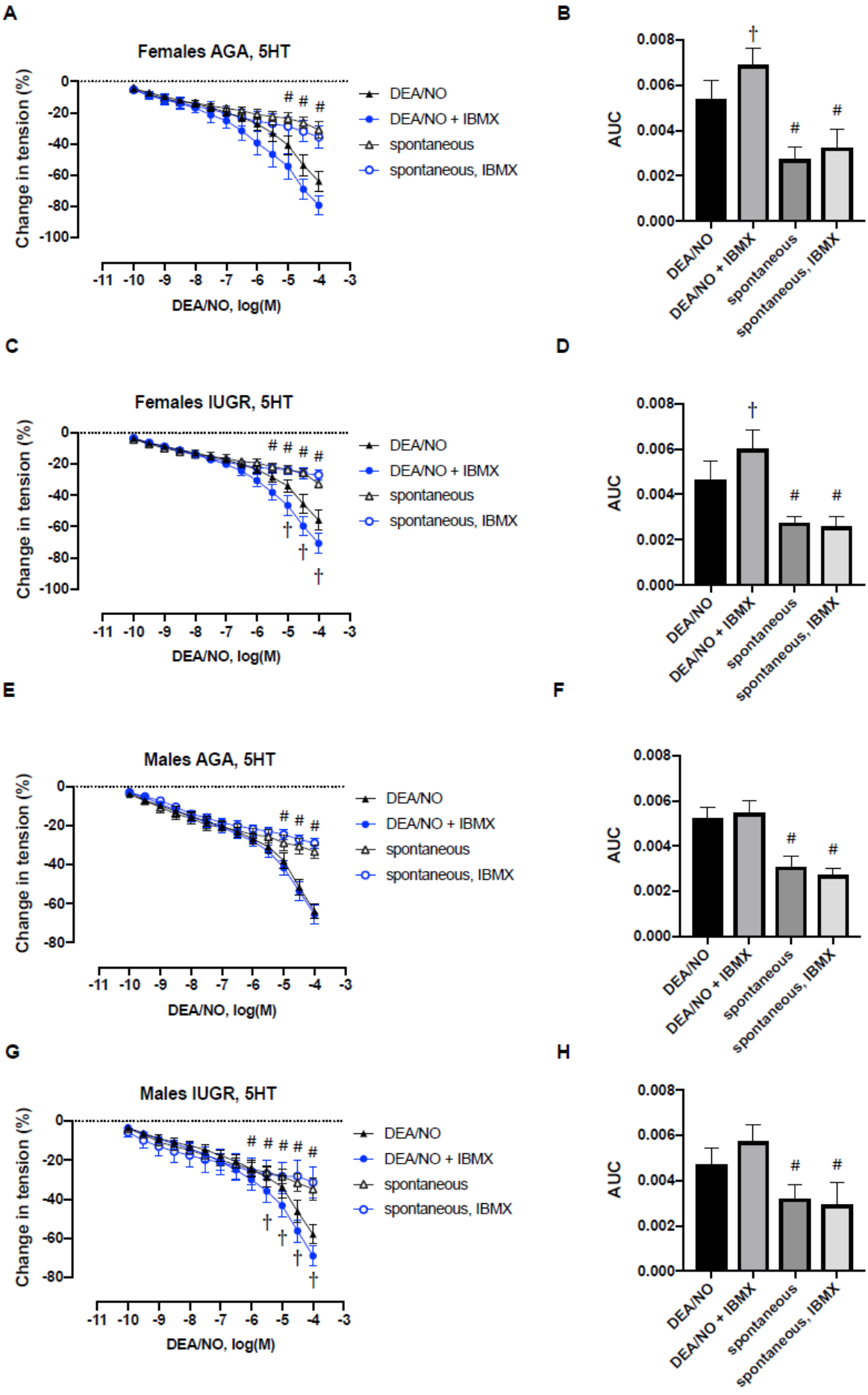
A
Females AGA, 5HT
Change in tension (%)
DEA/NO, log(M)
DEA/NO
DEA/NO + IBMX
spontaneous
spontaneous, IBMX
B
AUC
C
Females IUGR, 5HT
D
E
Males AGA, 5HT
F
G
Males IUGR, 5HT
H

Supplementary Figure 4. Spontaneous and NO-induced relaxation in isolated umbilical veins pre-contracted with 5-HT in the absence or presence of IBMX.

AGA, appropriate for gestational age neonates; IUGR, growth-restricted newborns. Cumulative concentrations of DEA/NO were applied to umbilical vein isolated from AGA females (A-B), IUGR females (C-D), AGA males (E-F) or IUGR males (G-H), pre-contracted with 5-HT 10-5 M, in the absence or presence of IBMX 10-4 M. Data are expressed as mean ± SEM of the percent of change in tension induced by the vasodilator (n=5-7 in females; n=6-7 in males). Data were analyzed by two-way ANOVA. † significant difference between DEA/NO + IBMX and DEA/NO alone; # statistical difference between DEA/NO-induced relaxation and the corresponding spontaneous relaxation ($P < 0.05$). Area under the curve (AUC) was calculated for each dose-response curve of the corresponding graph. Results are expressed as mean + SEM and were analyzed using two-way ANOVA. † significant difference between DEA/NO + IBMX and DEA/NO alone; # statistical difference between DEA/NO-induced relaxation and the corresponding spontaneous relaxation ($P < 0.05$). For each group, the four experimental conditions have been tested simultaneously in vascular rings isolated from the same patient.

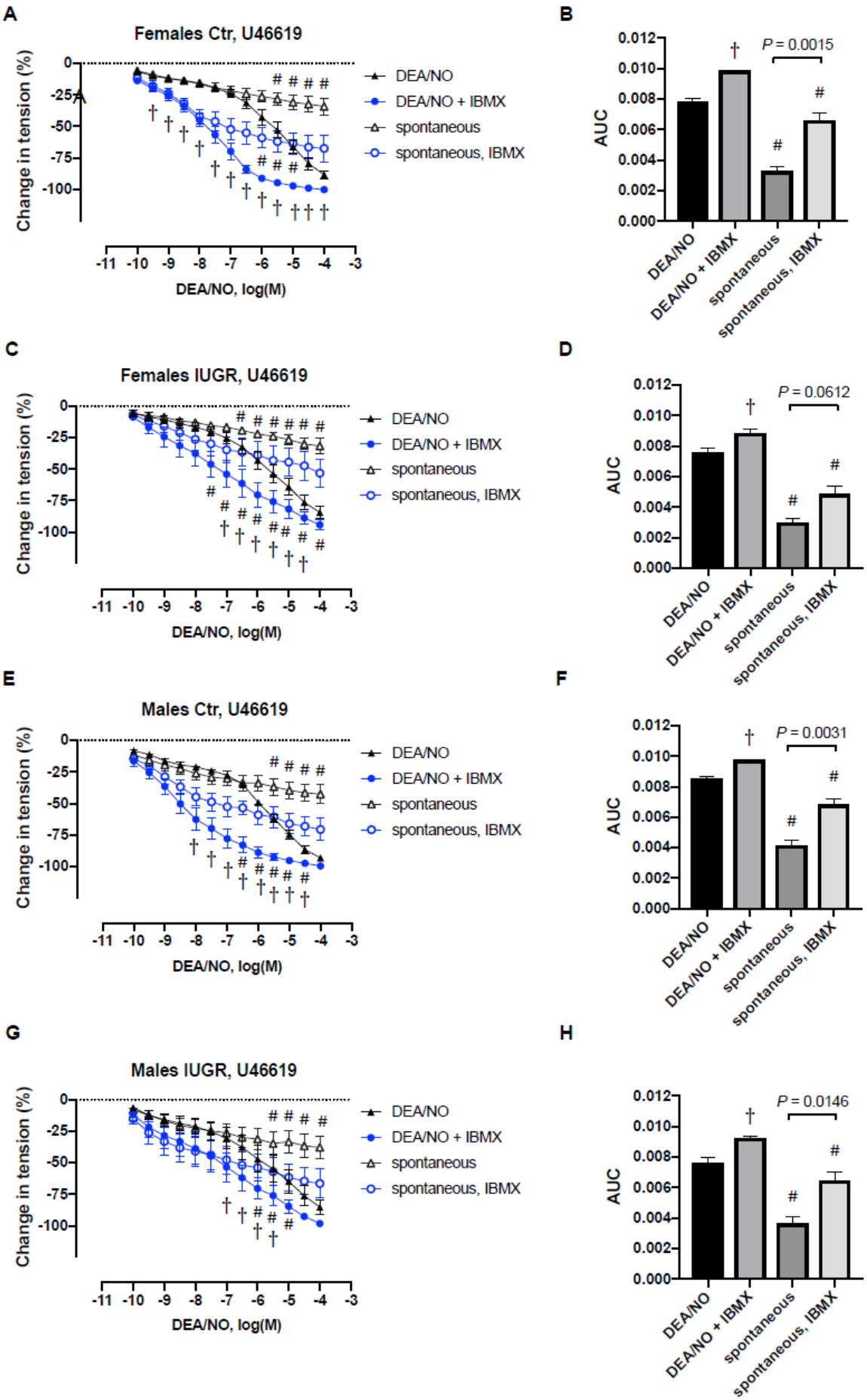
A
Females Ctr, U46619
Change in tension (%)
DEA/NO, log(M)
DEA/NO
DEA/NO + IBMX
spontaneous
spontaneous, IBMX
B
AUC
P = 0.0015
C
Females IUGR, U46619
D
P = 0.0612
E
Males Ctr, U46619
F
P = 0.0031
G
Males IUGR, U46619
H
P = 0.0146

Supplementary Figure 5. Spontaneous and NO-induced relaxation in isolated umbilical veins pre-contracted with U46619 in the absence or presence of IBMX.

AGA, appropriate for gestational age neonates; IUGR, growth-restricted newborns. Cumulative concentrations of DEA/NO were applied to umbilical vein isolated from AGA females (A-B), IUGR females (C-D), AGA males (E-F) or IUGR males (G-H), pre-contracted with U46619 10-6 M, in the absence or presence of IBMX 10-4 M. Data are expressed as mean ± SEM of the percent of change in tension induced by the vasodilator (n=6-7). Data were analyzed by two-way ANOVA. † significant difference between DEA/NO + IBMX and DEA/NO alone; # statistical difference between DEA/NO-induced relaxation and the corresponding spontaneous relaxation ($P < 0.05$). Area under the curve (AUC) was calculated for each dose-response curve of the corresponding graph. Results are expressed as mean + SEM and were analyzed using two-way ANOVA. † significant difference between DEA/NO + IBMX and DEA/NO alone; # statistical difference between DEA/NO-induced relaxation and the corresponding spontaneous relaxation ($P < 0.05$). For each group, the four experimental conditions have been tested simultaneously in vascular rings isolated from the same patient.

Supplementary Table 1. Patients inclusion and reclassification

	Patients already included in the study reported in *Placenta 2014* [1]	Patients newly included for the present study	Total of patients initially included	Patients excluded according to the 2018 clinical consensus [2]	**Patients finally included in the present report**
AGA females	82	71	153	2	**151**
IUGR females	55	59	114	24	**90**
AGA males	80	65	145	2	**143**
IUGR males	56	67	123	40	**83**
TOTAL	273	262	535	68	**467**

AGA, appropriate for gestational age neonates; IUGR, growth-restricted newborns. Data represent the number of patients. [1] Peyter *et al., Placenta* 2014; [2] All patients initially included were reclassified according to the criteria described in the "Consensus based definition of growth restriction in the newborn" (Beune *et al., J Pediatr* 2018). All patients who did not reach these criteria (mainly because of incomplete perinatal data) were excluded.

Supplementary Table 2. cGMP production in isolated umbilical veins

	Females			Males		
	AGA	**IUGR**		**AGA**	**IUGR**	
	(pmol cGMP/mg protein/min)		***P*-value**	(pmol cGMP/mg protein/min)		***P*-value**
	n = 10	n = 7		n = 10	n = 8	
basal	0.12 ± 0.04	0.32 ± 0.26	> 0.9999	0.16 ± 0.04	0.12 ± 0.03	> 0.9999
IBMX 10^{-4} M	0.43 ± 0.12	0.41 ± 0.14	> 0.9999	0.25 ± 0.06	0.53 ± 0.17	> 0.9999
DEA/NO 10^{-4} M	2.28 ± 1.58	22.64 ± 10.82	0.7378	2.30 ± 0.96	11.88 ± 5.25	0.8624
IBMX + DEA/NO	29.98 ± 14.16	96.39 ± 33.08 †‡# * §	**0.0011**	25.10 ± 11.77	50.94 ± 19.33 †‡# §	0.0891

AGA, appropriate for gestational age neonates; IUGR, growth-restricted newborns. Data are expressed as mean ± SEM, and were analyzed using a *two-way ANOVA*. *P*-values presented in the table are related to comparison between AGA and IUGR groups, and bold indicates significant *P*-values. * significant difference between AGA and IUGR; § significant difference between males and females; † significant difference as compared to basal cGMP production; ‡ significant difference as compared to cGMP production incubated with IBMX alone; # significant difference as compared to cGMP production in the presence of DEA/NO alone ($P<0.05$).

Supplementary Table 3. cGMP phosphodiesterases activity in umbilical vein homogenates

	Females		Males	
	AGA	**IUGR**	**AGA**	**IUGR**
	n = 8	n = 6	n = 8	n = 4
Total cGMP degradation (nmol cGMP/mg protein/min)	42.39 ± 3.07	42.03 ± 4.12	36.57 ± 3.57	36.93 ± 2.67
IBMX-sensitive cGMP degradation (nmol cGMP/mg protein/min)	14.89 ± 1.40 *	15.12 ± 1.40 *	11.53 ± 1.21 *	13.72 ± 1.66 *

AGA, appropriate for gestational age neonates; IUGR, growth-restricted newborns. Data are expressed as mean ± SEM. Data were analyzed using a two-way ANOVA. * significant difference between IBMX-sensitive and total PDEs activity ($P < 0.0001$). No significant difference was found between AGA and IUGR, nor between males and females.